

**Activity-Profiling of Vacuolar Processing Enzymes  
and the Proteasome  
during Plant-Pathogen Interactions**

Inaugural-Dissertation  
zur Erlangung des Doktorgrades  
der Mathematisch-Naturwissenschaftlichen  
Fakultät der Universität zu Köln

vorgelegt von  
**Johana C. Misas Villamil**  
aus Bogotá

Köln, August 2010

Die vorliegende Arbeit wurde am Max-Planck-Institut für Pflanzenzüchtungsforschung in Köln in der Abteilung für Molekulare Phytopathologie (Direktor: Prof. Dr. Paul Schulze-Lefert) angefertigt.



MAX-PLANCK-GESELLSCHAFT



Max-Planck-Institut für  
Pflanzenzüchtungsforschung

**DAAD**

Deutscher Akademischer Austausch Dienst  
German Academic Exchange Service

Berichterstatter:

Prof. Dr. Paul Schulze-Lefert

Prof. Dr. Marcel Bucher

Prof. Dr. Hermen Overkleef

Prüfungsvorsitzender:

Prof. Dr. Reinhard Krämer

Tag der Disputation:

18. Oktober 2010

# TABLE OF CONTENTS

<b>ABBREVIATIONS</b> .....	<b>I</b>
<b>SUMMARY</b> .....	<b>III</b>
<b>ZUSAMMENFASSUNG</b> .....	<b>IV</b>
<b>1 INTRODUCTION</b> .....	<b>1</b>
1.1 Plant caspase-like enzymes.....	1
1.2 Vacuolar Processing Enzymes (VPEs) .....	4
1.3 The plant proteasome .....	6
1.4 Activity-Based Protein Profiling (ABPP) .....	8
1.5 The natural interaction Arabidopsis - Hyaloperonospora arabidopsidis.....	9
1.6 The model pathogen <i>Pseudomonas syringae</i> .....	10
1.7 Aim and outline of the thesis .....	12
<b>2 RESULTS</b> .....	<b>13</b>
<b>2.1 VACUOLAR PROCESSING ENZYMES</b> .....	<b>13</b>
2.1.1 Screening of legumain probes on pumpkin seed extracts .....	13
2.1.2 Legumain probes target mainly $\gamma$ VPE .....	14
2.1.3 Labelling conditions .....	17
2.1.4 Characterization of VPE inhibitors .....	20
2.1.5 $\gamma$ VPE labelling increases upon Hpa infection.....	23
<b>2.2 THE PROTEASOME</b> .....	<b>27</b>
2.2.1 Epoxy-ketone probes label the plant proteasome .....	27
2.2.2 Proteasome inhibition by epoxomicin and syringolin A .....	30
2.2.3 Structure-Activity relationship of SylA.....	31
2.2.4 RhSylA labels Arabidopsis and <i>Nicotiana benthamiana</i> proteasome .....	32
2.2.5 Inhibition of <i>N. benthamiana</i> proteasome during infection.....	34
2.2.6 SylA-deficient mutant, sylC triggers early host cell death .....	36

2.2.7	SylA-deficient mutant growth is not affected by activation of immune responses .....	36
2.2.8	B728a WT bacteria spread and colonize distant tissue.....	39
2.2.9	B728a WT and sylC show the same phenotype on bean .....	42
2.2.10	Distant colonization is common for <i>Pseudomonas syringae</i> .....	43
2.2.11	Distant colonization is uncoupled from cell death suppression .....	46
2.2.12	Salicylic acid – mediated acquired resistance prevents distant colonization and is suppressed by SylA.....	48
2.2.13	sylC strain can colonize distant tissues in NahG plants .....	51
<b>3</b>	<b>DISCUSSION.....</b>	<b>54</b>
<b>3.1</b>	<b>VACUOLAR PROCESSING ENZYMES.....</b>	<b>54</b>
3.1.1	AMS-101 is a highly specific probe for $\gamma$ VPE in Arabidopsis leaf extracts .....	54
3.1.2	$\gamma$ VPE exhibits caspase-1 activity and distinct inhibitor specificity.....	56
3.1.3	$\gamma$ VPE is post-transcriptionally activated during compatible interactions.....	57
<b>3.2</b>	<b>THE PROTEASOME .....</b>	<b>59</b>
3.2.1	Epoxomicin-based probes are specific for the plant proteasome .....	59
3.2.2	SylA targets mainly $\beta$ 2 and $\beta$ 5 catalytic subunits of the plant proteasome .....	60
3.2.3	SylA is required for ETI suppression but not for bacterial growth at primary infection sites .....	62
3.2.3	SylA promotes distant colonization .....	64
3.2.4	Distant colonization is common for <i>P. syringae</i> .....	65
3.2.5	SylA is required for distant colonization but not always for HR suppression .....	66
3.2.6	A model for pathogen containment and distant colonization .....	67
<b>4</b>	<b>EXPERIMENTAL PROCEDURES.....</b>	<b>71</b>
4.1	Chemicals .....	71
4.2	Plant materials and growth conditions.....	71

4.3	Bacterial strains.....	71
4.4	In vitro labeling of leaf extracts.....	72
4.5	Generation of transgenic <i>Pseudomonas</i> strains .....	72
4.6	<i>Pseudomonas</i> infection assays.....	72
4.7	Quantification of bacterial densities.....	73
4.8	<i>Hyaloperonospora</i> infection assays .....	74
4.9	Agroinfiltration of VPEs .....	74
4.10	BTH treatment.....	75
4.11	PCR and RT-PCR.....	75
<b>5</b>	<b>REFERENCES.....</b>	<b>76</b>
<b>6</b>	<b>APPENDICES .....</b>	<b>84</b>
6.1	Appendix A. Structure of legumain probes used for VPE screening .....	84
6.2	Appendix B. Structure of the inhibitors used in this study .....	85
6.3	Appendix C. Syla and epoxomicin induce cell death in <i>Nicotiana benthamiana</i> .....	86
6.4	Appendix D. Table 1. <i>Pseudomonas syringae</i> strains.....	87
<b>7</b>	<b>ACKNOWLEDGMENT .....</b>	<b>88</b>
<b>8</b>	<b>ERKLÄRUNG .....</b>	<b>90</b>
<b>9</b>	<b>LEBENS LAUF .....</b>	<b>91</b>



## ABBREVIATIONS

-	fused to (gene/protein fusion constructs)
°C	degree Celsius
%	percentage
3'	three prime end of a DNA fragment
5'	five prime end of a DNA fragment
35S	35S promoter of Cauliflower Mosaic Virus
AALP	Arabidopsis Aleurain-Like Protein
AOMK	acyloxymethyl ketone
Asn	Asparagine
Asp	Aspartic acid
Avr	avirulence
bp	base pair (s)
BTH	benzo(1,2,3)thiadiazole-7-carbothioic acid S-methyl ester
Cala2	<i>Hyaloperonospora arabidopsidis</i> isolate Cala2
cDNA	complementary DNA
cfu	colony forming unit
C-terminal	carboxy terminal
Col-0	<i>Arabidopsis thaliana</i> ecotype <i>Columbia</i>
DAR	distant acquired resistance
DMSO	dimethylsulfoxide
DNA	deoxyribonucleic acid
dpi	day(s) post inoculation
DTT	dithiothreitol
E-64	(L-3-trans-Carboxyoxiran-2-Carbonyl)-L-Leucyl-Admat
EDS1	Enhanced Disease Susceptibility 1
ETI	effector-triggered immunity
ETS	effector-triggered susceptibility
Fig.	figure
FP	activity-based probe for serine proteases
g	gram(s)
<i>g</i>	gravity constant (9.81 ms <sup>-1</sup> )
GFP	green fluorescent protein
h	hour(s)
H <sub>2</sub> O <sub>2</sub>	hydrogen peroxide
<i>hrcC</i>	outer-membrane type III secretion protein
hpi	hour(s) post inoculation
HR	hypersensitive response
iVPE	intermediate Vacuolar Processing Enzyme isoform
kDa	kiloDalton(s)
KO	knock-out
l	litre(s)
log	decimal logarithm
LRR	leucine-rich repeat
m	milli
M	molar (mol/l)
μ	micro
MAMP	microbe-associated molecular patterns
min	minute(s)

ABBREVIATIONS

MgCl <sub>2</sub>	magnesium chloride
MS	mass spectrometry
mVPE	mature Vacuolar Processing Enzyme isoform
MW	molecular weight
<i>nahG</i>	bacterial SA-degrading enzyme salicylate hydroxylase
<i>N.</i>	<i>Nicotiana benthamiana</i>
NPC	no probe control
Noco1	<i>Hyaloperonospora arabidopsidis</i> isolate Noco1
Noco1	<i>Hyaloperonospora arabidopsidis</i> isolate Noco1
N-terminal	amino terminal
NYG	nutrient yeast extract-glucose
OD	optical density
OE	over-expressor
ORF	open-reading frame
PAGE	polyacrylamide gel-electrophoresis
PAMP	pathogen-associated molecular pattern
PCD	programmed cell-death
PCR	polymerase chain reaction
pH	negative decimal logarithm of the H <sup>+</sup> concentration
<i>Pac</i>	<i>Pseudomonas syringae</i> pv. <i>aceris</i>
<i>Pgl</i>	<i>Pseudomonas syringae</i> pv. <i>glycinea</i>
<i>Pma</i>	<i>Pseudomonas syringae</i> pv. <i>maculicola</i>
<i>Pph</i>	<i>Pseudomonas syringae</i> pv. <i>phaseolicola</i>
<i>Ppi</i>	<i>Pseudomonas syringae</i> pv. <i>pisii</i>
PPV	Precursor Protease Vesicle (s)
<i>Psy</i>	<i>Pseudomonas syringae</i> pv. <i>syringae</i>
<i>Pta</i>	<i>Pseudomonas syringae</i> pv. <i>tabaci</i>
<i>Pth</i>	<i>Pseudomonas syringae</i> pv. <i>thea</i>
<i>Pto</i>	<i>Pseudomonas syringae</i> pv. <i>tomato</i>
PTI	PAMP-triggered immunity
pv.	pathovar
R	resistance
RD21	Responsive to Dessication-21
RhSylA	Rhodamine tagged syringolin A
RNA	ribonucleic acid
ROS	reactive oxygen species
rpm	revolutions per minute
<i>RPP</i>	resistance to <i>Peronospora parasitica</i>
SA	salicylic acid
SAR	systemic acquired resistance
SDS	sodium dodecyl sulphate
<i>Sid2</i>	Salicylic Acid Induction-Deficient 2
SylA	syringolin A
<i>syIC</i>	Syringolin A deficient mutant
T3SS	type three secretion system
TMV	tobacco mosaic virus
TuMV	turnip mosaic virus
Tris	Tris-(hydroxymethyl)-aminomethane
Waco2	<i>Hyaloperonospora arabidopsidis</i> isolate Waco2
WT	wild-type
VPE	Vacuolar Processing Enzyme(s)



## SUMMARY

Programmed cell death (PCD) is an interesting natural phenomenon, common to many organisms. PCD has been extensively studied during animal apoptosis and several regulators have been identified. Cysteine proteases called caspases, and the proteasome were found to be main players in PCD in animals. In plants, PCD is regulated by vacuolar processing enzymes (VPEs) and the proteasome. Both proteolytic machineries exhibit caspase-like activities. In this work, the activity of VPEs and the proteasome were characterized using activity-based protein profiling (ABPP). ABPP involves fluorescent or biotinylated probes that react with the catalytic residue of proteases in an activity-dependent manner.

Specific probes that target  $\gamma$ VPE, the most abundant VPE in vegetative tissue, were selected from screen with legumain probes. Further characterization of  $\gamma$ VPE activity revealed an unexpected, post-transcriptional up-regulation of  $\gamma$ VPE activity during compatible, but not during incompatible interactions of *Arabidopsis* with *Hyaloperonospora arabidopsidis* (*Hpa*). Sporulation of *Hpa* was reduced in the absence of VPEs indicating that VPEs promote pathogen fitness. These findings introduce a new tool to study VPEs and reveal a new role of VPEs during compatible interactions.

New, selective probes that target the plant proteasome are also introduced in this thesis. The proteasome is a multi-subunit proteolytic complex containing three subunits with different catalytic activities:  $\beta$ 1,  $\beta$ 2 and  $\beta$ 5. ABPP was applied to further characterize the inhibition of the plant proteasome by Syringolin A (SylA), a non-ribosomal cyclic peptide produced by the bacterial pathogen *Pseudomonas syringae* pv. *syringae*. This work shows that SylA preferentially targets  $\beta$ 2 and  $\beta$ 5 of the plant proteasome. Structure-activity analysis revealed that dipeptide tail of SylA contributes to  $\beta$ 2 specificity and identified a nonreactive SylA derivative. The selectivity of SylA for the catalytic subunits is discussed and the subunit selectivity is explained by crystallographic data.

Importantly, it was discovered that SylA production promotes colonization of distant tissue by *Pseudomonas syringae* pv. *syringae*. SylA was found to suppress both effector-triggered immunity and salicylic acid-dependent acquired resistance. Distant colonization is a new phenomenon, common to other *P. syringae* strains, and undetected by classical pathogen assays.

## ZUSAMMENFASSUNG

Der programmierte Zelltod oder Apoptose ist ein natürliches Phänomen, das aktiv durch zelluläre Faktoren reguliert wird und zum Absterben der Zelle führt. Dieser Prozess spielt in der Entwicklung vieler Organismen eine entscheidende Rolle.

Der programmierte Zelltod tierischer Zellen wurde bereits intensiv untersucht. Dabei wurden eine Reihe von Regulatoren identifiziert, wobei Caspasen, die zu den Cystein-Proteasen gehören, und das Proteasom eine Schlüsselrolle einnehmen. In Pflanzen wird dieser Prozess durch die Vakuole prozessierende Enzyme (VPEs) und das Proteasom reguliert, wobei diese beiden proteolytische Maschinerien Caspase-ähnliche Aktivitäten aufweisen.

Im Rahmen dieser Dissertation fand mit Hilfe des so genannten *activity based protein profiling (ABPP)* eine Charakterisierung der Aktivität von VPEs und des Pflanzenproteasoms statt. ABPP nutzt fluoreszente oder biotinylierte Sonden, die mit dem katalytisch aktiven Rest der Enzyme kovalent und irreversibel reagieren, und somit die Visualisierung der Enzym-Aktivität ermöglichen.

Sonden, die spezifisch an  $\gamma$ VPE binden, dem vorherrschenden VPE in vegetativem Gewebe, wurden bei einem Screen mit Legumin Proben selektiert. Die weitere Charakterisierung der  $\gamma$ VPE-Aktivität zeigte eine unerwartete posttranskriptionale Hochregulation der  $\gamma$ VPE-Aktivität während kompatibler, aber nicht während inkompatibler Interaktionen von Arabidopsis mit *Hyaloperonospora arabidopsidis (Hpa)*. In Abwesenheit von VPEs nahm die Sporulation von *Hpa* ab. Dieses spricht dafür, dass VPEs die Fitness des Pathogens fördern. Diese Ergebnisse geben einen Hinweis darauf, dass ABPP ein sehr nützliches Werkzeug ist, um die Rolle von VPEs während kompatibler Interaktionen aufzuklären.

Des Weiteren wurden neue, selektive Sonden für das pflanzliche Proteasom identifiziert. Das Proteasom ist ein Multiproteinkomplex, welcher aus drei Untereinheiten mit unterschiedlichen katalytischen Aktivitäten besteht:  $\beta$ 1,  $\beta$ 2 and  $\beta$ 5. ABPP wurde auch hier genutzt, um eine Inhibition des pflanzlichen Proteasoms durch Syringolin A (SylA), einem nicht ribosomalen cyclischen Peptid, welches durch das bakterielle Pathogen *Pseudomonas syringae* pv. *syringae* produziert wird, nachzuweisen.

Die Ergebnisse dieser Arbeit zeigen, dass SylA vorzugsweise die  $\beta 2$  and  $\beta 5$  Untereinheiten des Proteasoms in ihrer Aktivität hemmt. Eine Struktur-Aktivitäts-Analyse mit SylA hat gezeigt, dass der Dipeptid-Rest des SylA Moleküls zu dessen  $\beta 2$  Spezifität beiträgt. Zusätzlich konnte eine nicht-reaktives Derivat identifiziert werden. Des Weiteren wurde die Selektivität von SylA für die katalytischen Untereinheiten durch Studien an Proteasommodellen verdeutlicht.

Innerhalb dieser Arbeit wird gezeigt, dass die Produktion von SylA eine Ausbreitung der Kolonisierung von Geweben durch *P. syringae* pv. *syringae* begünstigt. SylA hemmt sowohl die durch Effektoren-ausgelöste Immunität, als auch die Salicylicsäureabhängige basale Resistenz. Eine sich ausbreitende Kolonisierung ist ein Phänomen, welches auch für andere *P. syringae* Stämme beobachtet wurde, und die bis heute mit klassischen Methoden nicht detektierbar war. Die unerwartete biologische Funktion eines kleinen Effektormoleküls bietet einen wichtigen Einblick in einen ökologischen Aspekt, während der Interaktion zwischen Bakterien und Pflanzen, der bisher übersehen worden ist.



# 1 INTRODUCTION

Cell death is part of the life cycle of all living organisms. Plants and animals undergo programmed cell death (PCD) for controlling cell numbers, forming and deleting structures, and eliminating damaged cells. Three types of cell death have been recognized in animal systems, but the contribution of each pathway to PCD as well as their similarities and differences are still subject to debate.

Apoptosis is the most studied PCD in animals for which morphological, biochemical and molecular hallmarks have been defined. Apoptosis is often associated with chromatin condensation, cell shrinkage, plasma membrane blebbing, internucleosomal DNA cleavage, formation of apoptotic bodies and degradation in phagocytic lysosomes by adjacent cells (Hofius *et al.*, 2007). In contrast, autophagic cell death involves the sequestration of cytoplasmic components in double membrane vesicles, called autophagosomes, which fuse with the vacuole of lysosomes for degradation (Hofius *et al.*, 2007). The third type of cell death is called necrotic or non-lysosomal cell death which involves swelling of cells and organelles, followed by plasma membrane rupture and release of cytoplasmic material (Hofius *et al.*, 2007).

In plants, PCD is critical during development and immune responses. During development, the most predominant type of PCD is autophagic cell death (van Doorn & Woltering *et al.*, 2005). Despite the knowledge in plant PCD during development and abiotic stresses, the most well characterized form of PCD occurs during plant-pathogen interactions, the so-called hypersensitive response (HR) cell death. Different proteins are involved in PCD in animals. Caspases, a family of cysteine proteases and the proteasome, the cell degradation machinery, are main players of animal PCD. The role of these proteases in plant PCD is studied in this thesis.

## 1.1 Plant caspase-like enzymes

PCD has been extensively studied during apoptosis in animal cells with the characterization of caspases (Cysteine-containing ASpartate-specific ProteASES), a family of cysteine proteases that control PCD under stress conditions or during

development (Baehrecke, 2002). Cysteine proteases contain a catalytic cysteine (Cys) in their active site that acts as a nucleophile during proteolysis (Powers *et al.*, 2002). Based on sequence similarities and evolutionary relationships, cysteine proteases have been divided into 15 families which are grouped into five clans in the MEROPS database ([www.merops.ac.uk](http://www.merops.ac.uk)). CD clan proteases are highly selective for cleavage after specific residues: aspartic acid (Asp) for animal caspases (family C14A), arginine (Arg) for metacaspases (family C14B) and asparagine (Asn) for legumains (family C13) (van der Hoorn, 2008). Based on their biological functions, animal caspases have been subdivided in two classes: those involved in inflammation: caspases 1, 4, 5, 11, 12, 13 and 14, and in apoptosis: caspases 2, 3, 6, 7, 8, 9, and 10 (Okun *et al.*, 2006).

Although caspases have strong preferences for cleavage Asp at the P1 position, caspase substrate recognition is further determined by the substrate sequences adjacent to the cleavage site (P2-P4 positions) (Demon *et al.*, 2009). The major specificity determinant is the P4 position since most of the enzymes are promiscuous at P2 and P3 (Nicholson, 1999). For instance, based on screens using positional scanning combinatorial substrate libraries, animal caspases can be subdivided in three groups (Nicholson, 1999): Group I (caspases 1, 4, 5, and 13) prefers bulky hydrophobic amino acids at the P4 position. Group II (caspases 2, 3, and 7) requires Asp at the P4 position, consistent with the motif DExD which appears in many proteins that are cleaved during cell death. Group III (caspases 6, 8, 9 and 10) prefers branched chain aliphatic amino acids at the P4.

Many irreversible and reversible inhibitors used for the suppression of caspase-like activity are peptides that carry these residues at P4 and P1 positions and contain reactive groups such as chloromethyl ketones (-cmk), fluoromethyl ketones (-fmk) or aldehydes (-cho) (Evans & Cravatt, 2006). There are more proteases that cleave after Asp, and these have been generally named having caspase-like activity although they do not present the substrate selectivity of caspases. The  $\beta$ 1 subunit of the proteasome for example exhibits caspase 3-like activity (Groll *et al.*, 2008a). In this thesis caspase activity refers to the substrate specificity of a protease rather than its association to PCD. Caspase-like enzymes are defined as proteases that can convert caspase substrates such as DEVD (caspase-3 activity) or YVAD (caspase-1 activity) and that have sequence or structural homology to animal caspases.

There are no direct homologues of animal caspases present in plants. However, several studies in which the HR was suppressed by synthetic peptide caspase inhibitors demonstrated that proteases with caspase function that control PCD in plants exist. For instance, the irreversible caspase-1 inhibitor Ac-YVAD-cmk and the reversible caspase-3 inhibitor Ac-DEVD-cho, were found to suppress bacterial - induced PCD (del Pozo & Lam, 1998). VEIDase activity, which resembles caspase-6 activity, was implicated in plant embryogenesis (Bozhkov *et al.*, 2004). In addition, a tobacco protease with caspase specificity that cleaves *Agrobacterium tumefaciens* VirD2 protein and exhibits TATD proteolytic activity was shown to be essential for PCD-related responses to tobacco mosaic virus (TMV) and abiotic stresses (Chichkova *et al.*, 2004, Chichkova *et al.*, 2010).

Caspase-related proteins, called metacaspases, were identified by homology searches in plant databases (Uren *et al.*, 2000). Metacaspases belong to the family C14A and have been identified in plants, fungi and protozoa. The activity of Arabidopsis metacaspases depends on their catalytic cysteine, as for caspases (Watanabe & Lam, 2005). However, two Arabidopsis metacaspases, AtMCP1b and AtMCP2b, found to activate apoptosis-like cell death in yeast (Watanabe & Lam, 2005), exhibit arginine/lysine specific endopeptidase activity but not caspase-like activity, suggesting that there are other plant enzymes with caspase-like activities required to mediate cell death (Vercammen *et al.*, 2004).

Two apoplastic plant proteases involved in rubisco proteolysis, SAS-1 and SAS-2, have been identified in oat (*Avena sativa*) (Coffeen & Wolpert, 2004). SAS-1 and SAS-2 exhibit caspase specificity but display amino acid sequence homology to subtilisin-like Ser proteases. These proteases are classified as saspases in the clan SB of the MEROPS database (van der Hoorn, 2008). Furthermore, another subtilisin-like protease from tobacco and rice named phytaspase exhibits VEIDase activity, different from the Z-VAD-AFC hydrolytic activity of the two oat saspases (Chichkova *et al.*, 2010). Phytaspase are involved in the HR-response and resistance to TMV and in the cell death induced by abiotic stresses (Chichkova *et al.*, 2010).

## 1.2 Vacuolar Processing Enzymes (VPEs)

At present, the most likely proteases with caspase-like activities for execution of HR-cell death in plants are vacuolar processing enzymes (VPEs). VPEs are cysteine proteases classified in the legumain family C13 (clan CD). Legumains are lysosomal, Asn-specific endo-peptidases that in animal cells play a pivotal role in antigen processing (Kato *et al.*, 2005). VPEs share structural homology to animal caspases despite their low sequence similarities (Hofius *et al.*, 2007). For instance, VPE has specificity for P1= Asn/Asp and exhibits YVADase activity that contributes to defense against pathogens (Rojo *et al.*, 2004; Hatsugai *et al.*, 2004). Furthermore, the catalytic amino acids and surrounding motifs for caspase-1 activity are conserved in VPE (Hara-Nishimura *et al.*, 2005) and the autocatalytic conversion of functional VPE from the inactive precursor protein resembles the processing and activation of caspase-1 (Kuroyanagi *et al.*, 2002) (Fig. 1A).

Four VPE-encoding genes have been identified in *Arabidopsis*:  $\alpha$ VPE,  $\beta$ VPE,  $\gamma$ VPE and  $\delta$ VPE. These are classified into seed-type and vegetative-type (Yamada *et al.*, 2005). The seed-type  $\beta$ VPE plays a role in the maturation of seed proteins in protein storage vacuoles (Kinoshita *et al.*, 1999), while the vegetative-type  $\alpha$ VPE and  $\gamma$ VPE function in lytic vacuoles and are expressed during senescence or pathogen-induced defense response (Yamada *et al.*, 2005).  $\delta$ VPE is specifically expressed in the seed coat and regulates cell death (Nakaune *et al.*, 2005).



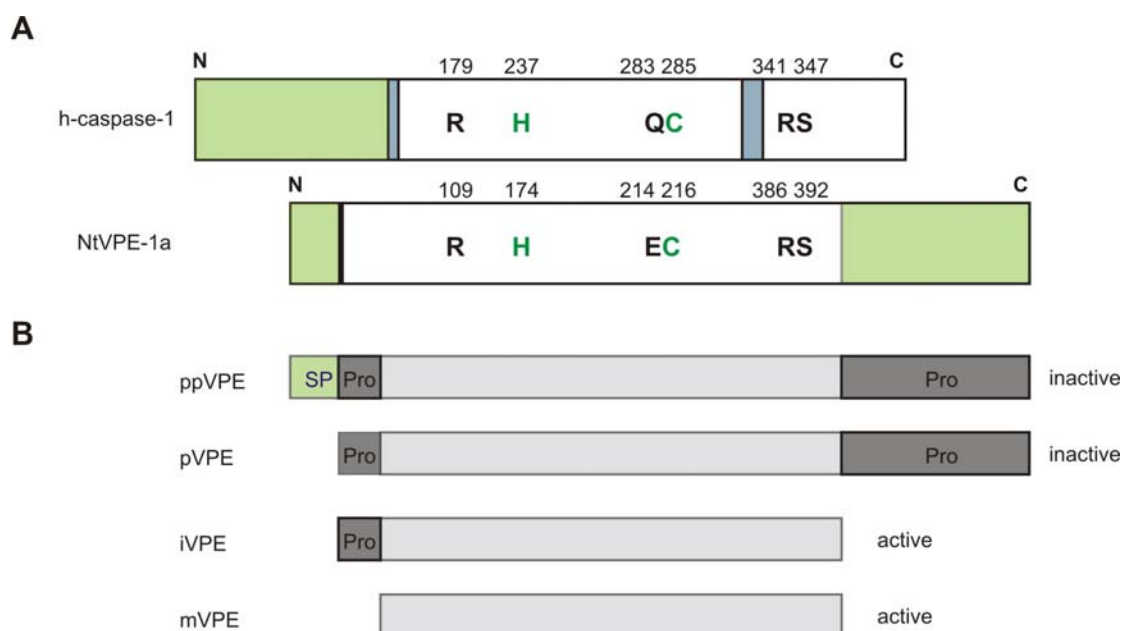


**Figure 1. Comparison of VPE with caspase-1 and VPE maturation process.**

**(A)** VPE has homology to human caspase-1. The essential amino acids between human caspase-1 (h-caspase-1) and *Nicotiana tabacum* VPE (NtVPE-1a) are conserved. His237 and Cys285 (green) form the catalytic dyad of h-caspase-1, whereas His174 and Cys216 (green) form the catalytic dyad of NtVPE-1a. Three essential amino acids, Arg179, Arg341 and Ser347, form the substrate-binding pocket of h-caspase-1. The corresponding amino acids are conserved in NtVPE-1a (adapted from Hara-Nishimura *et al.*, 2005). N and C represent the C- and N-terminus.

**(B)** Model of VPE maturation. The maturation of VPE occurs in three steps. First, the pro-protein precursor (ppVPE) is produced. ppVPE contains a signal peptide (SP) and two pro-peptides (Pro) at the N- and C-terminus of the protease. Cleavage of the SP from the ppVPE generates the pre-protein precursor (pVPE). Both forms are inactive. Under acidic conditions, sequential removal of the C- and N-terminal pro-peptide results in the immature (iVPE) and the mature (mVPE) isoforms. Both iVPE and mVPE are active (adapted from Kuroyanagi *et al.*, 2002).

VPE maturation has been elucidated by expressing Arabidopsis  $\gamma$ VPE in insect cells (Kuroyanagi *et al.*, 2002). First, an unglycosylated pre-protein precursor (ppVPE) is generated. ppVPE contains a 22-amino-acid N-terminal signal peptide that is removed to produce pVPE, a glycosylated pro-protein precursor. ppVPE and pVPE are both inactive. Under acidic conditions pVPE is self-catalytically converted into the intermediate isoform (iVPE) by removal of the C-terminal prodomain. The sequential removal of the N-terminal pro-peptide produces the mature isoform (mVPE). Both iVPE and mVPE are active (Kuroyanagi *et al.*, 2002) (Fig. 1B).

Several studies have described the function of VPE during incompatible plant-pathogen interactions. By inducing HR with tobacco mosaic virus (TMV) in *Nicotiana tabacum*, the Hara-Nishimura lab demonstrated that virus-induced HR is blocked by treatment with caspase-1 or VPE-specific inhibitors. Furthermore, VPE silencing prevents TMV-induced HR and increases virus replication (Hatsugai *et al.*, 2004). In parallel, the Raihkel lab confirmed caspase-1 activity of Arabidopsis  $\gamma$ VPE and found an early induction of  $\gamma$ VPE transcript levels upon infection with avirulent *Pseudomonas syringae* (Rojo *et al.*, 2004). Surprisingly, increased susceptibility of the  $\gamma$ vpe mutant was observed during infection with turnip mosaic virus (TuMV) and with the necrotroph pathogen *Botrytis cinerea* (Rojo *et al.*, 2004). The host cell death triggered by the fungal toxin fumosin B1 (FB1) was completely abolished in the Arabidopsis quadruple vpe mutant, which lacks all VPEs, but it was only partially suppressed in the  $\gamma$ vpe single-mutant, indicating a partial compensation of  $\gamma$ VPE by other VPEs (Kuroyanagi *et al.*, 2005). Together, these data show that VPE exhibits caspase-1 activity and is involved in the regulation of plant PCD.

### 1.3 The plant proteasome

Another protease exhibiting caspase-like activity is the proteasome, the major machinery to degrade and process damaged proteins in the cell. The 26S proteasome is a large multi-subunit protease residing in the cytosol and nucleus. It consists of a 20S core protease (CP) and a 19S regulatory particle (RP). The RP accepts ubiquitinated substrates, unfolds them and feeds them into the CP (Kurepa and Smalle, 2008). The CP is structured as a 670 kDa hollow cylinder formed by four stacked rings of seven subunits each (Groll *et al.*, 1997) (Fig. 2A). The proteolytic activity is located in the inner cavity of the cylinder and resides in three of the seven  $\beta$  subunits of the inner two rings. Subunit  $\beta$ 1 has caspase-like activity (cleaving after acidic residues);  $\beta$ 2 has trypsin-like activity (cleaving after basic residues); and  $\beta$ 5 has chymotrypsin-like activity (cleaving after hydrophobic residues) (Dick *et al.*, 1998) (Fig. 2B). Together, these subunits degrade the substrate proteins into peptides of 3-20 amino acids that are released into the cytosol or nucleus (Kurepa and Smalle, 2008).

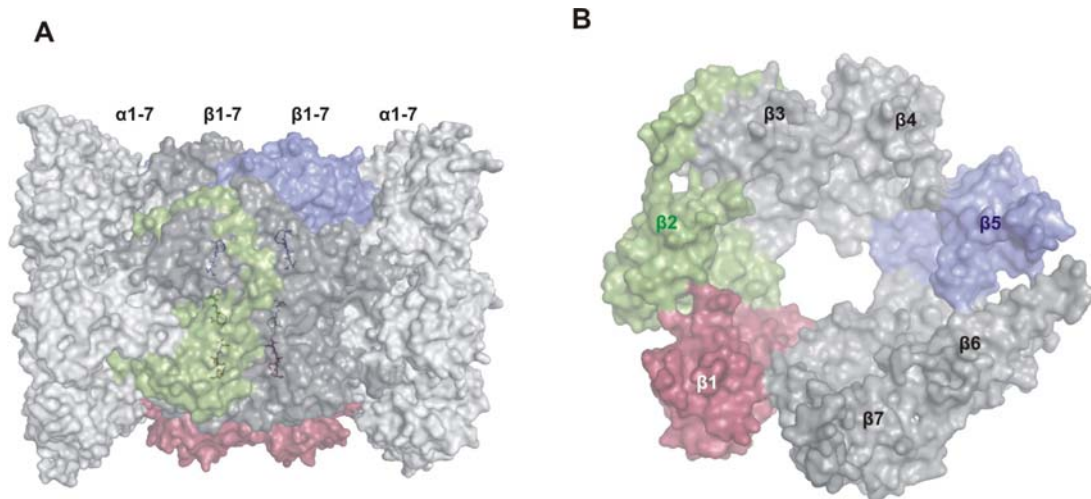


**Figure 2. Structure of the 20S core protease of the yeast proteasome.**

**(A)** The 20S core protease. The core protease of the proteasome consists of four rings of  $\alpha$  and  $\beta$  subunits: the outer rings of each seven  $\alpha$  subunits (light grey), and the inner rings of seven  $\beta$  subunits each (grey and colors).

**(B)** Position of the three catalytic subunits. One ring of seven  $\beta$  subunits shown from the side of the inner cavity contains the catalytic subunits:  $\beta 1$  (red),  $\beta 2$  (green), and  $\beta 5$  (blue).

The proteasome was recently demonstrated to play a role in HR in *Arabidopsis* infected with avirulent *P. syringae* strains (Hatsugai *et al.*, 2009). HR induced by avirulent bacteria involves the fusion of vacuolar membranes with the plasma membrane, which causes a release of the vacuolar content into the apoplast (Hatsugai *et al.*, 2009). Suppression of proteasome activity by RNA interference or proteasome inhibitors prevents membrane fusions and HR (Hatsugai *et al.*, 2009). Additionally, the proteasome is required for systemic acquired resistance (SAR), triggered by salicylic acid (SA) signaling (Spoel *et al.*, 2009). A key regulator in SA signaling and SAR is NPR1, a transcriptional co-activator of pathogenesis-related genes like *PR1* (Vlot *et al.*, 2009). Upon being phosphorylated during SA signaling, NPR1 becomes a transcriptional repressor, and proteasome-mediated degradation of phosphorylated NPR1 is required to maintain transcriptional activation of *PR1* (Spoel *et al.*, 2009).

#### 1.4 Activity-Based Protein Profiling (ABPP)

The activities of VPEs and the proteasome can be studied in plants by using activity-based probes (ABPs). ABPs are reporter-tagged inhibitors that react with active site residues of enzymes in a mechanism-dependent manner (Evans & Cravatt, 2006). ABPs are composed of three major parts: a warhead, or reactive group, the binding group and the reporter tag (Cravatt *et al.*, 2008). The warhead is designed to react with the active site-residue of enzymes resulting in the formation of a stable covalent bond. The reporter tag facilitates the display of labeled enzymes on protein gels, and/or the identification of labeled proteins by affinity capture and mass spectrometry (Sadaghiani *et al.*, 2007). Because probes only bind to active forms of enzymes, ABPs can be used as an indirect measurement of enzyme activities.

Activity-based protein profiling (ABPP) is a powerful tool to study the availability of active sites of proteins. ABPP has been extensively used in the animal field to study diverse protease families. For example, activities of most serine proteases can be profiled using FP probes (Liu *et al.*, 1999), whereas papain-like cysteine proteases (PLCPs) can be profiled using DCG-04 (Greenbaum *et al.*, 2000). DCG-04 is a biotinylated derivative of the wide range cysteine protease inhibitor E-64 (Greenbaum *et al.*, 2000). Six PLCPs has been identified in Arabidopsis leaf extracts using DCG-04 (van der Hoorn *et al.*, 2004), however none of the identified proteins belong to the CD clan. This can be explained by the lack of a P1 residue in DCG-04. Specific probes containing an aza-aspartate at the P1 position and either epoxide or michael acceptor warheads can potently label caspases (Sexton *et al.*, 2007). Additionally, probes with acyloxymethyl ketone (AOMK) warheads carrying P1 residues are selective for cysteine proteases (Kato *et al.*, 2005).

Proteasome activity profiling has been previously described with MV151, a fluorescent vinyl sulfone probe that targets the catalytic subunits of the proteasome in living cells (Verdoes *et al.*, 2006). Recently, proteasome activity profiling with MV151 has been introduced in plants. MV151 labels the  $\beta$ 1,  $\beta$ 2, and  $\beta$ 5 subunits of the Arabidopsis proteasome but also several PLCPs (Gu *et al.*, 2010). In search of more selective and specific proteasome inhibitors, probes

based on epoxomicin are strong candidates. The  $\alpha$ - $\beta$ -epoxyketone of epoxomicin forms an irreversible morpholino bond with the N-terminal catalytic threonine, making it highly specific for the small class of N-terminal nucleophilic hydrolases (Groll *et al.*, 2008a). Thus, epoxomicin does not react with PLCPs because the catalytic cysteine is not at the N-terminal position.

In this work, ABPP has been introduced to monitor the activity of VPEs and the proteasome during plant-pathogen interactions. VPE activity is studied during compatible interactions with *Hyaloperonospora arabidopsidis* whereas proteasome activity is monitored during infection with *Pseudomonas syringae*.

### 1.5 The natural interaction Arabidopsis - *Hyaloperonospora arabidopsidis*

*Hyaloperonospora* is a genus of downy mildews belonging to the class of oomycetes and the kingdom Stramenopiles, which makes it more closely related to brown algae and diatoms than to true fungi (Coates & Beynon, 2010). The species *Hyaloperonospora arabidopsidis* (*Hpa*) (formerly, *Peronospora parasitica*) is a highly specialized biotroph that cannot exist outside of its intimate association with the model plant *Arabidopsis thaliana* (Slusarenko & Schlaich, 2003). Different isolates have been identified to be pathogenic on different ecotypes of *A. thaliana* (Holub *et al.*, 1993) but not on other crucifers (Slusarenko & Schlaich, 2003). Pathogen races are named according to the geographic location and the ecotype they are found on. For example, isolate WELA derives from Weiningen and was found to be virulent on ecotype Landsberg *erecta*. NOCO was isolated in Norwich and is virulent on Columbia, EMWA is from East Malling and is virulent on Wassilewskija (Slusarenko & Schlaich, 2003).

During *Hpa* infections, incompatible interactions occur in a gene-for-gene dependent manner. This recognition triggers a typical HR cell death response accompanied by deposition of callose that varies in severity depending on the race-ecotype interaction (Soylu *et al.*, 2004). In compatible combinations, the degree and rate of colonization and sporulation also differs in a genotype-interaction specific manner (Rethage *et al.*, 2000). The timing and degree of asexual reproduction by *Hpa* varies depending on the host, providing an indirect assessment of pathogen colonization (Holub *et al.*, 1994).

To date several resistance genes that recognize *Hpa* avirulent proteins (*RPP* genes, for recognition of *Peronospora parasitica*) have been identified in *Arabidopsis* (Holub *et al.*, 1994). Many of the *RPP* genes are organized in clusters and recognize different pathogens. For example, *RPP8* confers resistance to cucumber mosaic virus and to turnip crinkle virus (Coales & Beynon, 2010). In contrast, little is known about the corresponding avirulent proteins of *Hpa*. Two *ATR* (*Arabidopsis thaliana* recognized) genes have been identified, *ATR1* and *ATR13* that are recognized by *RPP1* and *RPP13* respectively (Allen *et al.*, 2004; Rehmany *et al.*, 2005). Evidence of diversifying selection reported for *RPP13* and *ATR13* suggests that *Arabidopsis* and *Hpa* are locked in a co-evolutionary conflict (Allen *et al.*, 2004).

## 1.6 The model pathogen *Pseudomonas syringae*

*Pseudomonas syringae* is a Gram-negative bacterial pathogen capable of infecting hundreds of taxonomically diverse plant species and causing symptoms ranging from leaf spots to stem cancers (Hirano and Upper, 2000). Intensive studies have revealed many aspects of how the model plant pathogen *P. syringae* pathovar (pv.) *tomato* DC3000 interacts with its hosts, tomato and *Arabidopsis* (Katagiri *et al.*, 2002; Greenberg and Vinatzer, 2003; Melotto *et al.*, 2008; Jones and Dangl, 2006). Detection of pathogen-associated molecular patterns (PAMPs, e.g. bacterial flagellin) via pattern recognition receptors activates PAMP-triggered immunity (PTI). *P. syringae* suppresses PTI using effector proteins that are injected into the host through the type-III (T3) secretion system (Jones and Dangl, 2006, Guo *et al.*, 2009; Cunnac *et al.*, 2009). Resistant plants are able to directly or indirectly detect some effectors through the action of resistance (R) proteins, and thereby activate effector-triggered immunity (ETI). The immune response triggered by ETI is similar to that of PTI, but it is faster, more intense, and frequently includes HR (Jones and Dangl, 2006).

*Pseudomonas syringae* pv. *syringae* (*Psy*) B728a causes bacterial brown spot on bean plants. Brown spot is an economically important disease that has been studied intensively with respect to its ecology and epidemiology (Hirano and Upper, 2000). *Psy* can grow epiphytically on the leaf surface in aggregates consisting of millions of cells that are protected against low humidity (Monier and

Lindow, 2003). In the field, *Psy* is dispersed over the leaf surface by heavy rainfall, and enters the leaf tissue through stomata and wounds (Hirano *et al.*, 1996). *Psy* is able to create wounds at low temperatures using ice nucleation proteins that cause frost damage (Cochet and Widehem, 2000). Upon entering the plant, *Psy* propagates initially biotrophically, keeping the host cells alive, and later necrotrophically, causing host cell death (Greenberg and Yao, 2004). The genome of *Psy* B728a has been sequenced (Feil *et al.*, 2005), and some of its T3 effectors have been found to trigger cell death, whereas others prevented cell death (Vinatzer *et al.*, 2006).

*Psy* B728a and B301D-R secrete syringolin A (SylA) (Wäspi *et al.*, 1998), a small non-ribosomal cyclic peptide that covalently and irreversibly inhibits the eukaryotic proteasome (Groll *et al.*, 2008b). SylA is a non-ribosomal cyclic peptide that contributes to the development of disease symptoms (Groll *et al.*, 2008b). SylA is a 493 Da molecule that consists of a 12-atom macrocyclic lactam and a dipeptide tail (Wäspi *et al.*, 1999). The lactam ring contains an  $\alpha,\beta$ -unsaturated amide and a second double bond. This second unsaturated bond is absent in SylB, a minor, additional metabolite produced by *Psy* (Wäspi *et al.*, 1999). The dipeptide tail contains two L-valines, linked through an ureido bond. SylA is produced by *Psy* by non-ribosomal peptide and polyketide synthetases encoded by the *syIC* and *syID* biosynthesis genes and presumably secreted from bacteria by the product of *syIE*, which encodes a transporter-like protein (Amrein *et al.*, 2004; Ramel *et al.*, 2009; Imker *et al.*, 2009).

Crystallographic data revealed that the  $\alpha,\beta$ -unsaturated amide of SylA is attacked by the N-terminal threonine of the catalytic  $\beta$  subunits, resulting in an irreversible, covalent ether bond (Groll *et al.*, 2008b). Further studies showed that SylA has anti-apoptotic properties in mammalian cells and is therefore a promising novel anti-cancer drug, having different properties when compared to e.g. bortezomib, a proteasome inhibitor that is currently in clinical trials as anti-cancer drug (Coleman *et al.*, 2006; Clerc *et al.*, 2009a).

## 1.7 Aim and outline of the thesis

The aim of this work is to study the activities of VPEs and the proteasome during plant-pathogen interactions. These topics are introduced in chapter I. Chapter II describes the result section of VPEs and the proteasome. The first part introduces a new approach to detect the activity of VPEs in plants. Legumain probes were tested on plant extracts and three probes were selected. Optimal labelling conditions were determined and labeled proteins were identified through mutant analysis, transient overexpression and mass spectrometry. These experiments revealed that VPEs are targeted by legumain probes and that  $\gamma$ VPE is the main target in *Arabidopsis* leaf extracts. In the last part of this chapter the activity of  $\gamma$ VPE was monitored during infections with compatible and incompatible isolates of *Hpa* in *Arabidopsis*. Unexpectedly, an increased activity of  $\gamma$ VPE during compatible interactions was discovered. The relevance of this increment is further discussed in chapter III.

Proteasome labelling and the role of SylA were studied in the second part of chapter II using new selective probes based on the proteasome inhibitor epoxomicin. Comparisons between epoxomicin and SylA reveal a similar inhibitory strength but different subunit specificity. Further characterization of SylA using structure-activity relationship studies revealed the importance of the main components of SylA. Furthermore, labelling of *N.benthamiana* leaves challenged with different *P. syringae* strains, demonstrated that *Psy* B728a inhibits the host proteasome during infection. Experiments with the SylA-deficient mutant strain of *Psy* B728a revealed that SylA deficiency triggers early host cell death induced by bacterial type III effectors. SylA production promotes distant colonization. This phenomenon was investigated with GFP-expressing bacteria using tooth-pick inoculations. While addressing the mechanism of action of SylA it was noticed that cell death and distant colonization are unrelated and are strain-dependent. Chapter III discusses a new ecological aspect of the life cycle of *P. syringae* and the importance of the small effector molecule SylA for this pathogen.



## 2 RESULTS

### 2.1 VACUOLAR PROCESSING ENZYMES

#### 2.1.1 Screening of legumain probes on pumpkin seed extracts

Pumpkin seeds are known to contain a high amount of legumain proteases called Vacuolar Processing Enzymes (VPEs) (Hara-Nishimura *et al.*, 1998). Protein bodies from pumpkin seeds were isolated by using a nonaqueous isolation method described previously (Hara-Nishimura *et al.*, 1982) and extracts were analyzed by coomassie blue staining. Two major bands at 38 and 40kDa were visualized (Fig. 1A). In collaboration with Mathew Bogyo Lab at Stanford Medical School a screen of pumpkin seed extract with a series of legumain and caspase probes was performed. Pumpkin seed extracts were tested with nine probes containing different reactive groups and reporter tags at vacuolar pH 5 and cytosolic pH 7. Six probes caused two major bands at pH 5 that were visualized by in-gel fluorescent scanning (Fig. 1B). These signals correspond to the two bands stained with coomassie (Fig. 1A). AMS-101 showed the most intense signals at pH 5 (Fig. 1B) while probes AB13, AB46 and AB50 displayed similar labelling patterns but the signal intensity was lower compared to AMS-101 (Fig. 1B). The biotinylated probes JCP550 and D-AOMK did not show specific signals on streptavidin-HRP blots and therefore those probes were not used for further experiments (data not shown). Probes AB53, AB69 and AMS-101 were selected due to the high signal intensities and similar labelling pattern. AB53 and AB69 contain an AOMK reactive group and the fluorescent reporter tag Cy5 (Fig. 1C). AMS-101 contains an aza-epoxide reactive group and a Bodipy fluorescent tag (Fig. 1C). The aza-epoxide warhead from AMS-101 has been reported to efficiently label legumains (Sexton *et al.*, 2007). One should note that all these probes contain an asparagine or aspartic acid adjacent to the warhead according to the requirement of caspases. The probes with highest signal intensities have a

## RESULTS

proline at the P2 position. AMS-101 and AB69 do not have an amino acid at the P3 position, whereas AB53 contains a non natural amino acid (Appendix A).

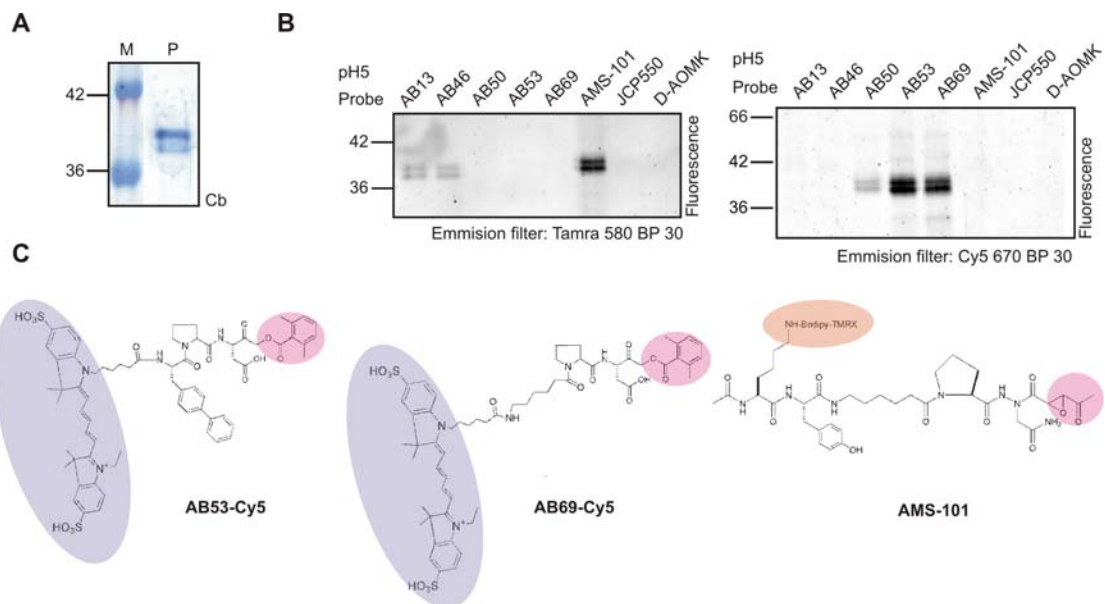


**Figure 1. Screening of legumain probes on pumpkin seed extracts.**

**(A)** Protein extract from pumpkin seeds (P). Sample was separated on protein gel and stained with coomassie blue (Cb). Two major proteins at 38 and 40 kDa were visualized. M: protein marker.

**(B)** Labelling of pumpkin seed extracts. Protein bodies from pumpkin seeds were isolated as described before (Hara-Nishimura *et al.*, 1982). Pumpkin seed extracts were incubated with different legumain probes at pH 5 for 2h. Samples were analyzed by in-gel fluorescence scanning with the emission filter Tamra (580 BP 30) or Cy5 (670 BP30) depending on the fluorescent tag of the probe. Three probes show an intense signal and were selected for further experiments.

**(C)** Structures of the three selected probes. The probes contain a reactive group (pink) and a fluorescent reporter tag Cy5 (purple) or Bodipy (orange).

### 2.1.2 Legumain probes target mainly $\gamma$ VPE

In order to identify the target of the selected probes, activity-based protein profiling was performed on leaf extracts of different *Arabidopsis* mutants. Two cysteine proteases, RD21 (Responsive to Dessication-21) and  $\gamma$ VPE, are known to be present in *Arabidopsis* precursor protease vesicles (PPVs) (Rojo *et al.*, 2003) and four VPE encoding genes have been identified in *Arabidopsis*:  $\alpha$ VPE,  $\beta$ VPE,  $\gamma$ VPE and  $\delta$ VPE (Shimada *et al.*, 2003).  $\alpha\beta\gamma\delta$ -KO is a quadruple *vpe* mutant lacking all four VPEs identified in *Arabidopsis* (Gruis *et al.*, 2004).  $\gamma$ -KO is a single *vpe* knock-out mutant and  $\gamma$ -OE is a 35S:: $\gamma$ VPE overexpressor line (Rojo *et al.*,

2004). The *ra* double mutant was used as a control since *ra* lacks both vacuolar cysteine proteases RD21 and AALP (Arabidopsis Aleurain-Like Protein). All Arabidopsis lines are in the Col-0 background. Labelling experiments on leaf extracts showed two signals in wild-type Col-0 plants (Fig. 2A). These signals were absent in both the quadruple *VPE* knock-out line and the  $\gamma$ *VPE* knock-out line (Fig. 2A) indicating that the signal originates from  $\gamma$ *VPE*. Over-expression of  $\gamma$ *VPE* results in increased labelling (Fig. 2A). In some cases, low intensity signals remain in the  $\gamma$ -KO. Those could represent  $\alpha$ *VPE*, the other vegetative *VPE*. The relatively low signal intensity in the Col-0 suggests that  $\gamma$ *VPE* is a low abundant protein or at least presents low reactivity under *in vitro* conditions (Fig. 2A). All three probes behave similarly (Fig. 2A). The presence of the signal in the *ra* mutant and the absence in the  $\alpha\beta\gamma\delta$ -KO showed how specific the probes are for *VPE*s since they do not label other cysteine proteases. These data indicate that AB69, AB53 and AMS-101 target  $\gamma$ *VPE* in Arabidopsis leaf extracts.

To further validate the target of the probes, all four Arabidopsis *VPE*s were cloned behind a 35S constitutive promoter in the T-DNA of a binary plasmid (Kaschani, unpublished). *Agrobacterium* cultures carrying these plasmids were infiltrated into *N. benthamiana* leaves for transient overproduction of each *VPE*. Protein extracts of *VPE* over-expressing leaves were incubated with AMS-101 and analyzed by in-gel fluorescent scanning. AMS-101 is able to label all four Arabidopsis *VPE*s (Fig. 2B).  $\alpha$ *VPE* labelling results in two major signals at 42 and 45 kDa.  $\beta$ *VPE* presents two strong signals at 35 and 46 kDa.  $\gamma$ *VPE* labelling correlates with previous results and the strongest signals are at 40 and 43 kDa, however two other low intensity signals appear at 38 and 30 kDa. Labelling of  $\delta$ *VPE* results in two bands at 38 and 40kDa (Fig. 2B).

To certify the identity of the probe target, mass spectrometry analysis was performed. Arabidopsis leaf extracts of  $\gamma$ -OE were labelled with *VPE*-B and *VPE*-R, two versions of AB69 containing the reporter tags biotin and rhodamine, respectively (Fig. 2C). A no-probe sample was used as the negative control. Biotinylated proteins were purified using streptavidin agarose beads from both the *VPE*-B labelled proteome and the no-probe control. Samples were separated on a protein gel flanked by leaf extracts labelled with *VPE*-R. The gel region of the purified proteins that were at the same height as the signals given by the fluorescent probe was excised and in-gel tryptic digest was performed. Four

peptides, specific for  $\gamma$ VPE, were identified in the MS analysis (Fig. 2D & appendix B). None of these peptides were found in the no-probe control. These data confirm that the main target of the probes in Arabidopsis leaves is  $\gamma$ VPE. (Gerrit Toenges, Farnusch Kaschani & Sherry Niessen).

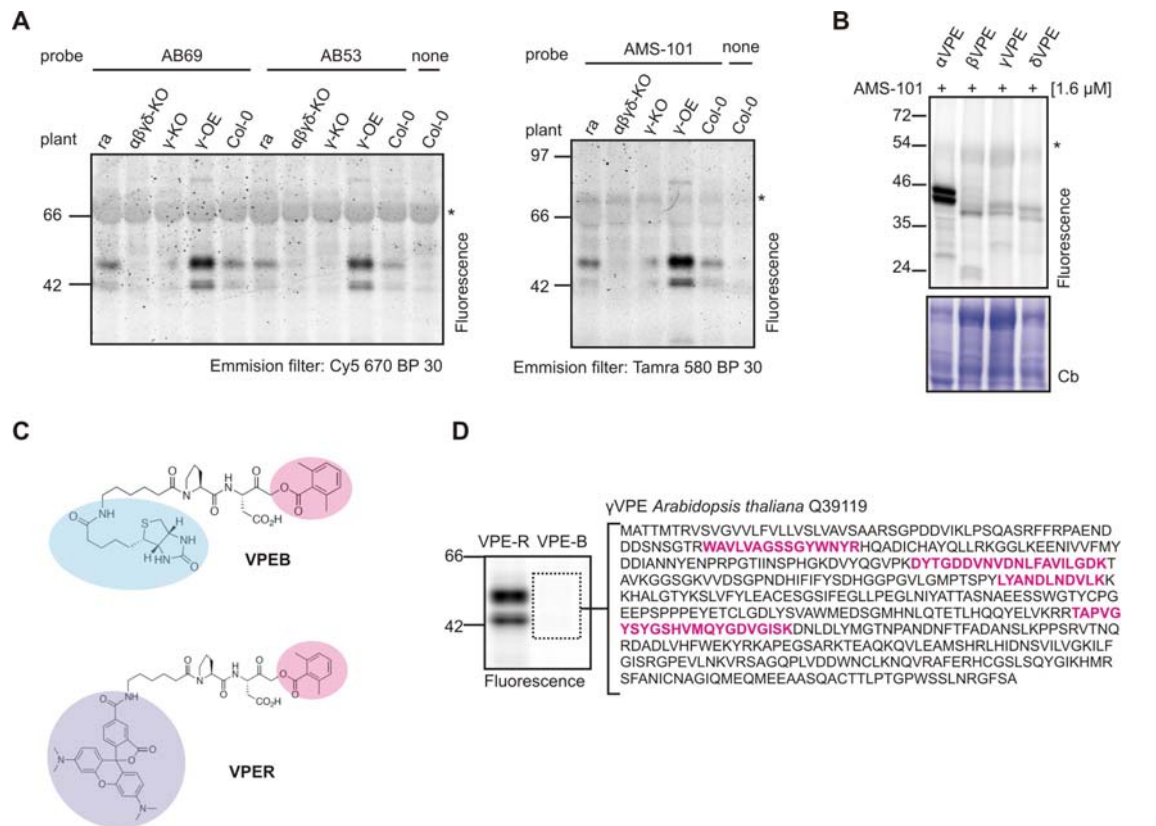


**Figure 2. Legumain probes target  $\gamma$ VPE in Arabidopsis leaves**

**(A)** Genetic evidence of the probe target. Leaf extracts of Arabidopsis  $\gamma$ -KO and  $\gamma$ -OE mutants were labeled for 2h at pH 5 with  $1\mu\text{M}$  probe. *ra*: double *rd21* and *aalp* knock-out,  $\alpha\beta\gamma\delta$ -KO: quadruple *vpe* knock-out,  $\gamma$ -KO: single *\gamma vpe* knock-out,  $\gamma$ -OE: *\gamma vpe* overexpressor, Col-0: wt control. \* unspecific signal.

**(B)** AMS-101 labels all four Arabidopsis VPEs.  $\alpha$ VPE,  $\beta$ VPE,  $\gamma$ VPE and  $\delta$ VPE from Arabidopsis were overexpressed in *Nicotiana benthamiana* by agroinfiltration (by Farnusch Kaschani & Bikram Pandey). Proteins were extracted and labeled at pH 5.5 with  $1.6\mu\text{M}$  AMS-101 for 2h. Samples were analyzed on protein gel with fluorescence scanning and coomassie staining (Cb).

**(C)** Structures of VPE-R and VPE-B probes. Analogs of AB69 were synthesized with different reporter tags. Probes exhibit a reactive group (pink) and the reporter tag biotin (blue) or Rhodamine (purple).

**(D)** Confirmation of labelling of  $\gamma$ VPE by mass spectrometry. Leaf extracts of Arabidopsis  $\gamma$ -OE were labeled with VPE-B and biotinylated proteins were purified. Sample was loaded on a gel flanked by VPE-R and scanned for fluorescence. The region next to the VPE-R fluorescent signal was excised and Mass Spectrometric analysis (MS) on tryptic digest was performed. Four unique peptides corresponding to  $\gamma$ VPE were identified (colored). Three peptides were identified once (red) and one peptide was identified six

times (purple). This experiment was performed by Gerrit Tonges, Farnusch Kaschani & Sherry Niessen.

In conclusion, by using three different approaches it was confirmed that AB53, AB69 and AMS-101 target VPEs in Arabidopsis. Of all VPEs,  $\gamma$ VPE is the most expressed in leaf tissue (Kinoshita *et al.*, 1999) and therefore causes the main signal in leaf extracts.

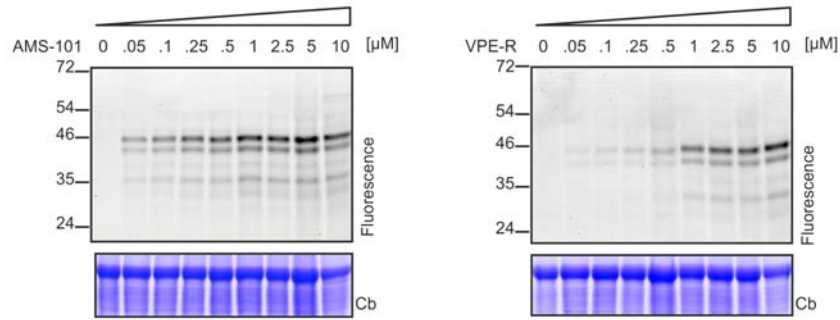
### 2.1.3 Labelling conditions

In order to characterize the optimal probe concentration, leaf extracts of  $\gamma$ -OE plants were labelled with different concentrations of AMS-101 or VPE-R. The two probes differ in signal intensity (Fig. 3A) but the concentration for maximal labelling is the same (Fig. 3B). AMS-101 reaches maximal labelling at 1  $\mu$ M, whereas VPE-R needs 10  $\mu$ M or even more to reach maximal labelling in 2h. A competition assay was performed in order to confirm that VPE-B targets the same protein as AMS-101 and VPE-R. VPE-B competes with AMS-101 and VPE-R for labelling, indicating that  $\gamma$ VPE is the main target of these probes (Fig. 3B). The fact that VPE-B suppresses VPE-R labelling more than AMS-101 indicates that AMS-101 has a higher affinity for VPE when compared to VPE-R.

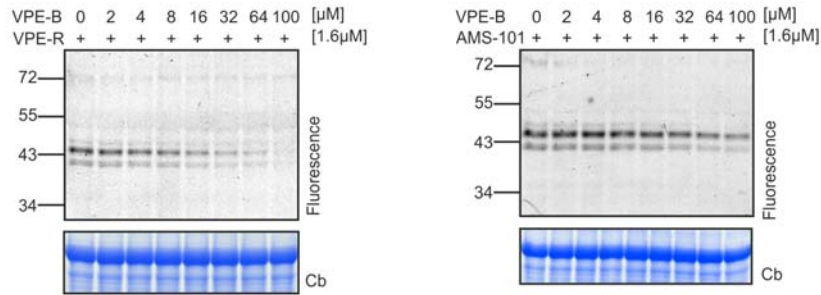
VPE is a vacuolar protein, so it is expected that the optimum pH for its activity is in the acidic range. Labelling with the probes AMS-101 and VPE-R at different pH showed that the maximum  $\gamma$ VPE labelling is around pH 5 - 5.5 (Fig. 3C).  $\gamma$ VPE is hardly labelled at neutral pH, consistent with its physiological environment.

## RESULTS

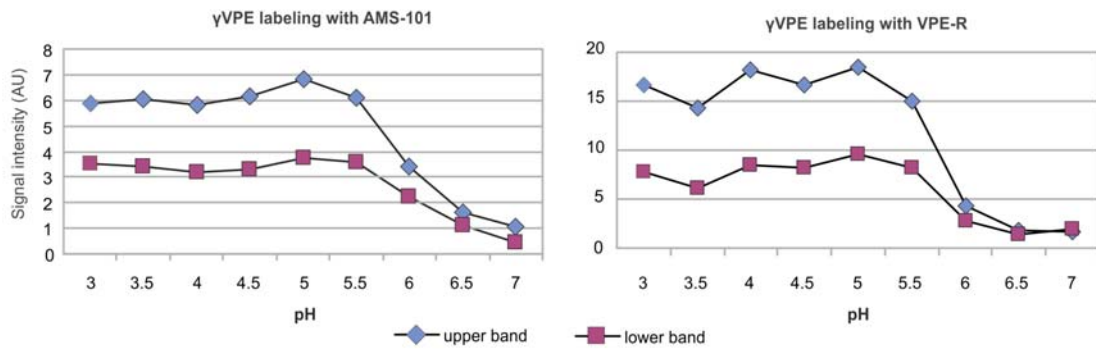
**A**



**B**



**C**



**D**

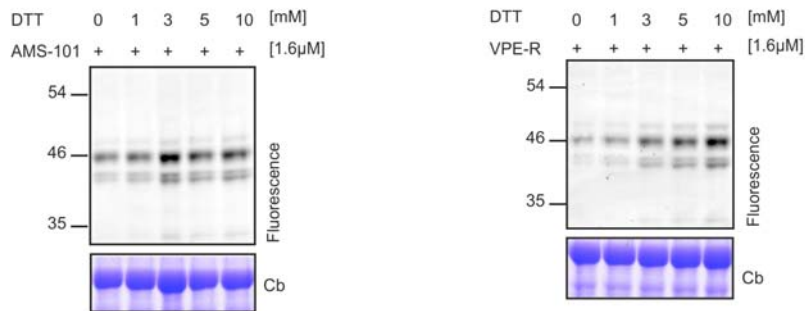


**Figure 3. Characterization of labeling conditions**

**(A)** Labelling with various probe concentrations. Leaf extracts of Arabidopsis  $\gamma$ -OE were incubated with different probe concentrations for 2h at pH 5.5. Samples were analyzed on protein gel with fluorescence scanning and coomassie blue staining (Cb).

**(B)** VPE-B competes on VPE-R and AMS-101 labelling. Leaf extracts of Arabidopsis  $\gamma$ -OE were pre-incubated for 30min with different VPE-B concentrations followed by 2h labelling at pH 5.5 with 1.6μM VPE-R (left panel) or AMS-101 (right panel). Samples were analyzed on protein gel with fluorescence scanning and coomassie staining (Cb).

**(C)** Vacuolar pH is optimum for labelling. Leaf extracts of Arabidopsis  $\gamma$ -OE were incubated at different pH and labeled for 2h with AMS-101 or VPE-R. Samples were analyzed on fluorescent protein gel. Two major signals at around 43 kDa, upper and lower band, were quantified and plotted. pH 5 - 5.5 is the optimum labelling pH for the probes AMS-101 and VPE-R. Experiment made by Gerrit Toenges (Internship).

**(D)** DTT increases VPE labelling. Leaf extracts of Arabidopsis  $\gamma$ -OE were labeled at pH 5.5 for 2h with 1.6 $\mu$ M AMS-101 or VPE-R at different DTT concentrations. Samples were analyzed on fluorescent protein gel and stained with coomassie blue (Cb). Experiment made by Gerrit Toenges (Internship).

Reducing conditions may assist *in vitro* labelling reactions and thereby improving signal intensities. The most common used reducing agent is dithiothreitol (DTT), an unusual strong redox agent due to its high propensity to form a six-membered ring with an internal disulphide bond. Higher concentrations of DTT can prevent inactivation of enzymes by spontaneous oxidation of cysteine residues (Okun *et al.*, 2006). By using different concentrations of DTT it was found that higher DTT concentrations improve *in vitro* labelling of  $\gamma$ VPE (Fig. 3D). In fact, maintaining a reducing environment might preserve  $\gamma$ VPE on its active state and consequently preventing or reverting the oxidation of the catalytic cysteine residue. L-cysteine also improves labelling (data not shown) and has been used for further experiments.

Altogether, AMS-101 showed better labelling than VPE-R and is an excellent tool to characterize  $\gamma$ VPE activity in plant extracts. Ideal labelling conditions are at pH 5 – 5.5 with 1 $\mu$ M AMS-101. Addition of a reducing agent like DTT or L-cysteine improves *in vitro* labelling.

#### 2.1.4 Characterization of VPE inhibitors

VPE is a caspase-like cysteine protease containing a nucleophilic cysteine. The most common inhibitor of cysteine proteases is E-64 (Barret *et al.*, 1982). However, pre-incubation with E-64 does not prevent  $\gamma$ VPE labelling by AMS-101 (Fig 4A lane 2). Several commonly used inhibitors for other types of proteases were also tested such as proteasome inhibitors epoxomicin and MG132. Epoxomicin was isolated from an *Actinomycetes* strain and is highly specific for the proteasome due to its  $\alpha',\beta'$ -epoxyketone “warhead” (Dick *et al.*, 1998). MG132 is a synthetic peptide aldehyde and one of the most frequently used proteasome inhibitors (Borissenko & Groll, 2007). N3 $\beta$ 1 is a selective  $\beta$ 1 proteasome inhibitor containing an epoxy-ketone analog (Ac-APnLL-ek) “warhead” (Britton *et al.*, 2008). All these three proteasome inhibitors block caspase-like activity of the proteasome, but none of them prevents labelling of  $\gamma$ VPE by AMS-101 (Fig 4A, lanes 1, 3, and 4). DEVD-cho is a reversible commonly used aldehyde-based caspase-3 inhibitor (Mashima *et al.*, 1995) that does not prevent labelling of  $\gamma$ VPE neither (Fig. 4A, lane 5). In contrast, YVAD-cmk, a covalent irreversible chloromethylketone-based caspase-1, 4 and 5 inhibitor (del Pozo & Lam, 1998) competes with AMS-101 labelling (Fig. 4A, lane 6). Furthermore, the AOMK legumain inhibitor xxAD also prevents VPE labelling (Fig 4A, lane 7). These data indicate that  $\gamma$ VPE can be inhibited by caspase-1 inhibitors. Interestingly, the different inhibitory abilities between DEVD and YVAD suggest that the P2 position might play an important role for the inhibitor recognition by  $\gamma$ VPE.



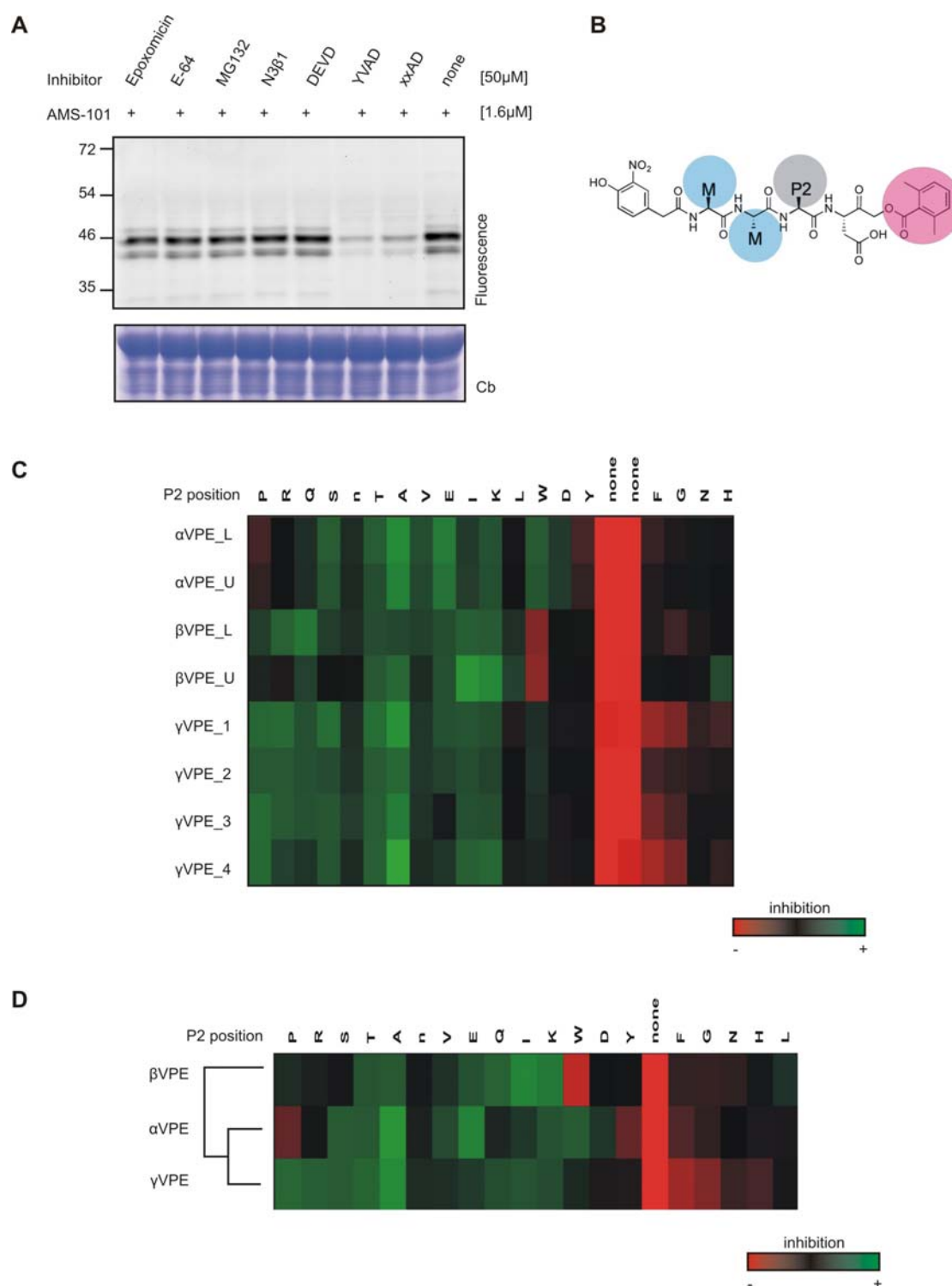


**Figure 4. Inhibition of VPE labeling.**

**(A)** Screening for VPE inhibitors. Leaf extracts of Arabidopsis  $\gamma$ -OE were pre-incubated for 30min with 50 $\mu$ M of the commonly used proteasome inhibitors epoxomicin, MG132 and N3 $\beta$ 1; E-64 cysteine protease inhibitor, DEVD-cho reversible caspase-3 inhibitor, YVAD-cmk covalent irreversible caspase-1 inhibitor and the irreversible legumain inhibitor xxAD (AOMK). After pre-incubation 2h labelling with 1.6 $\mu$ M AMS-101 was performed. Inhibition by YVAD and xxAD suggests that the P2 position plays a pivotal role for the specificity. Experiment made by Gerrit Toenges (Internship).

**(B)** Structure of the inhibitor library. The P1 position directly adjacent to the reactive AOMK group (pink) was held constant as aspartic acid. The P2 position (grey) corresponds to a fixed natural amino acid, a total of 19 excluding cysteine and methionine but including norleucine. P3 and P4 positions (blue) contain isokinetic mixtures of natural amino acids. Scheme modified from Berger *et al.*, 2006. P2 library was provided by Matt Bogyo (Stanford Medical School).

**(C)** Inhibitory profile for  $\alpha$ VPE,  $\beta$ VPE and  $\gamma$ VPE. Arabidopsis VPEs were over-expressed by agroinfiltration in *Nicotiana benthamiana*. Leaf extracts of over-expressed  $\alpha$ VPE,  $\beta$ VPE and  $\gamma$ VPE were pre-incubated with the P2 inhibitor library followed by 2h labelling with 1.6  $\mu$ M AMS-101. Samples were monitored by in gel fluorescent scanning.  $\alpha$ VPE and  $\beta$ VPE showed two bands: upper (U) and lower (L) at around 41KDa. For  $\gamma$ VPE four bands (1-4) were analyzed. Signal intensities were quantified and plotted in a heat map. Sample normalization was performed by using the internal control (DMSO + 1.6  $\mu$ M AMS-101). Green: inhibition, Red: no inhibition. None: internal control. These data correspond to a single experiment.

**(D)** Substrate selectivity of  $\alpha$ VPE,  $\beta$ VPE and  $\gamma$ VPE. An average value for the different signals analyzed by fluorescent scanning in (C) was generated. Values were plotted in a heat map and proteins were clustered according to their inhibitory profile.  $\alpha$ VPE and  $\gamma$ VPE are more closely related, based on similar P2 selectivity, than  $\beta$ VPE. Green: inhibition, Red: no inhibition. None: internal control (DMSO + 1.6  $\mu$ M AMS-101).

To verify the significance of the P2 position for the inhibition of VPEs, a P2 AOMK library of 19 compounds was screened for inhibiting labelling of  $\alpha$ VPE,  $\beta$ VPE and  $\gamma$ VPE over-expressed by agroinfiltration. VPEs exhibit substrate specificity towards an asparagine residue at the P1 position and this amino acid is conserved in the processing sites of storage protein precursors in many plant species (Gruis *et al.*, 2004). Therefore, in this library the P1 position was fixed as asparagine (N). In total 19 amino acids were used at the P2 position excluding cysteine and methionine, but including nor-leucine. The P3 and P4 positions were occupied by a mixture of amino acids (Fig. 4B).

A competitive assay was performed by pre-incubating for 30 min with 50  $\mu$ M of the compound followed by 2h incubation with AMS-101. For  $\alpha$ VPE and  $\beta$ VPE, two major bands were observed after in gel fluorescence scanning in the non-inhibited control. The signal intensity of both the lower (L) and the upper band (U), was quantified and visualized in a heat-map (Fig. 4C). Four bands were visualized and quantified for  $\gamma$ VPE. Two major bands at 45 and 43 kDa, referred as  $\gamma$ VPE\_1 and  $\gamma$ VPE\_2, respectively, and two lower bands at 35 and 33 kDa designated  $\gamma$ VPE\_3 and  $\gamma$ VPE\_4, respectively. The inhibitory profile for bands on gel appears similar within VPE types (Fig. 4C). Therefore, for each VPE type average of signal

intensity was calculated and plotted in a heat-map (Fig. 4D). Clustering analysis reveal inhibitory characteristic shared by the different VPE forms. The vegetative forms  $\alpha$ VPE and  $\gamma$ VPE cluster together in the heat-map, suggesting that both proteases have almost the same target affinity and that Alanine (A) at the P2 position is preferred. However, different from  $\gamma$ VPE,  $\alpha$ VPE prefers glutamic acid (E) and is sensitive for proline (P) at P2. In contrast to both  $\alpha$ VPE and  $\gamma$ VPE,  $\beta$ VPE favours isoleucine (I) and dislikes tryptophane (W) at P2, suggesting an affinity for different substrates (Fig 4D).

In conclusion, all three VPEs differ in their inhibitory profile and the P2 position plays an important role in their substrate selectivity.

### 2.1.5 $\gamma$ VPE labelling increases upon *Hpa* infection

$\gamma$ VPE contributes to defense against pathogens (Rojo *et al.*, 2004) and is involved in virus-induced hypersensitive cell death (Hatsugai *et al.*, 2004). To further investigate the role of  $\gamma$ VPE during infection, Arabidopsis plants were sprayed with benzothiadiazole (BTH) or challenged with the bacterial pathogen *Pseudomonas syringae* pv. tomato (*Pst*) or the oomycete pathogen *Hyaloperonospora arabidopsidis* (*Hpa*). Arabidopsis *sid2* mutants, impaired in the salicylic acid biosynthesis, are highly susceptible to *Pst* (Nawrath & Métraux. 1999). *sid2* mutant plants were spray-inoculated with *Pst* DC3000 or water. After three days post-inoculation (3dpi) leaves were collected and total protein extracts were generated. Leaf extracts were labelled for 2h with 2 $\mu$ M AB53 and AB69.  $\gamma$ VPE labeled with AB69 showed a slight increase in the signal intensity after *Pst* infection compared to the water-treated sample but this increment is not detected with AB53 (Fig. 5A).

Arabidopsis wild-type plants were spray-inoculated with BTH or water and five days after treatment samples were collected and protein leaf extracts were generated. Labelling of leaf extracts results in reduced signal intensity in comparison to the water-treated sample, suggesting a possible down-regulation of  $\gamma$ VPE activity during defense activation (Fig 5B).

*Hyaloperonospora arabidopsidis* (*Hpa*) is a natural pathogen of Arabidopsis. Arabidopsis *eds1-2* mutant plants are highly susceptible to disease caused by *Hpa*

isolates Noco1 and Waco2. *eds1-2* mutants were spray-inoculated with water or  $4 \times 10^4$  spores/ml *Hpa* Noco1. Samples were collected after 5 dpi and labelled with AB53, AB69 and AMS-101. Noco1-treated plants showed higher signal intensities of the two main signals at 43 and 45 kDa when compared to the non-treated plants, indicating that there is an up-regulated  $\gamma$ VPE activity after *Hpa* infection (Fig. 5C).

To further investigate  $\gamma$ VPE activation, Col-0 and  $\gamma$ -OE plants were inoculated with *Hpa* and extracts from leaves, taken at 5dpi, were labelled with AMS-101. Labelling is increased in both Col-0 and  $\gamma$ -OE plants, indicating that the activation is post-transcriptional since the 35S promoter of the  $\gamma$ -OE plants drives constitutive VPE expression (Fig. 5D).

Time course experiments revealed that increased VPE activity during infection is gradual (Fig. 5E, left), and this increment is absent during the incompatible interaction with *Hpa* isolate Cala2 (Fig. 5E, right). Again, VPE activation also occurs in the  $\gamma$ -OE line upon compatible, but not incompatible interactions (Fig. 5E). Please note that less was loaded for t=0 samples.

To monitor the effect of  $\gamma$ -VPE in the growth of *Hpa*, Arabidopsis wild-type, *eds1-1*,  $\gamma$ -KO and  $\gamma$ -OE plants were challenged with Noco1. Leaves were collected after 5 dpi and stained with trypan blue. Normal growth of the pathogen can be observed on both wild type and  $\gamma$ -OE plants, whereas the hyper-susceptible *eds1-2* mutant showed, as expected, enhanced growth of the mycelia and better tissue colonization (Fig. 5F). In contrast,  $\gamma$ -KO mutant showed a slightly reduced oomycete growth (Fig. 5F).

To further investigate the effect of  $\gamma$ -VPE during *Hpa* compatible interactions, sporulation was induced by spraying Arabidopsis wild-type, *eds1-1*,  $\gamma$ -KO,  $\gamma$ -OE and  $\alpha\beta\gamma\delta$ -KO plants with *Hpa* isolates Noco1 and Waco2. Conidiospore production was determined after 6-7 dpi. Both compatible isolates Noco1 and Waco2 present equal sporulation on wild-type and  $\gamma$ -OE plants (Fig. 5G). The indistinguishable sporulation phenotype is consistent with similar hyphal growth (Fig. 5F). In contrast, Noco1 sporulated less on  $\gamma$ -KO plants than on wild-type plants (Fig. 5G, left). Reduced sporulation correlates with reduced pathogen growth (Fig. 5F). However, this decreased in the sporulation is not statistically significant and was not observed with Waco2 (Fig. 5G, right). Interestingly, both

isolates of *Hpa* sporulated less on the  $\alpha\beta\gamma\delta$ -KO mutant, suggesting that VPEs might increase pathogen fitness and promote sporulation (Fig. 5G).

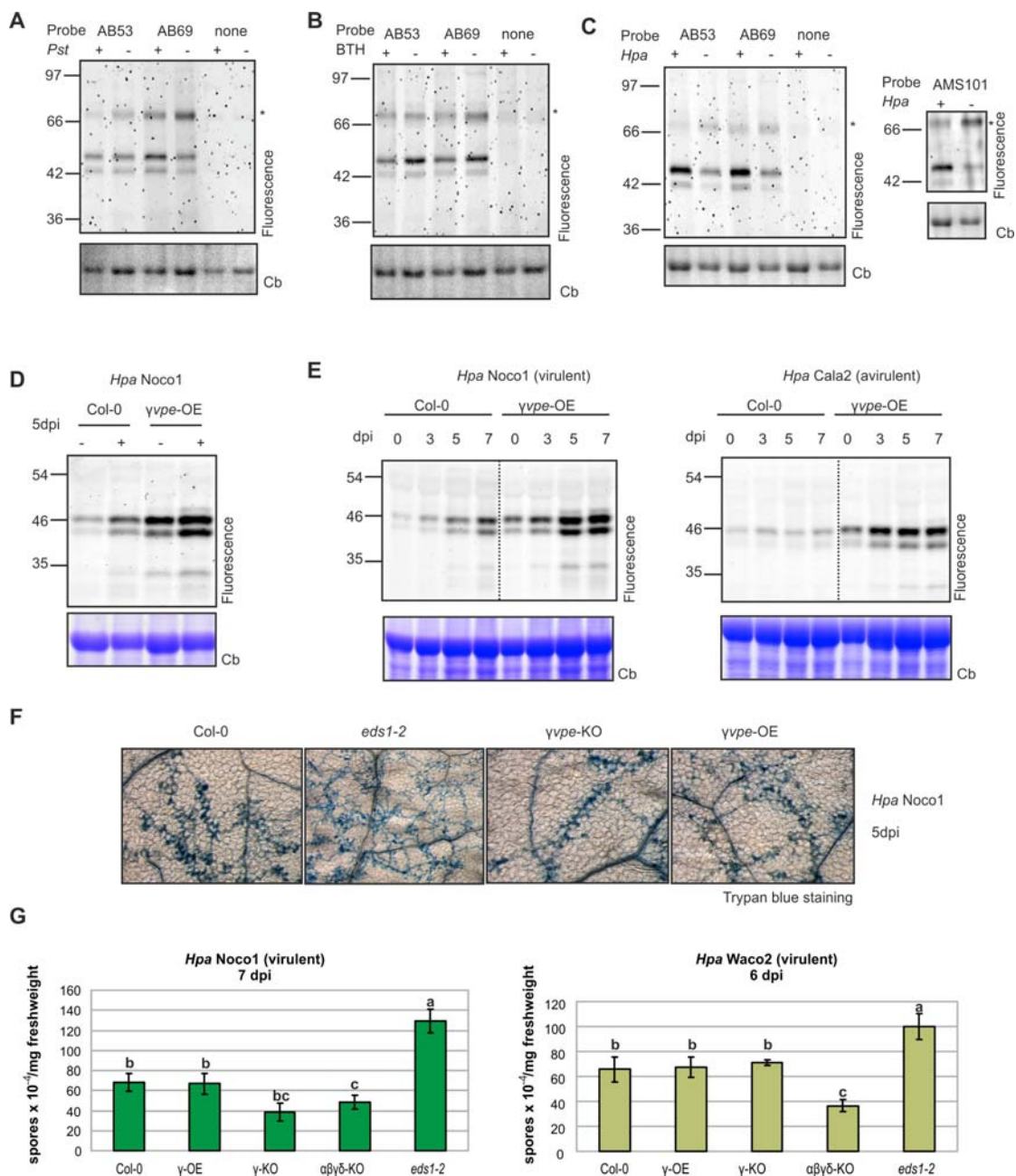


**Figure 5.  $\gamma$ VPE labeling increases upon *Hpa* compatible interactions**

**(A)** VPE labeling is unaltered upon *Pseudomonas* infection. 4 weeks old *Arabidopsis sid2* mutant plants were sprayed inoculated with 10mM MgCl<sub>2</sub> (-) or OD= 0.2 *Pseudomonas syringae* pv. *tomato* DC3000 (+). Leaves were harvested at 3 days post inoculation (dpi) and total protein extracts were generated. Leaf extracts were labeled with 2  $\mu$ M probe for 2h at pH 5. Protein samples were separated on protein gels and analyzed by fluorescent scanning and coomassie blue (Cb) staining.

**(B)** VPE labelling is unaltered upon BTH treatment. 4 weeks old *Arabidopsis* plants were sprayed with water (-) or 0.13 mg/ml Benzothiazole (BTH) (+). Leaves were harvested at 3

## RESULTS

days post treatment. Protein extracts were labeled with 2  $\mu\text{M}$  probes at pH 5 for 2h. Protein samples were separated on protein gels and analyzed by fluorescent scanning and coomassie blue (Cb) staining.

**(C)** VPE labelling increases upon *Hyaloperonospora* infection. 4-week old *Arabidopsis eds1-2* mutant plants were spray inoculated with water (-) or  $4 \times 10^4$  spores/ml *Hyaloperonospora arabidopsidis* (*Hpa* Noco1 (+)). Leaves were harvested at 5 days post inoculation (dpi) and total protein extracts were generated. Leaf extracts were labeled with 2  $\mu\text{M}$  probe for 2h at pH 5. Protein samples were separated on protein gels and analyzed by fluorescent scanning and coomassie blue (Cb) staining.

**(D)**  $\gamma$ VPE is upregulated during infection. *Arabidopsis* Col-0 wt and  $\gamma$ -OE plants were challenged with water (-) or  $4 \times 10^4$  spores/ml *Hpa* Noco1 (+). Leaves were harvested at 5 dpi and protein extracts were labeled at pH 5.5 with AMS-101 for 2h. Protein samples were separated on protein gels and analyzed by fluorescent scanning and coomassie blue (Cb) staining. Experiment made by Gerrit Toenges (Internship).

**(E)** Comparison between compatible and incompatible interactions. Col-0 and  $\gamma$ -OE were spray inoculated with  $4 \times 10^4$  spores/ml *Hpa* Noco1 (virulent) or Cala2 (avirulent). Leaves were harvested at 0, 3, 5 and 7 dpi and protein extracts were generated. Extracts were labeled with 1.6  $\mu\text{M}$  AMS-101 at pH 5.5 for 2h. Protein samples were separated on protein gels and analyzed by fluorescent scanning and coomassie blue (Cb) staining. Experiment made by Gerrit Toenges (Internship).

**(F)** Infection of *Hpa* Noco1 in different *Arabidopsis* genotypes. *Arabidopsis* Col-0 and the mutants *eds1-2*,  $\gamma$ -KO and  $\gamma$ -OE were spray inoculated with *Hpa* Noco1. Leaves were collected at 5dpi and stained with trypan blue for cell death detection. Experiment made by Gerrit Toenges (Internship).

**(G)** Infection assay with virulent and avirulent *Hpa*. *Arabidopsis* mutants were spray inoculated with *Hpa* Noco1 or *Hpa* Cala2. Spores on leaves were counted after 7dpi for the virulent isolate *Hpa* Noco1 or at 6dpi for the avirulent isolate Cala2. Error bars represent SD (n=3). Different letters represent significant differences between genotypes ( $\alpha=0.05$ , Tukey's Studentized Range). Similar data were obtained in a second repetition. Experiment made by Gerrit Toenges (Internship).

## 2.2 THE PROTEASOME

### 2.2.1 Epoxy-ketone probes label the plant proteasome

MVB003, MVB070 and MVB072 (Fig. 1A) are fluorescent probes that were synthesized based on the selective proteasome inhibitor epoxomicin, containing the epoxy-ketone reactive group (Meng *et al.*, 1999). The three probes differ in the additional tag. MV003 has a bodipy fluorescent group whereas MVB070 contain a bodipy with an azide minitag and MVB072 has a bodipy with a biotin (Fig. 1A). Arabidopsis leaf extracts were incubated with these probes to compare the labelling profiles. All three probes cause three bands at around 25 kDa (Fig 1B). MVB072-labelled proteins migrate slightly slower through the gel, consistent with a higher molecular weight of MVB072 due to the biotin when compared to MVB070 and MVB003. The middle band showed the most significant shift.

In order to identify the target of the probes, Arabidopsis leaf extracts were incubated with MVB072 or DMSO. Biotinylated proteins were purified from both the MVB072 labelled proteome and the no-probe control. Samples were separated on protein gel and fluorescent signals at ca. 25kDa were excised. In-gel tryptic digestion was performed and peptides were analyzed by mass spectrometry. Peptides of the three catalytic subunits of the Arabidopsis proteasome were identified (Fig. 1C). For PBA1, corresponding to the  $\beta$ 1 subunit, four unique peptides were identified. One unique peptide was identified for both PBB1 ( $\beta$ 2) and PBE1 ( $\beta$ 5). Additional two peptides were identified for  $\beta$ 2 that are identical between PBB1 and PBB2. Similarly, another two peptides were identified for  $\beta$ 5 that are shared between PBE1 and PBE2.

## RESULTS

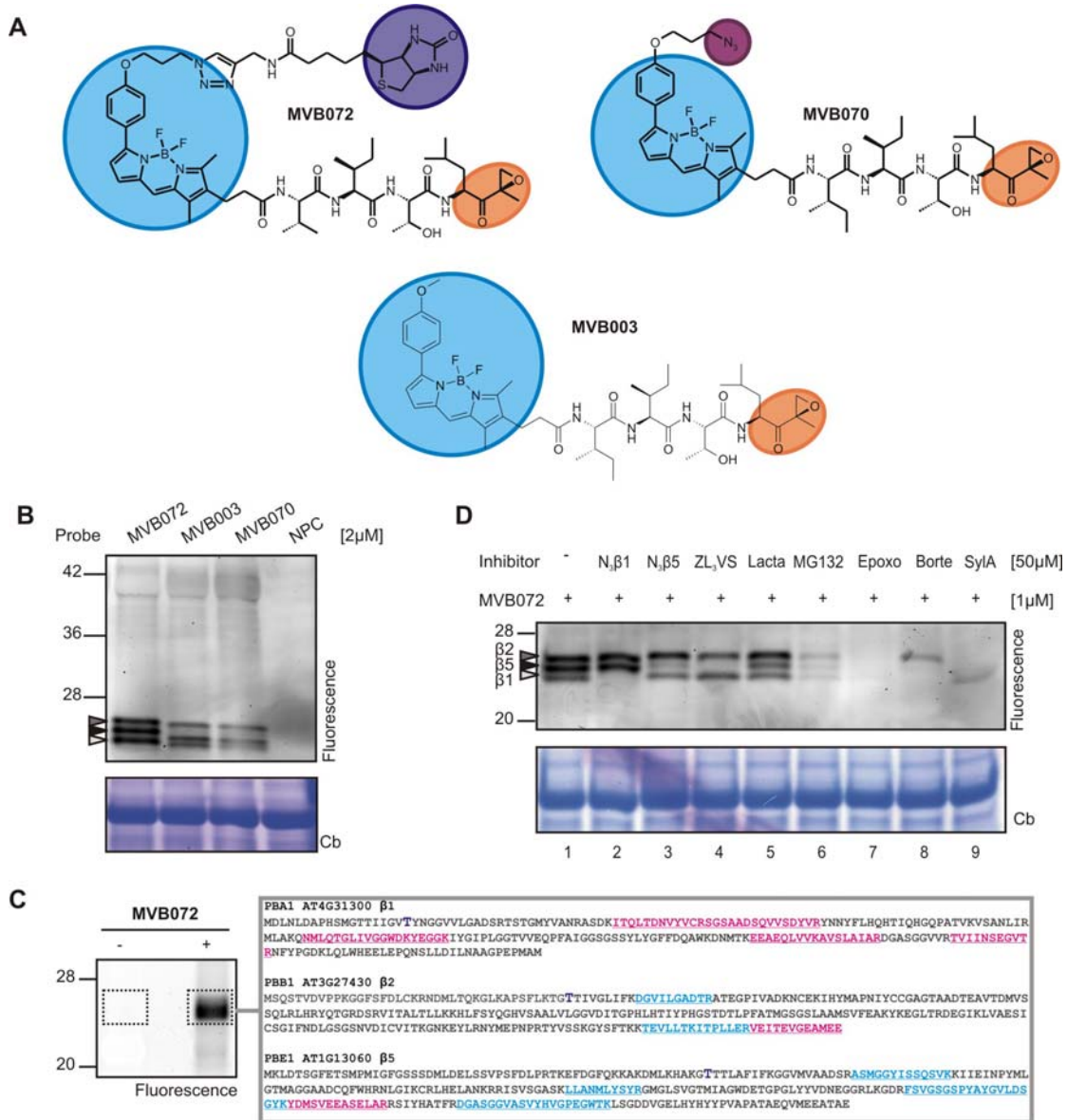


**Figure 1. Epoxy-ketone probes label the proteasome**

**(A)** Structure of proteasome probes. The probes contain an epoxide reactive group (orange) and the reporter tags biotin (purple), Bodipy (blue) or azide (purple).

**(B)** Comparison of labelling profiles of epoxy-ketone probes. Arabidopsis leaf extracts were labeled with MVB072, MVB003 and, MVB070 and fluorescently labeled proteins were detected from protein gels using fluorescence scanning and coomassie blue staining (Cb). NPC: no-probe control.

**(C)** Identification of MVB072-labeled proteins. Arabidopsis leaf extracts were incubated with MVB072 (+) or DMSO (-) for 2 hours. Biotinylated proteins were purified, separated on protein gels and the fluorescent signal at ~25 kDa was excised. Proteins were digested with trypsin and identified by mass spectrometry (Experiment done by Farnusch Kaschani and Tom Colby). Identified peptides are underlined in the full-length protein sequences of the three proteasome catalytic subunits:  $\beta 1$  (PBA1),  $\beta 2$  (PBB1) and,  $\beta 5$  (PBE1). Unique peptides are indicated in red and shared peptides between PBB1 and PBB2 or PBE1 and PBE2 are indicated in blue. The N-terminus catalytic threonine is colored in purple and the propeptide is indicated in grey.



**(D)** MVB072 signals identified using subunit-specific inhibitors. Arabidopsis leaf extracts were pre-incubated for 30 minutes with 50  $\mu$ M of different proteasome inhibitors and then labeled with 1  $\mu$ M MVB072 for 2 hours. N<sub>3</sub> $\beta$ 1 and N<sub>3</sub> $\beta$ 5 are selective inhibitors for caspase-like and chymotrypsin-like proteasome activity respectively (Britton *et al.*, 2009). ZL<sub>3</sub>VS is a vinyl sulfone irreversible proteasome inhibitor (Evans & Cravatt, 2006). Both MG132, a peptide aldehyde inhibitor, and, bortezomib (Borte), a boronate, are reversible proteasome inhibitors (Adams & Kauffman, 2004, Evans & Cravatt, 2006). To the natural and irreversible proteasome inhibitors belong Lactacystin (Lacta) produced by *Streptomyces spp.* (Fenteany *et al.*, 1995), epoxomicin (Epoxo) isolated from an *Actinomycetes* strain (Meng *et al.*, 1999) and SylA secreted by some *Pseudomonas* strains (Wäspi *et al.*, 1998). Samples were separated on protein gels and proteins were detected by fluorescence scanning and coomassie blue staining (Cb).

To determine the identity of the labelled signals, subunit-selective proteasome inhibitors were tested. Arabidopsis leaf extracts were pre-incubated for 30 minutes with the inhibitors followed by 2 hours incubation with MVB072. N<sub>3</sub> $\beta$ 1 competes for the labelling of the lower signal, indicating that this signal corresponds to the  $\beta$ 1 catalytic subunit (Fig. 1D, lane 2). N<sub>3</sub> $\beta$ 5 and ZL<sub>3</sub>VS suppressed labelling of the middle band, indicating that this signal corresponds to the  $\beta$ 5 catalytic subunit (Fig. 1D, lanes 3 and 4). Consistent with previous studies (Adams & Kauffman, 2004), bortezomib inhibits mainly the  $\beta$ 5 and  $\beta$ 1 subunits (Fig. 1D, lane 8), indicating that the upper signal represent the  $\beta$ 2 catalytic subunit. Similarly, lactacystin only suppresses labelling of the  $\beta$ 1 and  $\beta$ 5 subunits, leaving  $\beta$ 2 untouched (Fig. 1D, lane 5). The commonly used proteasome inhibitor MG132 suppresses the labelling of all three catalytic subunits but incompletely (Fig. 1D, lane 6). This partial suppression can be explained because MG132 binding is reversible whereas MVB072 binding is irreversible. In contrast, epoxomicin completely competes MVB072 labelling (Fig. 1D, lane 7). SylA suppresses mainly the  $\beta$ 2 and  $\beta$ 5 labelling and to a lesser extent  $\beta$ 1 (Fig. 1D, lane 9), consistent with its inhibition of the yeast proteasome (Groll *et al.*, 2008b).

## 2.2.2 Proteasome inhibition by epoxomicin and syringolin A

Epoxomicin (Fig. 2A, right) contains an  $\alpha$ - $\beta$ -epoxy-ketone warhead and a dipeptide tail (Meng *et al.*, 1999) while syringolin A (SylA) has a  $\beta$ -lactam ring coupled with two valines (Fig. 2A, left) (Wäspi *et al.*, 1999).

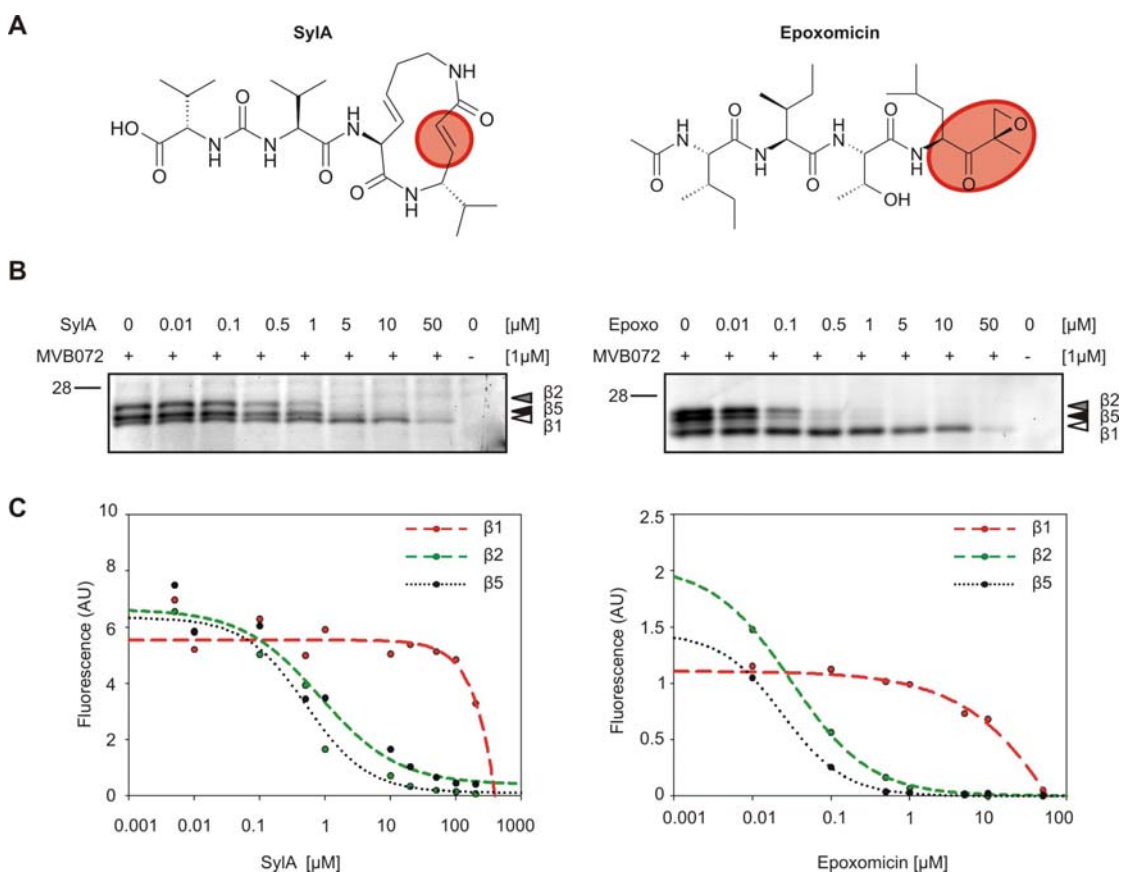


**Figure 2. Proteasome inhibition by epoxomicin and syringolin A**

**(A)** Structures of epoxomicin and SylA. Epoxomicin contains an  $\alpha$ - $\beta$ -epoxy-ketone that reacts covalently to the three catalytic subunits of the proteasome. SylA is a syrbactin and binds covalently to the N-terminal threonine via a Michael-type 1,4-addition. The reactive groups of the molecules are indicated with orange circles.

**(B)** Epoxomicin and SylA compete for MVB072 labelling. Arabidopsis leaf extracts were pre-incubated with different concentrations of Epoxomicin (Epoxo) and SylA for 30 minutes followed by 2 hours labelling with MVB072. Proteins were detected by fluorescence scanning.

**(C)** Inhibition curves for epoxomicin and SylA. Arabidopsis leaf extracts were pre-incubated with epoxomicin and SylA at various concentrations and non-inhibited proteasomes were labeled with 1 $\mu$ M MVB072. Signal intensities were quantified and plotted against the inhibitor concentration for the three catalytic  $\beta$  subunits. A four parameter logistic curve was generated for each subunit.

To compare the inhibitory strength of epoxomicin and SylA, a competition assay with MVB072 was performed. Leaf extracts of *Arabidopsis* were pre-incubated for 30 minutes with various inhibitor concentrations followed by 2 h labelling with the probe. To better visualize these results signal intensities were plotted against inhibitor concentrations and a four parameter logistic curve was fitted for each subunit (Fig. 2C). Similar concentrations of SylA and epoxomicin are needed to suppress MVB072 labelling (Fig. 2B). Interestingly, however, SylA and epoxomicin showed different subunit selectivity. SylA suppresses preferentially labelling of  $\beta 2$  and  $\beta 5$  whereas epoxomicin suppresses preferentially labelling of  $\beta 5$  followed by  $\beta 2$  and then  $\beta 1$ .

### 2.2.3 Structure-Activity relationship of SylA

SylA contains a 12-membered ring with two double bonds. A natural SylA variant, syringolin B (SylB), differs from SylA by having one of these bonds saturated (Fig. 3A). Preincubation of leaf extracts with SylB suppresses MVB072 labelling, but concentrations needed for inhibition are higher when compared to SylA (Fig. 3B, lane 7), consistent with the weaker binding of SylB to the yeast proteasome (Clerc *et al.*, 2009b). To verify the importance of the second unsaturated bond, SylA-sat, a SylA derivative where this bond is saturated was tested (Fig. 3A). Preincubation with SylA-sat does not prevent proteasome labelling (Fig. 3B, lane 6), indicating that the double bond is essential for proteasome inhibition. The importance of this double bond is consistent with the proposed inhibition mechanism because this is the Michael system that is attacked by the catalytic threonine of the proteasome (Groll *et al.*, 2008b).

Besides the 12-membered ring, SylA also contains two L-Val amino acids linked through an ureido bond. To test the importance of the conformation of these two valines, stereoisomers were generated and tested. Both SylA-D-L and SylA-D-D (Fig. 3A) carrying D-Val at the first position are able to inhibit  $\beta 5$  but not  $\beta 1$  or  $\beta 2$  (Fig. 3B lanes 4 and 5). In contrast, SylA-L-D which carries a D-Val at the position 2 (Fig. 3A) is still effective in proteasome inhibition when compared to the natural SylA (SylA-L-L) (Fig. 3B, lane 3), indicating that the conformation of the valine at the position 2 is not important for the selectivity of proteasome inhibition by SylA.

Thus, the Michael system is essential for overall reactivity, whereas specificity for inhibition of the  $\beta 2$  subunit requires the L-configuration of the Valine at position 1.

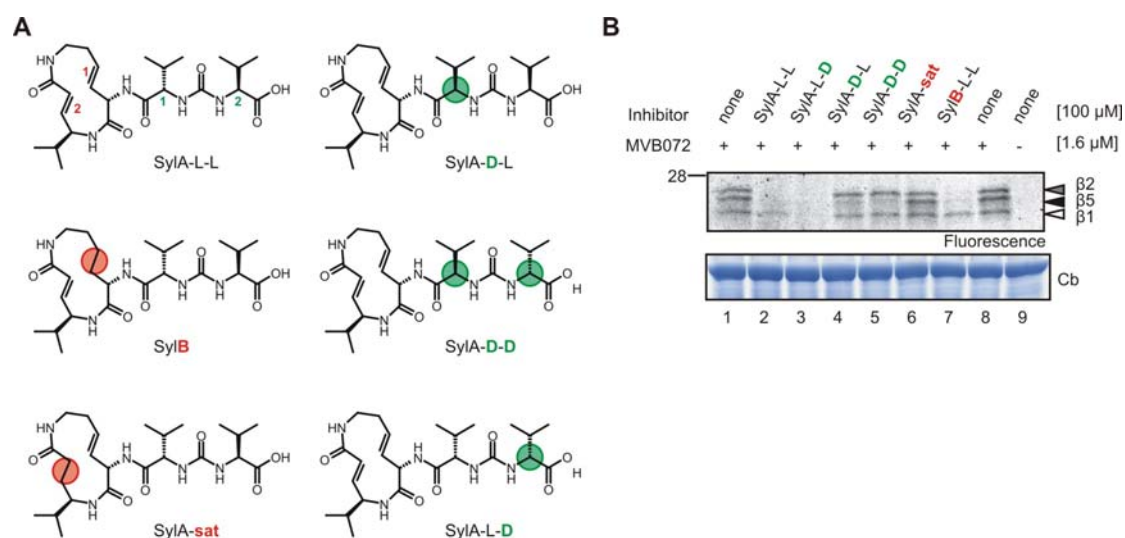


**Figure 3. Structure-activity relationship of SylA**

(A) Structures of SylA derivatives. Differences with the naturally occurring SylA-L-L are indicated with circles. Double bonds in the ring are labeled in red (1 and 2) and stereocenters of Valine 1 and 2 are circled in green.

(B) Inhibition of labelling by SylA derivatives. Arabidopsis leaf extracts were preincubated for 30 minutes with 100  $\mu$ M SylA derivatives and then labeled for 2 hours with 1.6  $\mu$ M MVB072. Labeled proteins were detected by in-gel fluorescent scanning and proteins were detected by coomassie blue staining (Cb).

#### 2.2.4 RhSylA labels Arabidopsis and *Nicotiana benthamiana* proteasome

A fluorescent version of SylA, RhSylA (Fig. 4A), was synthesized to investigate if the proteasome is the only target of SylA. Arabidopsis leaf extracts were pre-incubated with high concentrations of the inhibitors epoxomicin and SylA and then labelled with MVB072 or RhSylA (Fig. 4B). Labelling with RhSylA resulted in three bands that can be competed with an excess of epoxomicin or SylA, suggesting that the proteasome is the sole target of this small molecule (Fig. 4B, lanes 1-3). However, one can not exclude that SylA interacts with other molecules in a non-covalently manner. Consistent with SylA inhibitory specificity, RhSylA preferentially labels the  $\beta 2$  and  $\beta 5$  subunits and SylA incompletely competes MVB072 labelling of the  $\beta 1$  subunit (Fig. 4B, lane 7).

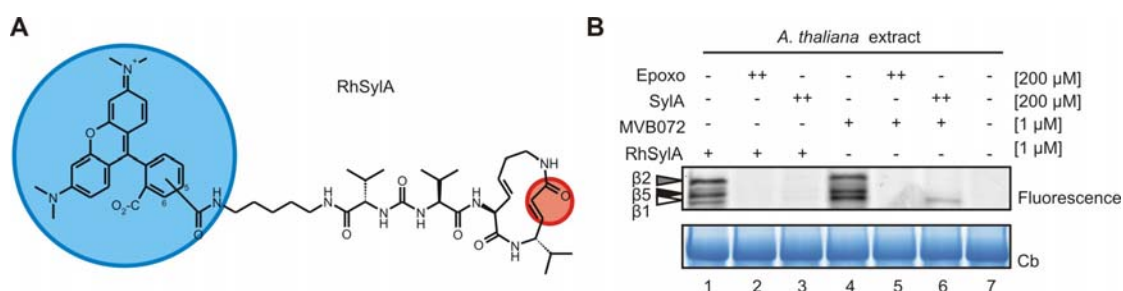


**Figure 4. RhSylA labels the Arabidopsis proteasome**

(A) Structure of RhSylA. Reactive group and fluorescent Rhodamine group are indicated in red and blue, respectively.

(B) Comparison and competition of MVB072 and RhSylA labelling. Arabidopsis leaf extracts were pre-incubated for 30 min with 200μM epoxomicin (Epoxo) or SylA and then labeled with 1μM MVB072 or RhSylA for 2h. Labeled proteins were detected by in-gel fluorescent scanning and proteins were detected by coomassie blue (Cb) staining.

Labelling of *N. benthamiana* leaf extracts with MVB072 produced a strong fluorescent signal at 25 kDa (Fig. 5A). Mass spectrometric analysis of purified labeled proteins showed that this signal represents the  $\beta 1$ ,  $\beta 2$  and  $\beta 5$  catalytic subunits of the proteasome (Fig. 5A). Pre-incubation of leaf extracts with SylA or epoxomicin prevented MVB072 labelling, indicating that SylA inhibits the proteasome of *N. benthamiana* (Fig. 5B). Labelling with RhSylA (Fig. 5B) produced only a 25 kDa signal and RhSylA-labelling was suppressed by pre-incubation with SylA or epoxomicin (Fig. 5B). Taken together, these data demonstrate that SylA targets the proteasome of Arabidopsis and *N. benthamiana* and that both RhSylA and MVB072 can be used to monitor the activity of the proteasome.

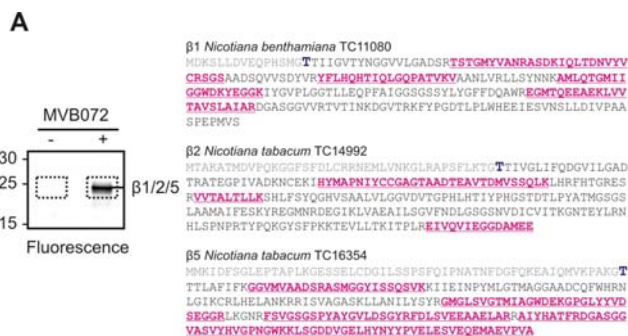


### Figure 5. SylA inhibits *Nicotiana benthamiana* proteasome

**(A)** MVB072 labels the catalytic proteasome subunits in *N. benthamiana* leaf extracts. *N. benthamiana* leaf extracts were incubated with (+) or without (-) MVB072. Biotinylated proteins were isolated and detected by in-gel fluorescence scanning (left) and identified by mass spectrometry (right). In-gel trypsin digests of the gel areas shown within the dashed lines were analyzed by tandem MS. Identified peptides are underlined and red colored in the sequences of the  $\beta$ 1,  $\beta$ 2, and,  $\beta$ 5 catalytic subunits of the proteasome. None of these peptides were found in the no-probe-control, the prodomain (grey) or the mature N-terminus, containing the catalytic Thr (purple bold).

**(B)** SylA targets the proteasome of *N. benthamiana*. Leaf extracts of *N. benthamiana* were preincubated with 200  $\mu$ M epoxomicin (Epoxo) or SylA for 30 minutes and then labeled for 2 hours with 2  $\mu$ M MVB072 or RhSylA. Labeled proteins were detected by in-gel fluorescent scanning and proteins were stained with coomassie (Cb).

#### 2.2.5 Inhibition of *N. benthamiana* proteasome during infection

*Nicotiana benthamiana* is an excellent host for *Psy* B728a bacteria (Vinatzer *et al.*, 2006). To monitor the proteasome activity during infection, *N. benthamiana* leaves were infiltrated with *Psy*. MVB072 labelling of extracts of leaf tissues infected with *Psy* B728a revealed a significant suppression of proteasome labelling at days 2 and 3 after inoculation relative to non-infected tissue (Fig. 6A). However, this suppression was incomplete and absent at later and earlier time points, suggesting that suppression of the proteasome activity by *Psy* during infection is time-regulated.

To investigate if other *P. syringae* strains can also inhibit *N. benthamiana* proteasome during infection, leaves were infiltrated with pathovar (pv.) *tomato* (*Pto*) DC3000, pv. *tabaci* (*Pta*) 11528R or pv. *thea* (*Pth*) K93001. MVB072 labelling was performed at 40 hours-post-inoculation (hpi) and compared to proteasome suppression by *Psy* B728a. In contrast to *Psy* B728a, no suppression of MVB072 labelling was observed with other *P. syringae* strains (Fig. 6B), indicating that these pathovars do not suppress the proteasome activity during infection.

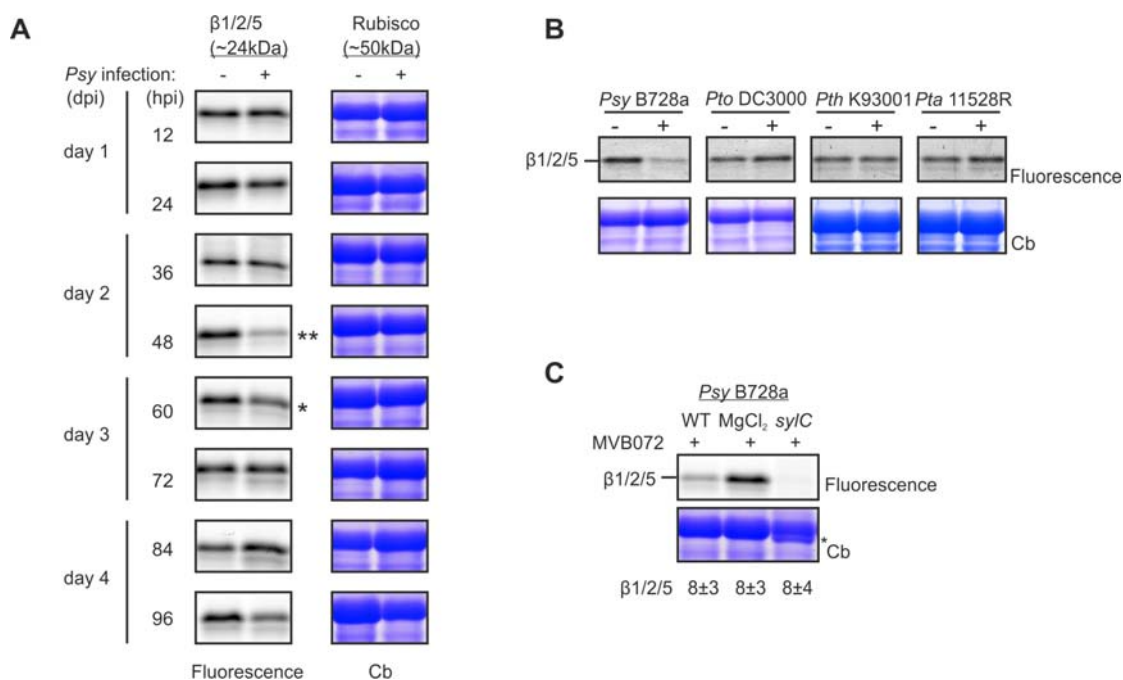


**Figure 6. Inhibition of *N. benthamiana* proteasome during infection**

**(A)** WT *Psy* B728a suppresses proteasome activity during infection. *N. benthamiana* leaves were infiltrated with  $2 \times 10^5$  bacteria/ml or 10 mM  $\text{MgCl}_2$ . Proteasome activity at various days after inoculation was visualized by labelling extracts with MVB072. A representative of four biological replicates is shown. \*/\*\*, reproducible suppression of proteasome labelling.

**(B)** Host proteasome activity during infection with *P. syringae* at 40hpi. *N. benthamiana* leaves were infiltrated with  $2 \times 10^5$  bacteria/ml or 10 mM  $\text{MgCl}_2$  and proteasome activity was determined using MVB072 labelling on extracts taken at 40 hours post-infiltration. Shown is a representative of three biological replicates.

**(C)** Proteasome activity and accumulation in *Psy* WT and *sy/C*-infected *N. benthamiana* tissue. Leaf extract at 48 hours-post-inoculation (hpi) was labeled with MVB072 and analyzed on protein gel with fluorescence scanning and coomassie staining (Cb). Accumulation of the catalytic subunits (in spectral counts) was determined by mass spectrometry on proteins in the 25 kDa region (MS analysis was performed by Farnusch Kaschani and Sherry Niessen). \*: cleaved rubisco.

Mass spectrometric analysis was performed at 40 hpi for *N. benthamiana* leaves infiltrated with *Psy* B728a at 40 hpi. Proteasome catalytic subunits accumulated to similar levels during infection by WT bacteria when compared to non-infected tissue (Fig. 6C), suggesting that the host proteasome is effectively inhibited during infection. No MVB072 labelling was detected in tissue infiltrated with a SylA-deficient knock-out strain (*sy/C*) (Fig. 6C), which lacks a critical component of SylA peptide synthetase (Groll *et al.*, 2008b). Proteasome

accumulation in the *sy/C*-treated sample is comparable to WT and non-infected samples, suggesting that, although the proteasome is present it is not active.

### 2.2.6 *SylA*-deficient mutant, *sy/C* triggers early host cell death

To determine the role of *SylA* during infection, the *sy/C* knock-out strain was used for infection experiments. Infiltration of the *sy/C* mutant triggered early host cell death, reminiscent of the hypersensitive response (HR) (Fig. 7A). The cell death induced by *sy/C* occurred already at 2 dpi, whereas the WT strain only caused cell death at 3-6 dpi (Fig. 7). The absence of MVB072 labelling in the previous experiment (Fig. 6C) can be explained by early host cell death, and is associated with cleavage of the rubisco large subunit (Fig. 6C), a common event during programmed cell death in plants (Navarre and Wolpert, 1999).

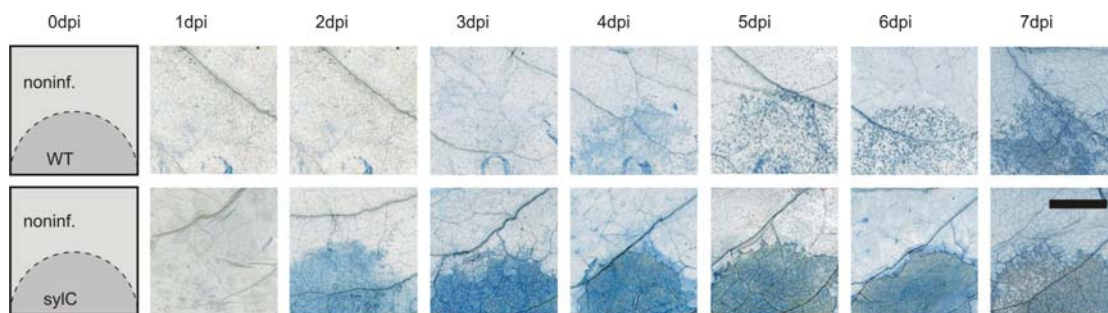


**Figure 7. *SylA*-deficient mutant strain triggers early cell death**

Time course of cell death induced by *Psy* WT and *sy/C* strains. 4-week old *N. benthamiana* plants were infiltrated with 10 mM  $MgCl_2$  buffer or  $2 \times 10^5$  bacteria/ml wild-type (WT) and *SylA*-deficient (*sy/C*) strains. Dead cells were stained with trypan blue at various days after infiltration. Scale bar: 10 mm.

### 2.2.7 *SylA*-deficient mutant growth is not affected by activation of immune responses

To determine if *sy/C*-induced cell death is associated with early immune responses, several markers of the hypersensitive cell death (HR) were tested. Cell death caused by *sy/C* infection was preceded by typical immune responses, such as callose deposition (Fig.8A) and up-regulation of transcript levels of the



hypersensitive cell death marker *NbHin1* at 24 hours-post-infection (hpi), followed by pathogenesis-related marker *NbPR1a* at 36 hpi (Fig. 8B). This sequence suggests that *syIC* mutant bacteria trigger hypersensitive cell death and associated immune responses. In contrast, infection by WT bacteria resulted in callose deposition at 7 dpi (Fig. 8A) and induction of *NbHin1* and *NbPR1a* transcript levels after 3 days (Fig. 8B), indicating that WT bacteria produce SylA to delay immune responses.

*Psy* B728a secretes around 30 type III (T3) effectors, among those, four were found to trigger cell death when expressed transiently in *N. benthamiana* leaves in the absence of *Psy* (Vinatzer *et al.*, 2006). To determine whether the cell death provoked by the *syIC* mutant bacteria was triggered by T3 effectors, *syIC/hrcC* double mutant, which lacks the T3 secretion system, was generated. The *syIC/hrcC* mutant strain did not trigger early cell death (Fig. 8C), also not when infiltrated at higher density, demonstrating that the cell death induced by the *syIC* mutant was triggered by T3 effectors, and suggesting that SylA suppresses effector-triggered immunity (ETI).

HR is aimed to create a barrier to the pathogens and in this way inhibiting the spreading of infection. Associated immune responses may directly affect the viability and propagation of biotrophic pathogens. To investigate endophytic bacterial population sizes, bacteria densities were determined in the infiltrated regions after sterilization of the leaf surface. In contrast to the expectations, no significant differences in growth or maintenance of bacterial population sizes between WT and *syIC* mutant bacteria were observed, indicating that the two strains grow at a similar rate and remain equally viable, despite the host cell death induced by the *syIC* mutant strain (Fig. 8D, top).

Since pre-invasive immunity cannot be detected by syringe infiltration (Melotto *et al.*, 2006), classical spray inoculations were also performed. Spray inoculations revealed no significant differences in endophytic bacterial population levels between the *syIC* and WT strains (Fig. 8D, bottom). Thus, despite strong host responses, population densities of SylA-deficient *syIC* mutant bacteria were unaffected in these pathogen assays.

## RESULTS

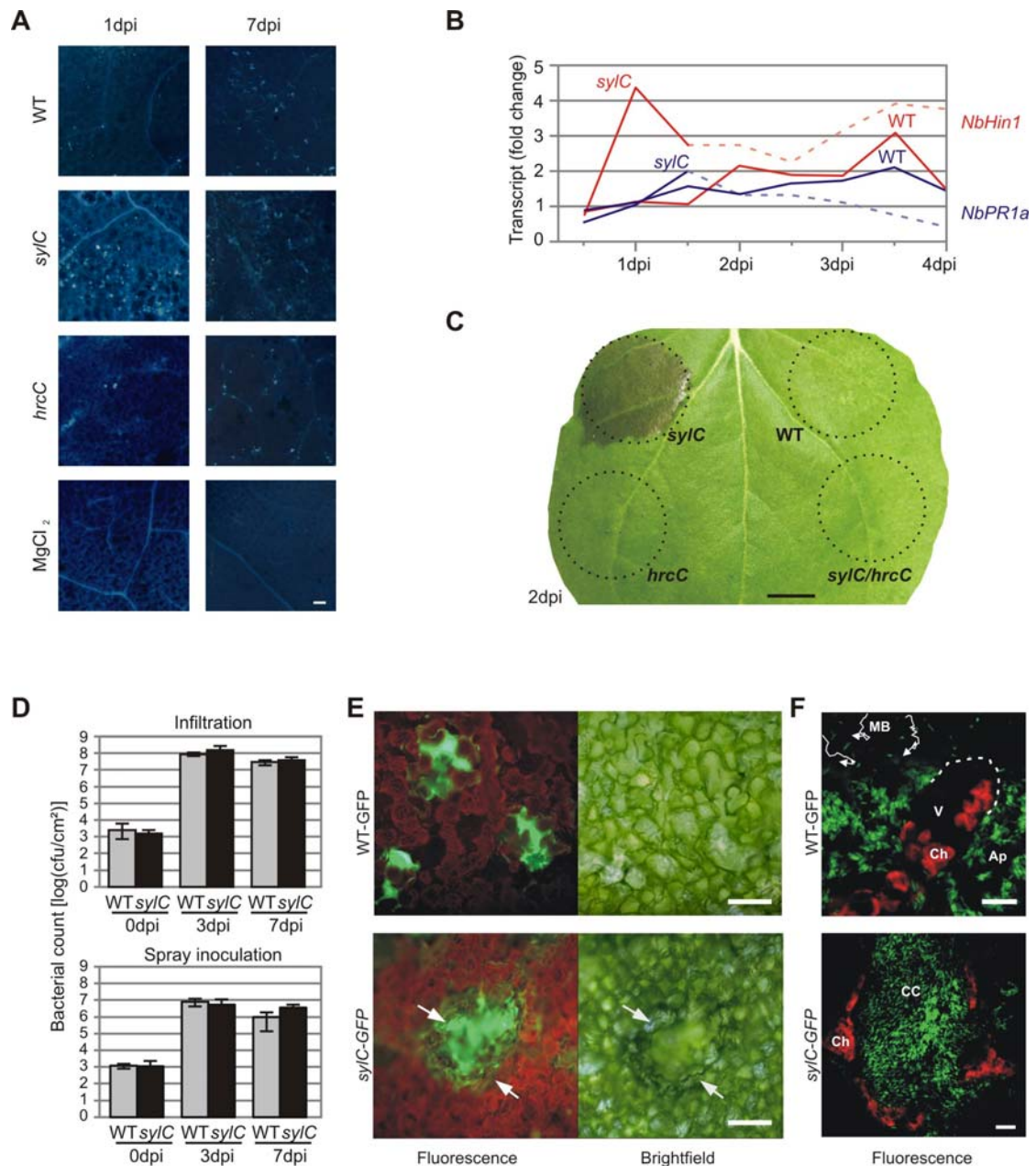


**Figure 8. SylA-deficient mutant triggers hypersensitive immune responses but grows normally**

**(A)** Cell death is preceded by callose deposition. *N. benthamiana* leaves challenged with *Psy* B728a WT and *sylC* were stained for callose at 1 day and 7 days after infiltration and then examined by fluorescence microscopy. Scale bar, 1  $\mu$ M.

**(B)** Cell death is preceded by upregulation of transcript levels of hypersensitive cell death marker *NbHin1* and pathogenesis-related protein marker *NbPR1a*. Semi-quantitative RT-PCR was performed on mRNA isolated after infiltration. Dashed lines indicate collapsed host tissue.

**(C)** *sylC*-induced cell death requires the T3 secretion system. *N. benthamiana* leaves were infiltrated with 10 mM MgCl<sub>2</sub> buffer or *Psy* WT, *sylC*, *hrcC* or *sylC/hrcC* mutant strains at  $2 \times 10^5$  or  $2 \times 10^8$  bacteria/ml. Symptoms were followed during various days. This is a representative picture taken at 2 days after infiltration. Scale bar: 10 mm.

**(D)** Growth of *Psy* B728a WT and *sy/C* on *N. benthamiana*. 4-week old *N. benthamiana* plants were infiltrated or sprayed inoculated with 10 mM MgCl<sub>2</sub> or 2x10<sup>5</sup> bacteria/ml (infiltration) or 2x10<sup>8</sup> bacteria/ml (spray inoculation) WT and *sy/C* bacteria. Bacterial population densities were determined at several time points after inoculation.

**(E)** Colonies of WT-GFP and *sy/C*-GFP bacteria differ in morphology. *N. benthamiana* leaves were infiltrated with 2x10<sup>5</sup> bacteria/ml GFP expressing *Psy* B728a WT and *sy/C* bacteria and analyzed by fluorescent microscopy at 3 dpi. Arrows indicate dead plant cells surrounding the *sy/C*-GFP colony. Scale bar: 0.5 mm. Fluorescent microscopy was done by Izabella Kolodziejek.

**(F)** WT-GFP and *sy/C*-GFP bacteria occupy different locations in the leaf tissue. WT-GFP bacteria (green) are in the apoplast surrounding living host cells (dashed line) with intact chloroplasts (red), whereas *sy/C*-GFP bacteria (green) invade collapsed host cells containing degenerating chloroplasts (red). Pictures were taken by confocal microscopy at 2 dpi. Ap, apoplast; Ch, chloroplast; V, vacuole; CC, collapsed cell; MB, 60 seconds path of motile bacteria. Scale bar: 10 µm. Microscopy was done by Izabella Kolodziejek.

To further investigate bacterial colonization, GFP-expressing WT and *sy/C* bacteria were generated. As with non-GFP expressing strains, the *sy/C*-GFP strain triggered early cell death relative to the WT-GFP strain (Fig. 8E). WT-GFP fluorescent colonies were formed at 2dpi in the apoplastic space and were surrounded by living host cells (Fig. 8F, top). In contrast, colonies of *sy/C*-GFP bacteria were larger and associated with collapsed cells (Fig. 8E, bottom) and bacteria in these colonies were inside and outside dead host cells (Fig. 8F, bottom).

Overall, these microscopic observations confirmed that WT and *sy/C* mutant bacteria accumulated to similar bacterial population levels, irrespective of differences in their colonization environments.

### 2.2.8 B728a WT bacteria spread and colonize distant tissue

It was unexpected that HR-like responses observed for the *sy/C* bacteria did not affect bacterial densities. HR is a mechanism thought to prevent the spread of infection by microbial pathogens; therefore symptoms at later time points after inoculation were investigated. Remarkably, spreading of cell death surrounding the WT but not the *sy/C* mutant infiltrated areas was frequently noticed (Fig. 9A). Although bacterial densities of WT and *sy/C* in the infiltrated region maintain the same, *sy/C* bacteria grow less than WT bacteria in the areas surrounding the infiltrated region (Fig. 9B).

## RESULTS

Two weeks after inoculation, disease symptoms appeared around WT but not *sy/C*-infiltrated regions (Fig. 9C). To investigate if these symptoms are accompanied by spreading bacteria, WT-GFP and *sy/C*-GFP strains were infiltrated and colonization of non-infiltrated regions was monitored. Within two weeks, fluorescent colonies appeared around WT-GFP infiltrated regions, but not around *sy/C*-GFP infiltrated regions (Fig. 9D). These distant WT-GFP colonies contained bacteria surrounded by living host cells (Fig. 9D, inset) and frequently occurred along veins.

To exclude the possibility that distant colonization was caused by pressurized infiltration, toothpick inoculations were performed, mimicking infections at wounded sites. Fluorescence imaging at 30 dpi revealed new WT-GFP colonies up to a centimeter from the primary infection site, associated with spreading chlorosis and occasional cell death (Fig. 9E). GFP-fluorescent colonies distant from the toothpick inoculation site followed the vasculature and could be detected from 5 dpi onwards.

Colonization by WT-GFP bacteria distant from the toothpick inoculation sites was observed at a high frequency (Fig. 9F). In contrast, the majority of *sy/C*-GFP colonies remained at the toothpick inoculation site (Fig. 9E and 9F). The distinct difference in distal colonization was associated with a >10.000-fold higher bacterial densities in distal tissue of WT-GFP compared to *sy/C*-GFP infected tissue (Fig. 9G). No *sy/C*-GFP colony-forming units were detected in extracts taken outside the primary infection site in the majority (73%, n = 22) of these bacterial count assays, indicating that *SylA*-deficient bacteria were efficiently confined to the site of inoculation.

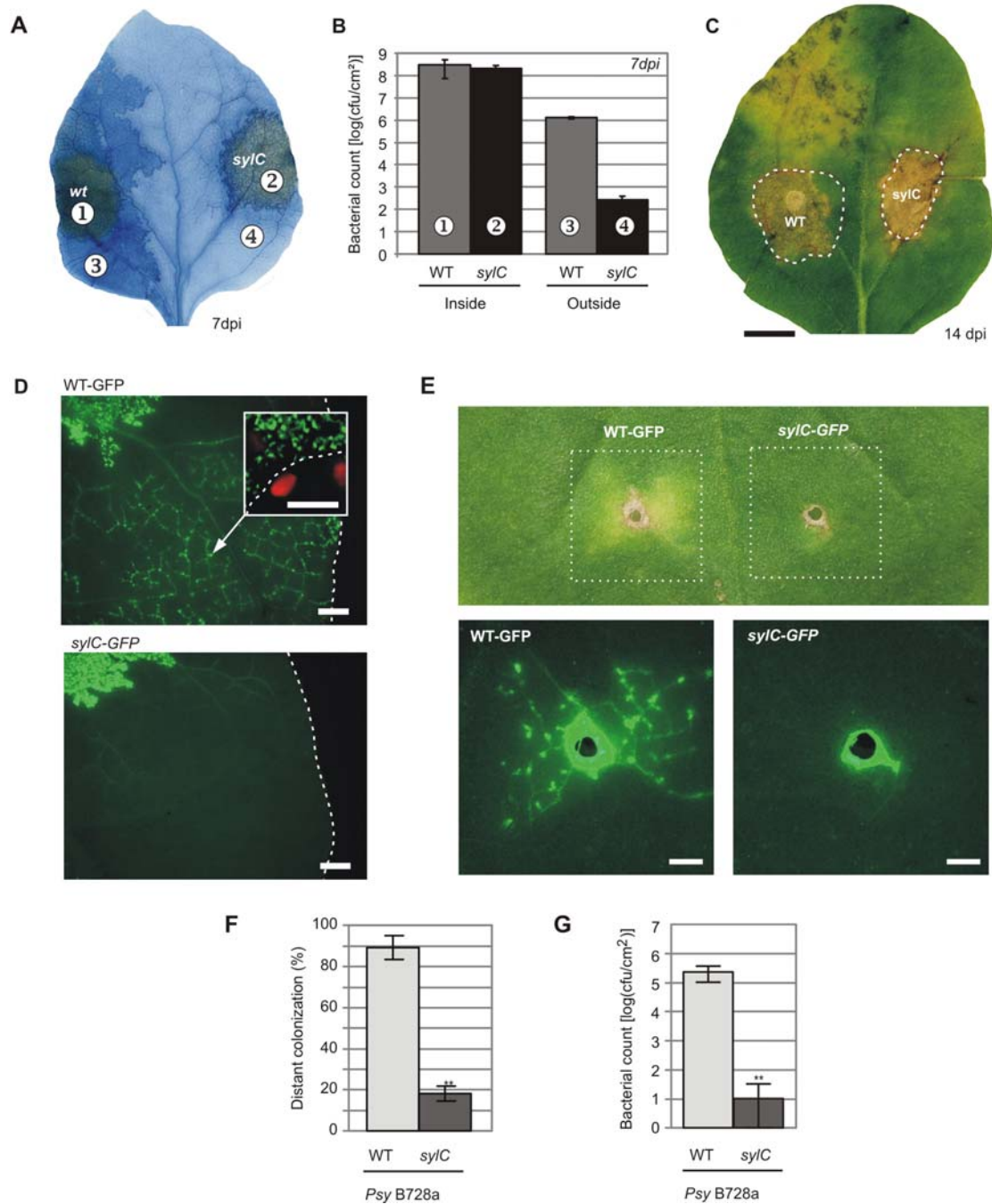


**Figure 9. B728a WT bacteria spread and colonize distant tissue**

**(A)** Spreading of cell death outside from WT infiltrated region. *N. benthamiana* leaves were infiltrated with WT or *syIC* bacteria at  $2 \times 10^5$  bacteria/ml and leaves were stained with trypan blue at 7 dpi.

**(B)** *Psy* WT bacteria spread outside the infiltrated region. Bacterial densities were determined for the infiltrated regions (1 and 2) or outside (3 and 4) of the infiltrated area at 7 dpi.

**(C)** Bacterial disease symptoms spread from the WT-inoculated site. WT-GFP and *syIC*-GFP strains were infiltrated at  $2 \times 10^5$  bacteria/ml into regions of opposite leaf halves (dashed lines). Picture was taken at 14 dpi. Scale bar: 10 mm.

**(D)** WT-GFP bacteria colonize tissues distant from the primary infection site. WT-GFP and *syIC*-GFP strains were infiltrated at  $2 \times 10^5$  bacteria/ml (left upper corner) and colonization was visualized at 14 dpi by stereo fluorescence microscopy. Colonies are present outside the WT-GFP infiltrated area up to the leaf edge (dashed line). Scale bar: 2 mm. Inset: confocal microscopy image of WT-GFP bacteria (green) in distant colony outside sponge parenchyma cell, containing chlorophyll (red) inside the host cell wall (dashed line). Scale bar: 10  $\mu$ m. Confocal microscopy was done by Izabella Kolodziejek.

**(E)** WT-GFP bacteria spread and colonize from toothpick inoculation sites in contrast to *syIC*-GFP bacteria. WT-GFP and *syIC*-GFP bacteria were toothpick-inoculated and colonization was examined at 14 dpi for symptoms (upper panel) and by stereo fluorescence microscopy (lower panel). Scale bars: 1 mm.

**(F)** WT-GFP bacteria spread more frequently from toothpick inoculation sites than *SylA* deficient mutant. Frequency of *Psy* B728a distant colonization from toothpick inoculation sites at 10-14 dpi. Bars represent SEM of five independent biological experiments, each with >10 toothpick inoculations. Students *t*-test:  $P = 0.000313$ .

**(G)** WT-GFP Bacterial populations accumulate in tissue distant from the toothpick inoculation site. Bacterial densities in tissue at 2-12.5 mm from the toothpick inoculation site were determined at 13 dpi. The bars represent SD of five leaves. This experiment is a representative of four biological replicates. Students *t*-test:  $\alpha = 0.05$ ; \*\*  $P < 0.003$ .

### 2.2.9 B728a WT and *syIC* show the same phenotype on bean

*Psy* B728a has been most frequently studied on bean (*Phaseolus vulgaris*), which is its natural host. As with *N. benthamiana*, infiltration of the *syIC* mutant into bean leaves triggered early cell death within 2 days, whereas infiltration of WT bacteria caused host cell death only after 5 days (Fig. 10A). WT-GFP bacteria were able to colonize distant tissues in bean leaves upon toothpick inoculation, but *syIC*-GFP bacteria did not colonize distant tissues (Fig. 10B). Quantification of spreading frequencies revealed that the difference in distant colonization between WT-GFP and *syIC*-GFP bacteria was even more pronounced when compared to *N. benthamiana*: in bean, *syIC*-GFP bacteria hardly colonized tissues distant from the toothpick inoculation site (Fig. 10C). These data suggest that *SylA* deficiency produced phenotypes that are similar in both *N. benthamiana* and bean, making *N. benthamiana* a suitable model plant to study this phenomenon further.

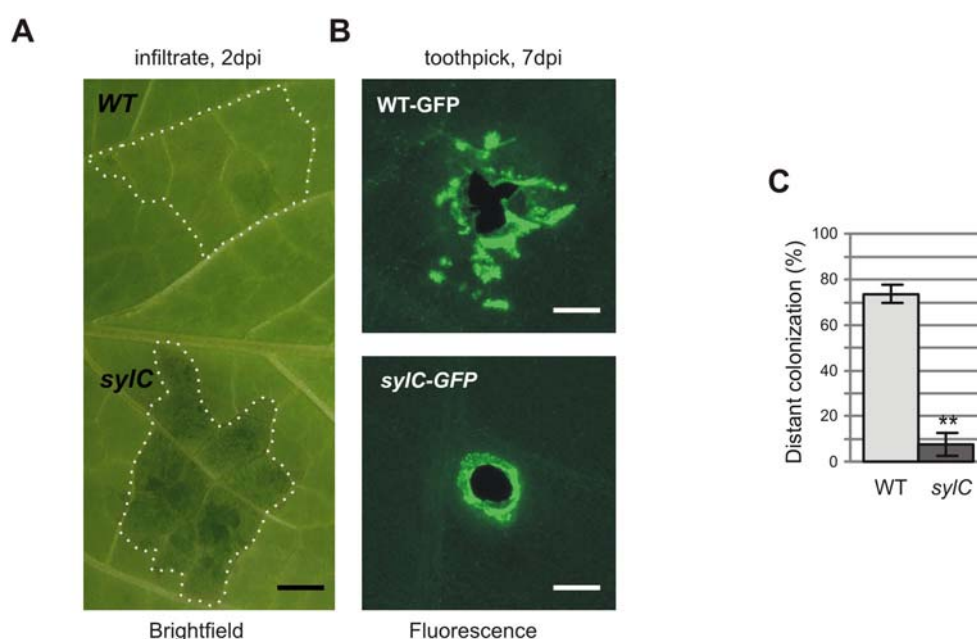


**Figure 10. B728a WT and *syIC* show the same phenotype on bean**

(A) The *syIC* mutant strain triggers early cell death on bean leaves upon infiltration. WT and *syIC* mutant bacteria were infiltrated at  $10^5$  bacteria/ml. Pictures were made at 2 dpi from the lower side of the infiltrated leaf. Scale bar: 5 mm.

(B) WT-GFP bacteria spread and colonize from toothpick inoculation sites on snap bean, the natural host of *Psy* B728a. B728a WT-GFP and *syIC*-GFP bacteria were toothpick-inoculated on leaves of bean plants and colonization was examined at 7 dpi by stereo fluorescence microscopy. Scale bar: 1 mm.

(C) Frequency of distant colonization from toothpick inoculation sites by WT-GFP and *syIC*-GFP bacteria on bean plants. Bars represent SEM of three independent biological experiments, each with >10 toothpick inoculations. Students *t*-test:  $P = 0.0131$ .

### 2.2.10 Distant colonization is common for *Pseudomonas syringae*

Thirteen *Pseudomonas syringae* pathovars (Fig. 11A and 11B), representing different phylogenetic groups of *P. syringae* (Hwang *et al.*, 2005), were screened to determine if the ability to colonize distant tissue is a more general property of *P. syringae* strains. Syringe infiltration of GFP-expressing derivatives caused fluorescent colonies within 2 days of infiltration, indicating that all strains are able to colonize *N. benthamiana* tissue (Fig. 11A). For some bacterial strains host cell death was observed at different time points after infiltration (Fig. 11C). Among those, pathovars *tomato* (*Pto*) DC3000, *aceris* (*Pac*) A10853, *Psy* B301D-R and *maculicola* (*Pma*) YM7930 caused tissue collapse within 3 days of infiltration. The remaining eight colonizing pathovars only caused late and/or incomplete cell death, similar to *Psy*B728a (Fig. 11C).

## RESULTS

After toothpick inoculations seven pathovars colonized the primary inoculation site, but were unable to colonize distant tissues (Fig. 11D). This group includes the notorious model pathogen *Pto*DC3000. In contrast, pathovars *thea* (*Pth*) K93001, *phaseolicola* (*Pph*) RW60, *tabaci* (*Pta*) 11528R, *Psy* B64 and *Psy* B301D-R were able to colonize distant tissue with frequencies close to 80%, similar to that of *Psy* B728a (Fig. 11D). These distant colonizer strains belong to three of the five phylogenetic groups, and have been isolated from various plant species, including monocots (Hwang *et al.*, 2005, Fig. 11B).

*Pto* DC3000 and *Pph* 1448A genomes do not contain homologs of SylA biosynthesis genes (Feil *et al.*, 2005; Joardar *et al.*, 2005). The presence of a SylA biosynthesis cluster in the other strains was investigated using PCR with primers specific for the *sy/C* gene. PCR products were identified from four of the six phylogroup II pathovars, and were absent for all other pathovars (Fig. 11E). These data indicate that SylA biosynthesis is common to many, but not all, phylogroup II strains, and is absent in the other phylogroups.



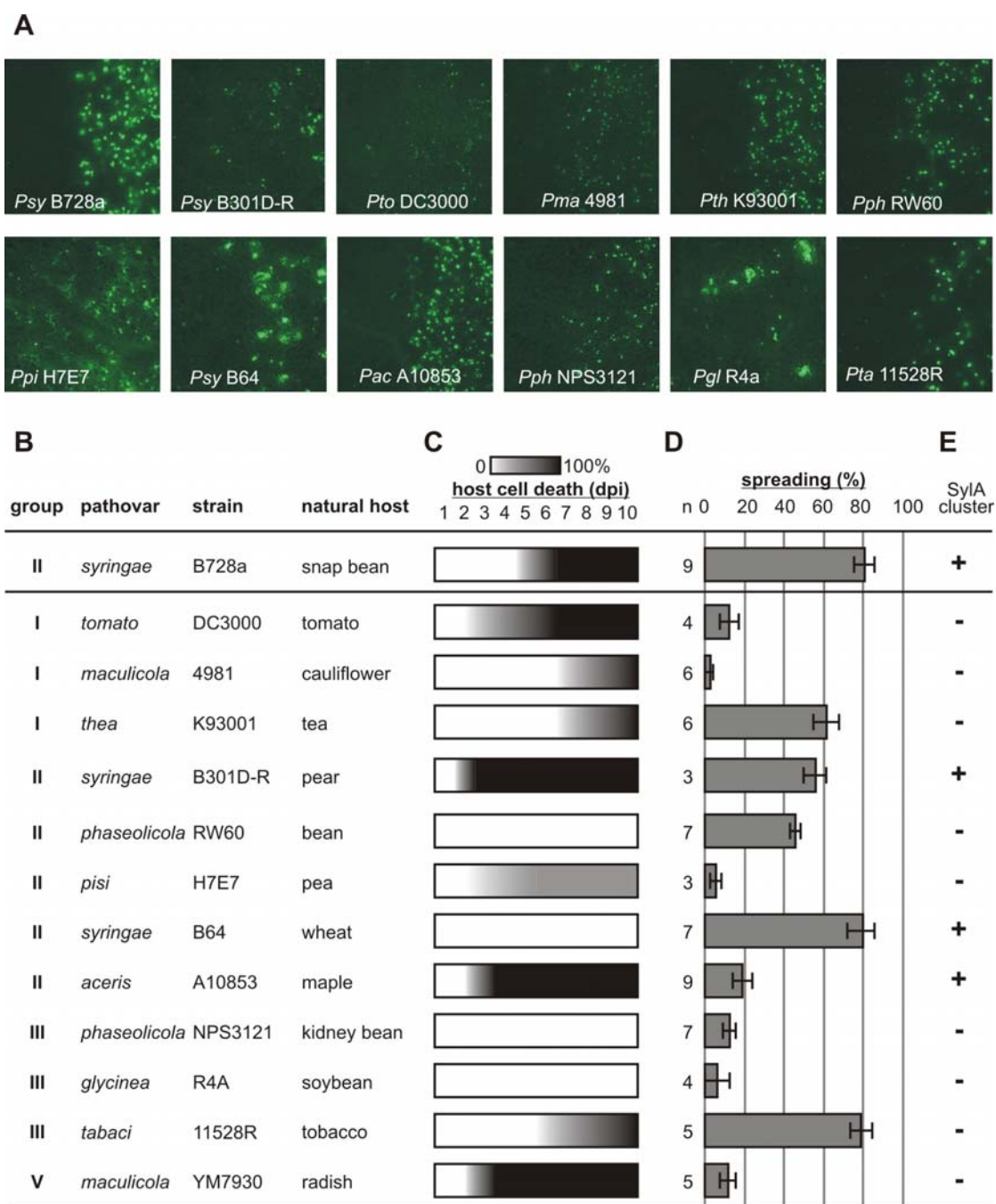


**Figure 11. Distant colonization is common for *Pseudomonas syringae***

**(A)** Colonization on *N. benthamiana* by *P. syringae* strains. GFP-expressing pathovars were infiltrated into *N. benthamiana* leaves at  $2 \times 10^5$  bacteria/ml, and pictures were taken at 5-6 dpi using fluorescence microscopy at the edge of the infiltrated area (right) and non-infiltrated area (left).

**(B)** Properties of the used strains (Hwang *et al.*, 2005).

**(C)** Strains trigger host cell death at different time points. Bacterial cultures were infiltrated at  $2 \times 10^5$  bacteria/ml and tissue collapse was monitored visually at different days-post-infiltration (dpi). White: no cell death; black: full cell death.

**(D)** Frequency of distant colonization (in percentage) from toothpick inoculation sites differs between *Pseudomonas syringae* strains. Error bars represent SEM of *n* independent biological experiments, each with >10 toothpick inoculations.

**(E)** Presence of the *syC* gene, indicated by PCR using gene-specific primers.

### 2.2.11 Distant colonization is uncoupled from cell death suppression

*Pac* A10853 was used to test if transformation of a non-spreading pathovar with the SylA biosynthesis cluster promotes distant colonization. Attempts to transform other strains with the SylA biosynthesis cluster were unsuccessful. The GFP-expressing wild-type strain, *Pac* WT-GFP, was unable to spread from toothpick inoculation sites (Fig 12A, top), even though *Pac* WT-GFP naturally carries genes that encode for SylA biosynthesis. To test if more SylA production would promote distant colonization, *Pac* WT-GFP was transformed with the SylA biosynthesis cluster. In contrast to *Pac* WT-GFP, *Pac* SylA-GFP were able to colonize distant tissue (Fig 12A, bottom), with high frequency (Fig. 12B), confirming that SylA production is required and sufficient to promote spreading.

To investigate if SylA suppresses cell death *N. benthamiana* leaves were infiltrated with SylA-producing and non-producing (*syIC*) strains. Both *Pac* WT and *Pac* SylA strains triggered early cell death (Fig. 12C) and no differences in timing and severity of host tissue collapsed could be observed. Similar early cell death was observed for *Psy* B301D-R WT and its *syIC* mutant derivative (Fig. 12D). In contrast, *Psy* B728a WT does not trigger early cell death. Despite the cell death, SylA production promotes distant colonization for all the strains (Fig. 12E). Surprisingly, distant colonization was also observed for *Psy* B64 *syIC* strain with almost the same frequency as the WT (Fig. 12E) but cell death was not triggered by both *Psy* B64 WT and *syIC* strains (Fig. 12D). These data indicate that suppression of cell death is not necessary but can contribute to distant colonization. Thus, SylA production promotes distant colonization without suppressing cell death in both *Psy* B301D-R and *Pac* A10853.

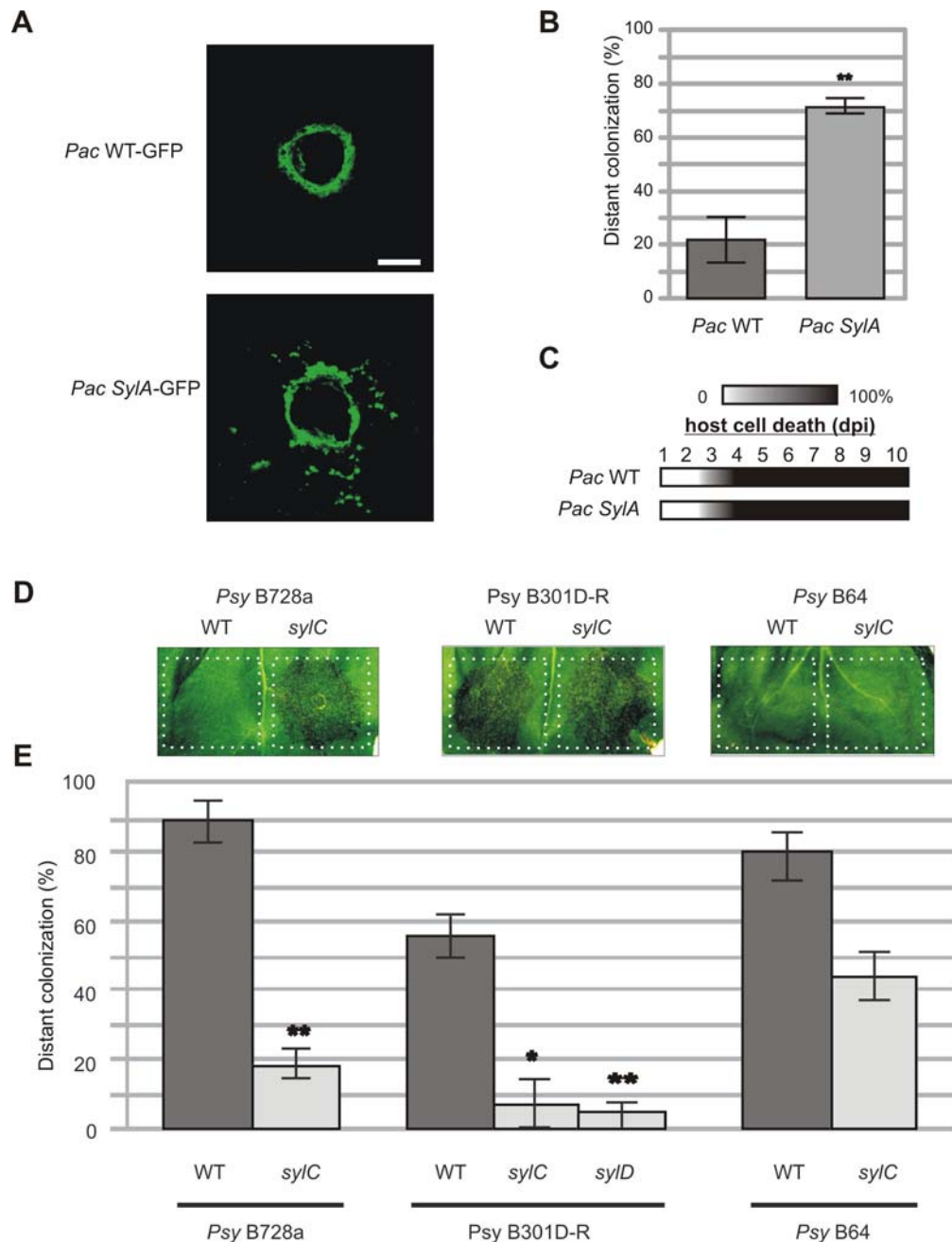


**Figure 12. Distant colonization is uncoupled from cell death suppression**

**(A)** SylA biosynthesis cluster promotes distant colonization of the non-spreading pathovar *aceris*. Representative pictures of distant colonization by GFP-expressing pathovar *aceris* (*Pac* WT-GFP) and the transformant carrying the SylA biosynthesis cluster *Pac* SylA-GFP at 14 dpi. Scale bar, 1 mm.

**(B)** SylA is required and sufficient for promoting distant colonization. The frequency of distant colonization (in percentage) from toothpick inoculation sites was determined at 5-10 dpi. Error bars represent SEM of four independent biological experiments, each with >10 toothpick inoculations. Students *t*-test:  $P = 0.0151$ .

**(C)** Host cell death triggered by *Pac* WT and *Pac* SylA. Bacterial cultures were infiltrated at  $2 \times 10^5$  bacteria/ml and tissue collapse was monitored visually at different dpi. White: no cell death; black: full cell death.

**(D)** Cell death is independent of SylA production. *N. benthamiana* leaves were infiltrated with *P. syringae* WT strains and their respective SylA-deficient mutants at  $2 \times 10^5$  bacteria/ml. Pictures were taken at 3dpi.

**(E)** Strains that naturally produced SylA can colonize distant tissue. Frequency of distant colonization from toothpick inoculation sites were measured for *Pseudomonas syringae* SylA producing strains and their respective SylA-deficient mutants. Error bars represent SEM of n independent biological replicates, each with >10 toothpicks.\*  $P < 0.090$ , \*\*  $P < 0.095$ . Students *t*-test:  $P = 0.000313$   $n = 5$  (*Psy* B728a WT/*syIC*);  $P = 0.0537$  (*Psy* B301D-R WT/*syIC*  $n = 3$ );  $P = 0.01278$  (*Psy* B301D-R WT/*syID*  $n = 3$ );  $P = 0.0151$  (*Pac* A10853 WT/*SylA*  $n = 4$ ). Experiment was done in collaboration with Izabella Kolodziejek and Renier van der Hoorn.

### **2.2.12 Salicylic acid – mediated acquired resistance prevents distant colonization and is suppressed by SylA**

In addition to the hypersensitive immune response at the primary infection site, *syIC* bacteria could also induce immune responses in the surrounding tissue. This tissue surrounding the infection site is called 'distant', to distinguish it from local tissue (the infection site itself) and systemic tissue (the entire plant). To test for distant acquired resistance (DAR), *NbPR1a* expression in tissue distant from *syIC* infiltrated regions was monitored using RT-PCR. *NbPR1a* transcripts accumulated in the infiltrated tissue at 24 hpi, and accumulated in the adjacent tissue 12 hours later, at 36 hpi (Fig. 13A). Thus, *syIC* bacteria also induce immune responses in tissue adjacent to the primary infection site.

To test if *syIC*-induced distant immune response limits distant colonization, *N. benthamiana* plants were toothpick-inoculated with WT-GFP at 1 dpi next to WT or *syIC* infiltrated regions. Importantly, when inoculated next to *syIC*-infiltrated regions, WT-GFP was unable to spread (Fig. 13B). This finding demonstrates that *syIC* induces DAR, which can prevent distant colonization, even of WT-GFP strains.

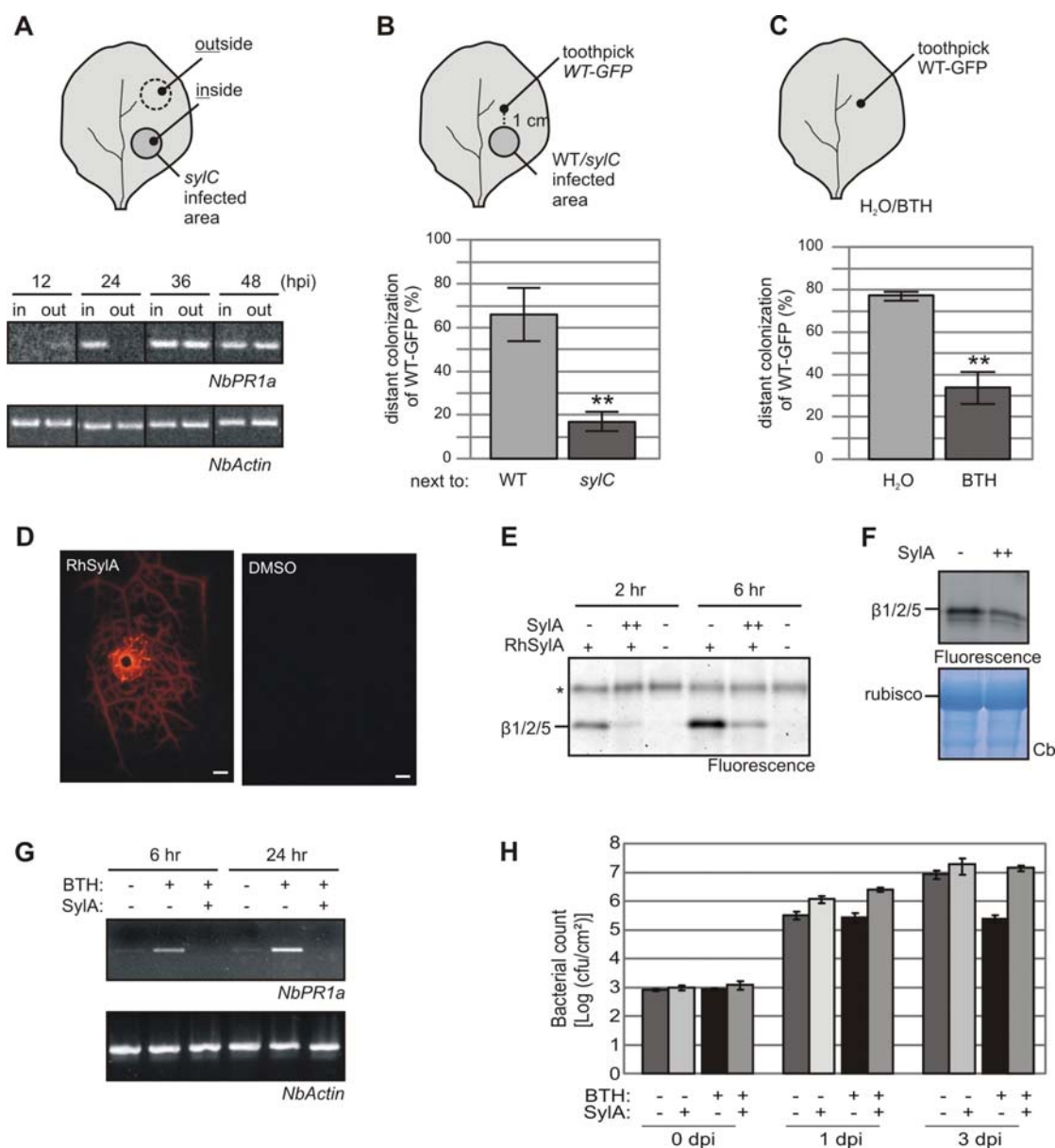


**Figure 13. SA-mediated acquired resistance prevents distant colonization and is suppressed by SyIA**

**(A)** *NbPR1a* gene expression is activated in tissue adjacent to *sy/C*-infiltrated regions. *N. benthamiana* leaves were locally infiltrated with *Psy sy/C* and RNA was isolated from the infiltrated region (in) and adjacent tissue (out) at various time points after infiltration.

**(B)** WT-GFP cannot colonize distant tissue when inoculated next to *sy/C* infiltrated regions in an SA-dependent manner. Leaves of *N. benthamiana* plants were infiltrated with *Psy WT* or *sy/C* bacteria and WT-GFP was toothpick-inoculated one day later at 1 cm from the border of the infiltrated region. Distant colonization of WT-GFP was monitored at seven days after toothpick inoculation. Error bars represent SEM of three independent biological experiments, each with >10 toothpick inoculations. Students *t*-test:  $P = 0.0326$ .

**(C)** Activation of SA signaling cascade suppresses distant colonization. *N. benthamiana* plants were sprayed with water or BTH and WT-GFP bacteria were tooth-pick inoculated one day later and distant colonization was scored at seven days after toothpick inoculation. Error bars represent SD of at least three independent biological experiments, each with >10 toothpick inoculations. Students *t*-test:  $P = 0.0207$ .

## RESULTS

**(D)** RhSylA spreads through the vasculature. A 1- $\mu$ l aliquot of 2 mM RhSylA or DMSO was applied at a toothpick wounding site and a fluorescent image was taken 2 hours later. Scale bar, 1 mm.

**(E)** SylA targets the proteasome in distant tissue. A 1- $\mu$ l aliquot of 2 mM SylA was applied to a toothpick-inoculation site and preincubated for 30 minutes. Subsequently, 1  $\mu$ l of 2 mM RhSylA was added and incubated for another 2 hours or 6 hours. Proteins were extracted from tissue at 1-10 mm from the application site and labeled proteins were detected by fluorescent scanning.

**(F)** SylA moves into distant tissue. A 1- $\mu$ l aliquot of 1 mM SylA was applied at a toothpick-wounding site and incubated for 4 hours. The application site was removed and extracts from distant tissues were labeled with MVB072 and fluorescently labeled proteins were detected.

**(G)** SylA blocks BTH-induced *NbPR1a* expression. Leaves were infiltrated with 50  $\mu$ M SylA or water and immediately sprayed with 300  $\mu$ M BTH. RNA was isolated from infiltrated tissues at 6 and 12 hours after treatment and used as template for semiquantitative RT-PCR with gene-specific primers for *NbPR1a* and *NbActin*.

**(H)** SylA prevents BTH-induced acquired resistance. *N. benthamiana* leaves were infiltrated with or without SylA and immediately sprayed with BTH. *sylC* mutant bacteria were infiltrated at  $2 \times 10^5$  bacteria/ml at 6 hours after SylA/BTH treatment and bacterial populations were determined at 0, 1 and, 3 dpi. Error bars represent SEM of four independent bacterial counts.

Acquired resistance is thought to be mediated through the salicylic acid (SA) signaling cascade (Vlot *et al.*, 2009). To test if activation of SA signaling is sufficient to prevent distant colonization, plants were toothpick inoculated with WT-GFP at one day after spraying with water or benzothiadiazole (BTH). BTH mimics SA and triggers SA-dependent responses (Kohler *et al.*, 2002). BTH-treatment significantly reduced the frequency of distant colonization by WT-GFP (Fig. 13C). Thus, up-regulation of the SA signaling cascade is sufficient to suppress distant colonization.

The above data suggest that WT bacteria may be able to suppress SA-dependent immune responses by producing SylA. To test if SylA itself can act at a distance, RhSylA was inoculated on a toothpick site and the migration of this molecule was monitored. Fluorescent signals emerged from the vascular tissue and reached tissue  $>1$  cm from the inoculation site within 3 hours (Fig. 13D). Protein extraction from fluorescent tissue demonstrated that the proteasome was labeled by RhSylA distant from the inoculation site (Fig. 13E). Proteasome labelling was suppressed when an excess of SylA was added to the application site (Fig. 13E), indicating that SylA itself also inhibits the proteasome at a distance. Furthermore, application of SylA, followed by MVB072 labelling of extracts made

from distant tissues also showed suppressed labelling, confirming that SylA itself diffuses and suppresses the proteasome on a distance (Fig. 13F).

To determine if SylA can suppress SA-signaling, leaves were infiltrated with SylA or DMSO and then sprayed with water or BTH. At 6 and 12 hours after spraying, BTH induced *NbPR1a* expression (Figure 13G). However, BTH-induced *NbPR1a* induction was absent in the presence of SylA, demonstrating that SylA prevents SA-induced immune responses.

To test if SylA also suppresses BTH-induced acquired resistance to SylA-deficient bacteria, the *sy/C* mutant was infiltrated at 6 hours after treatment with BTH and SylA. Classical bacterial count assays showed a 10-fold lower bacterial population upon BTH treatment when compared to water-treatment, indicating that SA-mediated acquired resistance suppresses bacterial growth (Fig. 13H).

Importantly, SylA treatment prevents BTH-mediated suppression of bacterial growth, demonstrating that SylA suppresses SA-mediated acquired resistance (Figure 13H). Taken together, these data indicate that SylA can move through the vasculature and suppress SA-dependent immune responses and acquired resistance at a distance.

### **2.2.13 *sy/C* strain can colonize distant tissues in *NahG* plants**

*NahG*-transgenic *N. benthamiana* lines (Wulff *et al.*, 2004) were used to determine if SA signaling is not only sufficient but also required to prevent distant colonization in DAR tissue. SA cannot accumulate in these plants since *NahG* expresses a bacterial salicylate hydroxylase that degrades SA. Infiltration of *sy/C* bacteria into *NahG* plants triggered hypersensitive cell death indistinguishable in timing and severity from responses triggered in wild-type plants (data not shown). However, when WT-GFP was toothpick-inoculated next to *sy/C* infiltrated regions, distant colonization was observed with the same frequency as spreading near areas infiltrated with WT bacteria (Fig. 14A). In addition, the intensity (distance and number of colonies) of distant colonization was indistinguishable in the two conditions (Fig. 14B). These data demonstrated that SA accumulation is required to prevent distant colonization of WT-GFP in DAR tissue.

## RESULTS

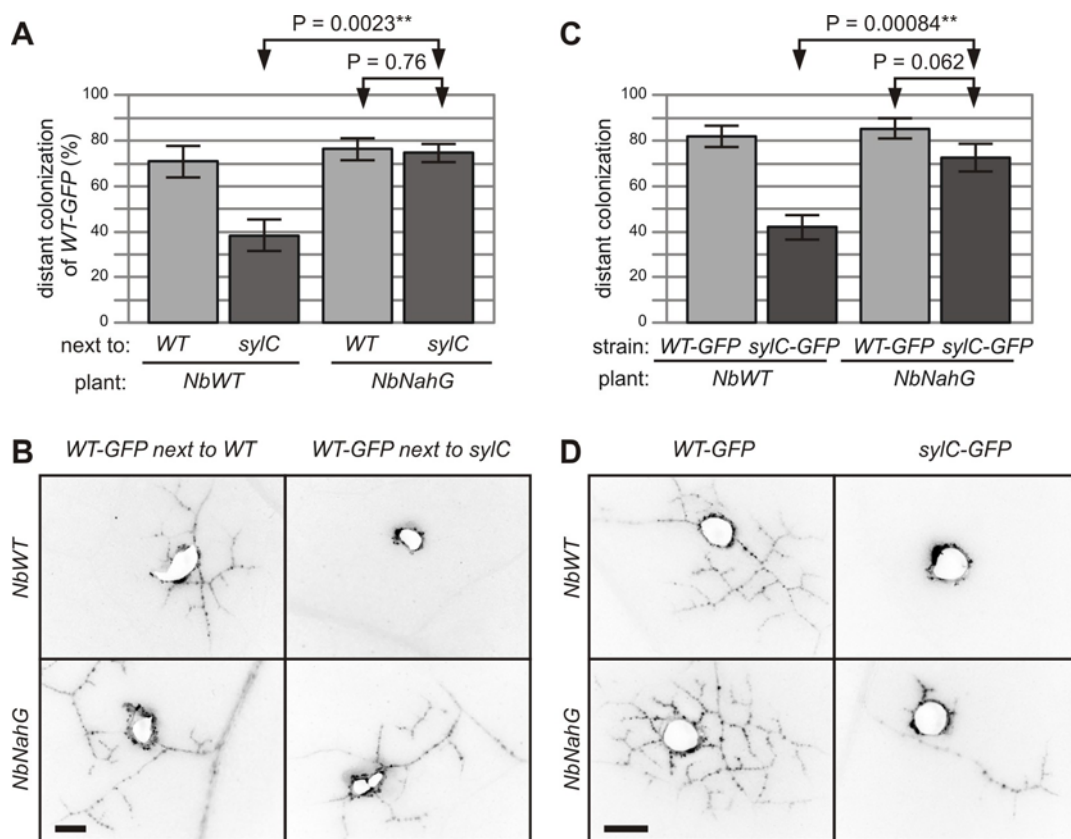


**Figure 14. SyIA-deficient bacteria can colonize distant tissue in *NahG* plants**

**(A)** WT-GFP can spread in *NahG* plants when tooth-pick inoculated next to *syIC* infiltrated sectors. Leaves of *N. benthamiana* WT and *NahG* plants were infiltrated with WT or *syIC* bacteria and WT-GFP was toothpick-inoculated one day later at 1 cm from the border of the infiltrated region. Distant colonization of WT-GFP was monitored at seven days after toothpick inoculation. Error bars represent SEM of at least three independent biological experiments, each with >10 toothpick inoculations. P-values of Students *t*-test are indicated.

**(B)** Representative pictures of distant colonization of WT-GFP when inoculated next to WT or *syIC* infiltrated sectors in WT or *NahG* plants. Fluorescence pictures were inverted and converted to grayscale for better visibility of the colonies (black). Scale bar: 1 mm.

**(C)** *syIC*-GFP can colonize distant tissues in *NahG* plants. WT-GFP and *syIC*-GFP bacteria were toothpick inoculated in NbWT and Nb*NahG* plants and distant colonization was scored after seven days. Error bars represent SEM of at least three independent biological experiments, each with >10 toothpick inoculations. P-values of Students *t*-test are indicated.

**(D)** Representative pictures of colonization pattern of WT-GFP or *syIC*-GFP at 7 days after toothpick inoculation in WT or *NahG* plants. Fluorescence pictures were inverted and converted to grayscale for better visibility of the colonies (black). Scale bar, 1 mm.



Interestingly, when toothpick-inoculated, *sy/C-GFP* strains were able to colonize distant tissues significantly more frequently in *NahG* plants when compared to WT plants (Fig. 13C), confirming that SA signaling is required to restrict distant colonization. The frequency of distant colonization of *sy/C-GFP* bacteria was still slightly less than that of WT-GFP bacteria, and also the number of distant colonies was reduced (Fig. 13D), indicating that the hypersensitive immune response in local tissues contributes to the containment of *sy/C* bacteria, independent from SA.

### 3 DISCUSSION

#### 3.1 VACUOLAR PROCESSING ENZYMES

The activity of VPEs and their inhibitory profile was characterized using activity-based protein profiling (ABPP). A screen of legumain probes in different plant extracts resulted in specific labelling of  $\gamma$ VPE, the most abundant VPE type in vegetative tissue. The fluorescent activity-based probe AMS-101 was selected due to its potent and highly specific labelling of  $\gamma$ VPE in *Arabidopsis* leaves extracts. Further characterization of  $\gamma$ VPE function in the *Arabidopsis-Hpa* model reveals an unexpected post-transcriptional up-regulation of  $\gamma$ VPE during compatible interactions but not during incompatible interactions, suggesting a role of  $\gamma$ VPE during compatible interactions.

##### 3.1.1 AMS-101 is a highly specific probe for $\gamma$ VPE in *Arabidopsis* leaf extracts

VPEs are plant legumains that share similarities with caspases, a family of cysteine proteases. Both, VPEs and caspases, need aspartic acid (Asp) or asparagine (Asn) at the P1 position in substrate cleavage sites (Haraiwa *et al.*, 1999; Berger *et al.*, 2006) and both are involved in PCD (Hatsugai *et al.*, 2004; Rojo *et al.*, 2004). Specific labelling of pumpkin seed extracts suggested that the target of legumain probes is VPE (Fig. 1A). The acyloxymethyl ketone (AOMK) warhead has been described as a very suitable reactive group for cysteine proteases of the clan CD (Kato *et al.*, 2005). Addition of Asn or Asp at the P1 position results in specific labelling of VPEs. Labelling with AMS-101 caused stronger signals when compared to VPE-R (Fig. 3A). Both AMS-101 and VPE-R contain the same P1 and P2 position amino acids, so differences must reside in the warhead or the fluorophore. Quantification of the concentration range for VPE-R and AMS-101 showed that saturation of labelling occurs at the same probe concentration but signal intensities differ even at saturating probe concentrations, suggesting that

rhodamine is less fluorescent than bodipy. Rhodamine is a relative inexpensive fluorophore, but has rapid photobleaching and low quantum yields (Sadaghiani *et al.*, 2007). In contrast, bodipy displays high absorption coefficients, high quantum yields and narrow absorption peaks. However, it is extremely expensive (Sadaghiani *et al.*, 2007).

The main VPE expressed in Arabidopsis leaves is  $\gamma$ VPE (Kinoshita *et al.*, 1999). Three different approaches confirmed that  $\gamma$ VPE also is the main target of AMS-101, VPE-B and VPE-R in Arabidopsis leaf extracts. Labelling of VPE knock-out and over-expressor lines showed that  $\gamma$ VPE is the main target of these probes. This result was confirmed by mass spectrometry analysis. In addition, labelling of *N. bentamiana* leaves transiently overexpressing Arabidopsis VPEs demonstrated that AMS-101 can label all four VPEs and not only  $\gamma$ VPE. These results confirmed that  $\gamma$ VPE is the main VPE expressed in vegetative tissue and that AMS-101 specifically labels VPEs. Moreover the inhibitory profiling showed that proline at the P2 position might favour  $\gamma$ VPE targeting more than  $\alpha$ VPE, making AMS-101 more specific for  $\gamma$ VPE.

Animal caspases reside mainly in the cytoplasm and sometimes in the nucleus depending on the cell and the caspase (Shikama *et al.*, 2001). VPEs in plants, however, have been found in vesicles or in the vacuole (Hara-Nishimura *et al.*, 1998; Rojo *et al.*, 2003).  $\alpha$ VPE and  $\gamma$ VPE reside mainly in the lytic vacuoles of the vegetative organs of Arabidopsis (Kinoshita *et al.*, 1999). The subcellular localization of VPEs in acidic environments explains two experimental observations: First, labelling occurs at acidic pH (pH 5 – 5.5) which is consistent with the maximum activity of  $\gamma$ VPE at pH 5.5 and inactivity at pH 7.5 (Kuroyanagi *et al.*, 2002). Second, VPEs accept both Asp and Asn at the P1 position. This is consistent with the labelling of human legumain with Asp-AOMK which occurs only at a low pH whereas labelling with Asn-AOMK occurs at a broader pH window (Kato *et al.*, 2005). These observations can be explained by the low pH, causing protonation of the side chain of Asp and so eliminating its negative charge and allowing binding to the legumain or the VPE.

### 3.1.2 $\gamma$ VPE exhibits caspase-1 activity and distinct inhibitor specificity

Various inhibitors for caspase activities were used to determine the biochemical characteristics of  $\gamma$ VPE. Epoxomicin, MG132 and N3 $\beta$ 1 block the caspase-3-like activity of the  $\beta$ 1 catalytic subunit of the proteasome but did not inhibit  $\gamma$ VPE. This is correlated with the fact that VPEs exhibit caspase-1 activity and not caspase-3 activity (Rojo *et al.*, 2004; Hatsugai *et al.*, 2004). For the same reason, the specific caspase-3 inhibitor DEVD-cho does not block the activity of  $\gamma$ VPE and neither does E-64, the broad band cysteine protease inhibitor. E-64 does not have any amino acid at the P1 position and as a consequence does not meet the requirement of P1 Asn/Asp for inhibition of caspase-like proteases. That YVAD-fmk prevents  $\gamma$ VPE labelling is consistent with previous results. Biotin-YVAD-fmk labels VPE in tobacco leaves (Hatsugai *et al.*, 2004). Interestingly, the caspase-1 inhibitor Ac-YVAD-cho suppresses TMV-induced cell death (Hatsugai *et al.*, 2004) and Ac-YVAD-CMK is able to inhibit HR caused by *Pseudomonas syringae* pv. *phaseolicola* in tobacco plants (del Pozo & Lam, 1998). Taking together these findings indicate that  $\gamma$ VPE exhibits caspase-1 activity and that  $\gamma$ VPE might be involved in cell death activation.

YVAD-fmk blocks the self-processing of the intermediate to the mature isoform of  $\gamma$ VPE (Rojo *et al.*, 2004). The intermediate (43kDa) and mature (40kDa)  $\gamma$ VPE isoforms are active whereas the precursor (56kDa) is inactive (Kuroyanagi *et al.*, 2002). This indicates that the two signals at 40 and 43 kDa correspond to the mature and intermediate  $\gamma$ VPE isoforms that become labelled by AMS-101 because they are active.

To further characterize the inhibitor specificity of VPEs, a P2 AOMK library was tested against  $\alpha$ ,  $\beta$  and  $\gamma$  over-expressed Arabidopsis VPEs in *N. benthamiana* by agroinfiltration. The three VPEs tested exhibit differential inhibitory profile.  $\alpha$ VPE prefers the combinations xxAD or xxED whereas  $\beta$ VPE prefers xxID or xxKD.  $\gamma$ VPE preferentially recognizes xxAD. These data suggest that  $\alpha$ VPE and  $\gamma$ VPE have similar substrate specificities and indicates that these enzymes might fulfil redundant roles. *Nt*VPE can be inhibited by Ac-ESEN-cho (Hatsugai *et al.*, 2004). This correlates with the specificity of Arabidopsis  $\alpha$ VPE for xxED and the fact that Asp (D) and Asn (N) behave similarly at acidic pH. It would

be interesting to test if  $\alpha$ VPE and  $\gamma$ VPE also have functional redundancy, since both enzymes are present in leaves. Overall these data suggest that there is a substrate preference for each of the VPEs and that specific inhibitors for VPEs could be synthesized by using different amino acids at the P2 position.

### 3.1.3 $\gamma$ VPE is post-transcriptionally activated during compatible interactions

$\gamma$ VPE contributes to defense against pathogens by regulating vacuole-mediated cell disruption during cell death, especially during the hypersensitive response (HR) elicited during incompatible interactions (Rojo *et al.*, 2004).  $\gamma$ VPE has been studied during incompatible interactions because it exhibits caspase-1-like activity but little is known about the role of  $\gamma$ VPE during incompatible interactions. VPE deficiency suppressed HR in response to infection with TMV (tobacco mosaic virus). As a consequence, the virus can replicate more abundantly in VPE-silenced plants (Hatsugai *et al.*, 2004). However, inhibition of pathogen growth is not always a consequence of HR. For instance, blocking HR in tobacco leaves using the saspase inhibitor biotinyl-TADT-cho does not affect TMV accumulation (Chichkova *et al.*, 2004), indicating that biotinyl-TADT-cho is involved in the inhibition of TMV-triggered HR rather than in the suppression of TMV accumulation. Moreover, infection with an incompatible strain of *Pseudomonas syringae* pv. *phaseolicola* on tobacco plants that were treated with the  $\gamma$ VPE inhibitor Ac-YVAD-CMK did not show activation of the HR markers *HSR203J* and *HIN1* but induction of *PR1* was unaltered compared to the mock-inoculated control (del Pozo & Lam, 1998). These data suggest that host defense and HR cell death might be regulated by different pathways and that  $\gamma$ VPE might function up-stream of *HSR203J* and *HIN1* regulation (del Pozo & Lam, 1998; Chichkova *et al.*, 2004).

$\gamma$ VPE expression levels were induced after treatment with the obligate biotroph TuMV (turnip mosaic virus), which does not cause PCD (Rojo *et al.*, 2004). This thesis described that  $\gamma$ VPE activity increases gradually in Arabidopsis plants challenged with the biotroph *Hyaloperonospora arabidopsidis* isolate Noco1. However, the increment in  $\gamma$ VPE was present in wild-type plants as well as in  $\gamma$ -OE lines in which  $\gamma$ VPE is constitutively expressed through the 35S promoter.

This finding indicates that upregulation of  $\gamma$ VPE activity during a compatible interaction is post-transcriptional. Increased  $\gamma$ VPE activity might be explained by its self activation (Kuroyanagi *et al.*, 2002). Sequential removing of the C-terminal and N-terminal pro-peptides under acidic conditions leads to a self-catalytic conversion of pVPE precursor into an active 43kDa intermediate form (iVPE) and an active 40kDa mature form (mVPE) (Kuroyanagi *et al.*, 2002). To confirm that self-activation is responsible for the increased signals during infection it will be necessary to perform western blot analysis with specific  $\gamma$ VPE antibodies.

$\gamma$ VPE activity increases after *Hpa* compatible interactions. Two explanations are possible to interpret this result: First,  $\gamma$ VPE has a function in a late defense response that does not involve HR. Second, the pathogen manipulates the host activating  $\gamma$ VPE for its own benefit. The absence of all VPEs decreases *Hpa* sporulation for two virulent isolates, suggesting that VPEs might be beneficial for *Hpa* rather than activating defense. This enhanced resistance was not detected in the  $\gamma$ -KO mutant, indicating that another VPE, perhaps in addition to  $\gamma$ VPE, contributes to *Hpa* sporulation. VPEs could be required for nutrient release. VPE function is thought to be part of a cellular suicide strategy in which disruption of the vacuole during pathogenesis and development elicits PCD (Hatsugai *et al.*, 2006). Reduced vacuolar disruption in the absence of VPE might be associated with less nutrient availability decreasing pathogen proliferation. However, there is no PCD during the compatible interaction with *Hpa*. Interestingly, this case might be similar to the human pathogen *Salmonella enterica* which delivers the virulence factor SopE into the host to elicit caspase-1 maturation triggering gut inflammation without cell death (Müller *et al.*, 2010). This activation of VPEs in the absence of PCD might be achieved by *Hpa* effectors and be beneficial for *Hpa* infection.

In conclusion, a new method to display the activity of VPEs was developed by using fluorescent and biotinylated probes. By using different inhibitors it was shown that VPEs exhibit caspase-1 activity and that the P2 position provides specificity to different VPEs.  $\gamma$ VPE is the main VPE expressed in Arabidopsis leaves and therefore prominently labelled.  $\gamma$ VPE shows a gradual up-regulation during *Hpa* compatible interactions which is probably post-translational. Pathogen proliferation decreases in the absence of VPEs, suggesting that VPE activity promotes sporulation.

## 3.2 THE PROTEASOME

Three probes based on the well-characterized proteasome inhibitor epoxomicin were introduced in this study. MVB072 was mainly used to monitor the activity of the plant proteasome *in vitro* and during pathogen infection. MVB072 labelling was used to study syringolin A, a small effector molecule produced by some *Pseudomonas syringae* strains. This study revealed the role of SylA in the interaction with the host plant. Furthermore, this thesis introduces a long-overlooked and important aspect in the life of *P. syringae* pv. *syringae*, facilitated by the production of the small molecule proteasome inhibitor SylA.

### 3.2.1 Epoxomicin-based probes are specific for the plant proteasome

Several proteasome inhibitors and probes have been identified and are currently used for medical studies. For example the fluorescent probe MV151, a vinyl sulfone, has been used for proteasome profiling in animal (Verdoes *et al.*, 2006) and plant cells (Gu *et al.*, 2010). MV151 is a broad spectrum proteasome probe that can be used for *in vivo* and *in vitro* profiling (Verdoes *et al.*, 2006). However, vinyl sulfones can react with cysteine proteases (Britton *et al.*, 2009). Indeed, Gu *et al.* showed that MV151 labels the three catalytic subunits of the Arabidopsis proteasome but also labels the abundant cysteine protease RD21 (Gu *et al.*, 2010). Labelling of RD21 becomes even stronger when Arabidopsis cell cultures are incubated *in vivo* with MV178, an alkyne-tagged version of MV151 (Kaschani *et al.*, 2009). In contrast, MVB072 only labels the three catalytic subunits of the plant proteasome and does not label other proteins in plant extracts. This is consistent with the specificity of epoxomicin for the proteasome (Meng *et al.*, 1999). The N-terminal threonine of the catalytic subunits of the proteasome attacks the epoxy-ketone group of epoxomicin resulting in the formation of a morpholine ring (Groll *et al.*, 2008a). This unique mechanism of inhibition gives the specificity to the proteasome and not to other cysteine proteases. Imaging studies with MVB003 showed high specificity of the probe for

both cytoplasmic and nuclear proteasomes (Kolodziejek *et al.*, submitted). These features make MVB072 and its derivatives a powerful tool to monitor the activity of the proteasome *in vitro* and *in vivo*.

### **3.2.2 SylA targets mainly $\beta 2$ and $\beta 5$ catalytic subunits of the plant proteasome**

RhSylA preferentially labels the  $\beta 2$  and  $\beta 5$  subunits. This subunit selectivity does not reside in the reporter tag since SylA itself also preferentially competes with  $\beta 2$  and  $\beta 5$  in MVB072 labelling.  $\beta 1$  labelling is slow for both RhSylA and MVB072, though  $\beta 1$  is best labeled by MVB072.

The subunit selectivity of SylA was also observed with studies on the yeast proteasome (Groll *et al.*, 2008) and can be explained using the crystal structure of the yeast proteasome inhibited by SylA (Groll *et al.* 2008, PDB code 2ZCY). The crystal structure of the 20S yeast proteasome contains six SylA molecules, three on each of the two middle rings of  $\beta$  subunits (Fig. 15A). SylA is covalently bound to the N-terminal threonine of  $\beta 1$ ,  $\beta 2$  and  $\beta 5$ . The dipeptide tail of SylA also interacts with the adjacent subunit (Fig. 15B). The structure of the adjacent subunits has important implications on how SylA can bind to each of the three binding pockets. Overlay of the SylA structures shows that the dipeptide tail of SylA is pushed downwards when bound to the  $\beta 1$  subunits but not when bound to the  $\beta 2$  and  $\beta 5$  subunits (Fig. 15C). This is caused by a bulky H116 side chain in the subunit adjacent to the  $\beta 1$  subunit which makes the  $\beta 1$  binding pocket smaller when compared to that of the  $\beta 2$  and  $\beta 5$  subunits (Figs. 15D-F). Consequently, SylA bound to the  $\beta 1$  binding pocket is unable to make a hydrogen bond with D114 of the adjacent subunit, which is an important interaction of SylA bound to the binding pocket of  $\beta 2$  and  $\beta 5$  (Figs. 15D-F). The presence of the D114 interaction in  $\beta 2$  and  $\beta 5$  binding pockets explains why SylA preferentially targets the  $\beta 2$  and  $\beta 5$  subunits. Since many properties including H116 and D114 are conserved in the proteasome subunits of Arabidopsis, it seems likely that this interpretation from the yeast crystal structure might also apply for the Arabidopsis proteasome.



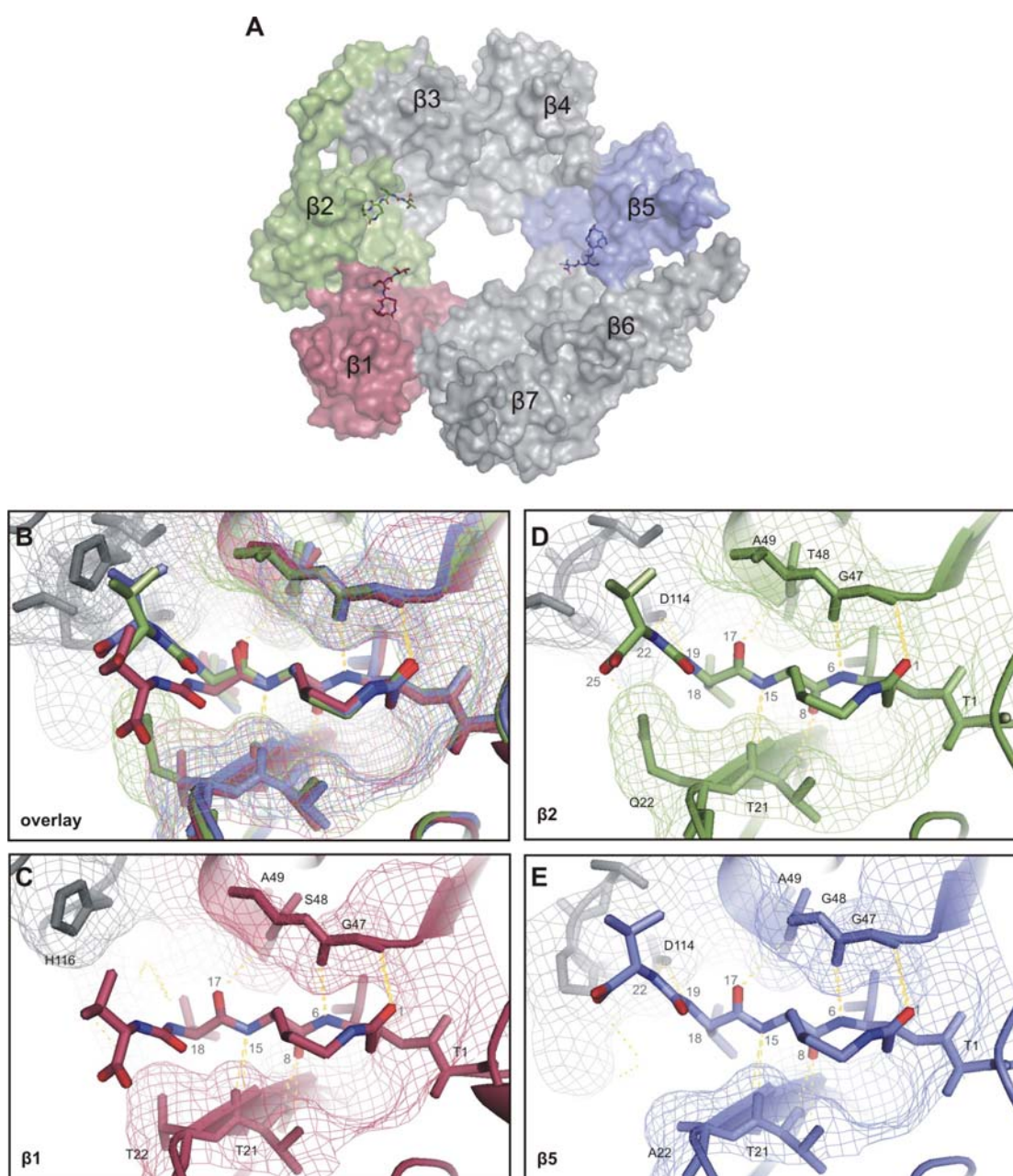


**Figure 15. Affinities of SylA (-derivatives) explained by crystallographic data**

**(A)** Conformation of one ring of seven  $\beta$  subunits from the side of the inner cavity of the 20S core proteasome. Three molecules of SylA bound to the catalytic subunits:  $\beta 1$  (red),  $\beta 2$  (green), and,  $\beta 5$  (blue) are shown. Please note that the tail of SylA interacts with the adjacent subunit.

**(B)** Overlay of SylA bound to the three catalytic subunits. Please note the distinct confirmation of the tail of SylA bound to  $\beta 1$  (red).

**(C)** SylA bound to  $\beta 1$ . SylA (middle, ball-and-stick) is bound to Thr1 (T1) of the  $\beta 1$  subunit (red). Hydrogen bonding between SylA and T21, G47 and S48 exist, but H116 of the adjacent  $\beta 2$  subunit (grey) pushes the tail of SylA downwards, preventing hydrogen bonding with D114 of the adjacent subunit.

**(D)** SylA bound to  $\beta 2$ . SylA (middle, ball-and-stick) is bound to Thr1 (T1) of the  $\beta 2$  subunit (green). Hydrogen bonding between SylA and T21, G47, T48 of  $\beta 2$  exist, as well as with D114 of the adjacent  $\beta 3$  subunit. However, the substrate binding cleft is relatively narrow compared to that of  $\beta 1$  and  $\beta 5$ , because of the Q22 side chain.

**(E)** SylA bound to  $\beta 5$ . SylA (middle, ball-and-stick) is bound to Thr1 (T1) of the  $\beta 5$  subunit (blue). Hydrogen bonding between SylA and T21, G47, G48 of  $\beta 5$  exist, as well as with D114 of the adjacent  $\beta 6$  subunit. The substrate binding cleft is relatively wide compared to that of  $\beta 2$ , because of the small A22 side chain.

**(A-E)** Figures were made by Renier van der Hoorn.

The conformation of the valine at position 1 of the dipeptide tail of SylA contributes to the specificity for the  $\beta 2$  subunit since the SylA derivatives carrying a D-Val at this position have a reduced affinity for  $\beta 2$  (Fig. 3B). Also this observation can be explained using the crystal structure of the yeast proteasome bound to SylA (Fig. 15). The binding cleft of  $\beta 2$  is narrower compared to  $\beta 5$  because it carries glutamine at position 22 (Q22) when compared to alanine (A22) in  $\beta 5$ . The side chain of D-Val at position 1 (atom 18 in SylA) would clash with the narrow cleft of  $\beta 2$  (Fig. 15E), but not with the wider cleft of  $\beta 5$  (Fig. 15F).

Subunit selectivity might be an important aspect of SylA function. Hatsugai et al. (2009) demonstrated that the proteasome mediates the discharge of the vacuolar content into the apoplast during the hypersensitive response, triggered by avirulent *P. syringae* bacteria. Inhibition studies indicated that this is regulated through the caspase activity of the  $\beta 1$  proteasome subunit (Hatsugai et al., 2009). Consistent with this observation, SylA-producing bacteria are able to prevent early host cell death but most likely mediated by inhibition of the  $\beta 2$  and  $\beta 5$  subunits of the host proteasome. Subunit selectivity is also an important aspect of drug development since proteasome inhibitors are important anti-cancer drugs. Interestingly, SylA was found to induce apoptosis and inhibit cancer proliferation (Coleman et al., 2006) and selectively targets the proteasome, also in cancer cells that have adapted to the proteasome-targeting drug bortezomib (Clerc et al., 2009a).

### **3.2.3 SylA is required for ETI suppression but not for bacterial growth at primary infection sites**

The fact that SylA-deficient mutants trigger early cell death and associated immune responses indicates that SylA production suppresses immunity. The immune responses were absent with the double *sylC/hrcC* mutant, which was not able to translocate T3 effectors into the host (Fig. 8C). This observation excludes

the possibility that *sy/C*-induced cell death was caused by PAMPs, even though it has been demonstrated that flagellin induces hypersensitive cell death in *N. benthamiana* (Hann and Rathjen, 2007). Thus cell death triggered by *sy/C* must be produced by effectors.

That ETI can be suppressed by inhibiting the proteasome is consistent with previous reports. Hatsugai and colleagues found that silencing of the  $\beta 1$  proteasome subunit in *Arabidopsis* carrying the RPM1 immune receptor suppressed the hypersensitive cell death induced by *P. syringae* pv. *tomato* DC3000 that carries the corresponding T3 effector *avrRpm1* (Hatsugai *et al.*, 2009). Furthermore, the caspase-1 and caspase-3 inhibitors YVAD and DEVD inhibited the  $\beta 1$  catalytic subunit of the plant proteasome (Hatsugai *et al.*, 2009; Gu *et al.*, 2010) and these inhibitors were also found to inhibit early cell death induced by *P. syringae* pv. *phaseolicola* in tobacco (Del Pozo and Lam, 1998) and pv. *tabaci* in tobacco (Krzymowska *et al.*, 2007). DEVD also suppressed cell death induced by virulent *P. syringae* pv. *tabaci* in tobacco (Richael *et al.*, 2001). Taken together, these studies implicate the involvement of the proteasome in cell death triggered by *P. syringae*.

The idea that proteasome inhibition would prevent cell death seems counter-intuitive, since proteasome inhibitors generally are assumed to cause cell death. SylA alone, for example, induces apoptosis and thereby inhibits cancer proliferation in mammalian cells (Coleman *et al.*, 2006). However, medical research on proteasome inhibitors has demonstrated that proteasome inhibition can also promote cell survival or cell death, depending on the concentrations and potencies of the proteasome inhibitors used (Meiners *et al.*, 2008). When 100  $\mu$ M SylA was infiltrated into *N. benthamiana* leaves, it caused a collapse of the infiltrated tissue at day 5 (Appendix C). During *Psy* infection, however, SylA intercepts a pro-death program, implying that SylA production is carefully timed and targeted by *Psy* during infection to provide a sublethal dosis. Proteasome inhibition also seems counter-intuitive since many effectors like *avrPtoB*, *HopM1* and coronatin depend on proteasome activity to execute degradation of their host targets (Rosebrock *et al.*, 2007; Melotto *et al.*, 2006; Nomura *et al.*, 2006). The *Psy* B728a genome lacks biosynthesis genes for coronatin, but contains *avrPtoB* and *HopM1* homologs (Sarkar *et al.*, 2006; Lin *et al.*, 2006). Therefore, SylA

concentration, timing, subcellular targeting and subunit specificity may be essential parameters that act in concert with the expression of other effectors. This may be reflected in the observation that suppression of proteasome activity in the infected tissue is transient and incomplete.

The observation that *sy/C* mutants grow as fast as WT bacteria demonstrates the striking ability of *Psy* to survive in dead host tissue, despite the widely accepted view that the hypersensitive response suppresses pathogen survival. As a facultative saprophyte and epiphyte, *Psy* is apparently able to survive and even grow in the presence of dead host tissue, despite the likely presence of toxic components generated by immune responses of the dying host. Aggregates of *Psy* on the leaf surface are notorious for sustaining dry periods (Monier and Lindow, 2003), an ability that might also explain their survival in dead host tissue. Unaffected bacterial populations in dying host tissue were previously observed in tobacco plants infiltrated with *P. syringae* pv. *maculicola* M2 and pv. *tabaci* (Krzymowska *et al.*, 2007). Similarly, the growth rate of avirulent *P. syringae* pv. *tomato* strains is typically increased by 10- to 100-fold when inoculated on resistant *Arabidopsis* plants (e.g. Katagiri *et al.*, 2002). These data suggest that the immune response against *P. syringae* only acts by limiting the growth space, rather than by harming the bacteria.

### 3.2.3 *SylA* promotes distant colonization

The absence of significant differences in bacterial populations of WT and *sy/C* strains upon spray inoculation and syringe infiltration, despite host cell death triggered by the *sy/C* strain, was a motivation to search for additional phenotypes. This search resulted in the discovery of an important aspect in the life of *P. syringae*: the ability to colonize distant tissues. The initial discovery came from the observation that symptoms spread from WT infiltrated sites (Fig 9A-B). However, spreading from infiltrated areas was conditional and relatively rare, possibly since the inoculated leaves were too stressed by infiltrating bacteria. The toothpick inoculation of GFP-expressing strains, however, is a robust and quantifiable assay for measuring the frequency of spread from primary infection sites and enables the study of an important aspect that would not have been discovered using traditional

pathogen assays. This finding underlines the need for additional assays to identify important novel aspects of *P. syringae* pathogenicity. Pre-invasive immunity, for example, which was undetected by widely used hand infiltration methods, was revealed by spray inoculation (Melotto *et al.*, 2006).

The ability of *P. syringae* strains to colonize distant tissues has not been described before. Given their extracellular lifestyle, it seems likely that the bacteria use an apoplastic transportation route and enter the xylem. Indeed, colonization was always observed along the vascular tissues. Furthermore, *Psy* has been detected in xylem vessels of petioles and shoots of plum trees by electron microscopy (Roos and Hattingh, 1983). The ability to colonize xylem tissue is common for other pathogenic bacteria. *Xanthomonas oryzae* pathovar *oryzae*, for example, is a bacterial rice pathogen shown to colonize the vasculature (Nino-Liu *et al.*, 2006). Additionally, *Ralstonia solanacearum* colonizes the xylem of Arabidopsis and solanaceae species (Hayward, 1991; Deslandes *et al.*, 1998).

### **3.2.4 Distant colonization is common for *P. syringae***

The ability to colonize distant tissues is common to many *P. syringae* strains, including strains across different phylogroups that infect various hosts. However, not all strains with this ability do so in a manner that relies on SylA production; there are SylA-independent mechanisms that promote distant colonization. So far, suppression of proteasome activity in tissues infected with *Pta11528R* or *PthK93001* has not been seen (Fig 6B), indicating that these strains mediate distant colonization without inhibiting the host proteasome. Identification of mechanisms that other strains use to facilitate distant colonization will be important for unraveling the mechanism underlying pathogen containment.

The SylA biosynthesis cluster is common to phylogroup II strains. Interestingly, the SylA biosynthesis cluster was also found in *Psy642*, a phylogroup II strain that can grow on *N. benthamiana* but lacks a classical T3 secretion system (Clarke *et al.*, 2010). However, the SylA biosynthesis cluster was not detected in all phylogroup II strains. The polymorphic character of SylA production is common to many other virulence-related characters in *P. syringae*. Moreover, the production of other toxins and T3 effectors is remarkably

polymorphic in this species (Hwang *et al.*, 2005) and probably reflects the bacterial ability to acquire gene clusters through horizontal gene transfer and to adapt to different hosts (Lovell *et al.*, 2009).

### **3.2.5 *SylA* is required for distant colonization but not always for HR suppression**

Effector-triggered immunity (ETI) is a sophisticated mechanism that is initiated upon recognition of microbial effectors by R proteins. Resistance is the consequence of ETI activation that leads to abrogation of pathogen growth and HR induction in the infected tissue. HR typically does not extend beyond the infected cell (Jones & Dangl, 2006) and is not always a consequence of an ETI response. Nevertheless, ETI suppression might be accompanied by cell death suppression but it is difficult to differentiate between HR-associated cell death and disease symptoms since both responses share almost the same hallmarks. *SylA* promotes spreading in *Psy* B728a, *Psy* B301D-R and *Pac* A10853, but it only suppresses host cell death in *Psy* B728a. If host cell death is part of an immune response, as might be the case for B728a, then HR-cell death explains the inability of B728a *syfC* to colonize distant tissue. However this explanation does not apply for the other pathovars.

Five effectors of *Psy* B728a that were transiently expressed in *Nicotiana benthamiana* triggered HR-like cell death (Vinatzer *et al.*, 2006). However, infiltrations of *Psy* B728a itself did not trigger early cell death but late disease symptoms, suggesting that production of other effectors or *SylA* are able to suppress HR in this strain. In contrast, *Psy* B301D-R WT triggers early cell death, indicating that the effector repertoire may differ between *Psy* B728a and *Psy* B301D-R. One could hypothesize that *Psy* B728a may carry effectors that trigger proteasome-dependent cell death, whereas *Psy* B301D-R and *Pac* A10853 may carry effectors that trigger proteasome-independent cell death. This could explain why *SylA* prevents cell death in one strain but not in the others. *Psy* B64 does not trigger cell death and is able to colonize distant tissue even in the absence of *SylA*, suggesting that other effectors different than *SylA* suppress immune responses. In contrast, *SylA* promotes spreading also of the cell death-inducing

strains, indicating that cell death does not fully suppress distant colonization. Thus, SylA promotes distant colonization by suppressing immune responses different from cell death itself. These findings confirm that cell death is not necessary for host immunity (del Pozo & Lam, 1998, Chichkova *et al.*, 2004).

SA is essential for cell death activation and many components acting in the SA pathway are disease related. Interestingly, *Psy* B728a *sy/C* triggers the same early cell death phenotype in *NahG* and WT plants. However *sy/C*-GFP bacteria are able to colonize distant tissue in *NahG* plants (Fig. 14D), indicating that *sy/C*-induced cell death is independent of SA signaling whereas distant colonization is SA dependent. SA mediated-immunity might be accompanied by cell death to cause pathogen containment. This is consistent with previous results where *Psy* B64 *sy/C* does not trigger cell death but is able to colonize distant tissue almost as good as WT strains such as *Psy* B301D-R which triggers early cell death (Fig. 12D). Overall these data indicate that cell death and distant colonization are unrelated, although cell death can assist in the containment of the pathogen.

### 3.2.6 A model for pathogen containment and distant colonization

From the data described above, the following mechanistic model for SylA action is proposed (Fig. 16). *Psy sy/C* bacteria are stopped from colonizing distant tissues by two barriers. The hypersensitive immune response at the primary infection site, triggered by *sy/C*, produces a local barrier (Fig. 16A, red triangles). This local barrier is associated with the release of the host cellular content into the apoplast (Hatsugai *et al.*, 2009) and is triggered by T3 effectors (ETI) since the hypersensitive immune response is absent in the *hrcC/sy/C* double mutant (Fig. 8C).

In addition to hypersensitive immune responses, *sy/C* bacteria also trigger DAR, which forms a second barrier that prevents distance colonization (Fig. 16A). The existence of this second barrier was demonstrated by the inability of WT-GFP bacteria to colonize distant tissues in tissue adjacent to *sy/C*-infiltrated regions (Fig. 13B). DAR requires SA signaling, since the suppression of WT-GFP spreading in DAR tissue is absent in *NahG* plants (Fig. 14A), and BTH-treatment is sufficient to suppress distant colonization of WT-GFP bacteria (Figure 13C).

WT bacteria are able to suppress ETI and DAR by producing SylA. SylA production might prevent host cell death and associated immune responses (Fig. 16B). Inhibition of the proteasome prevents the fusion of the vacuolar membrane with the plasma membrane and the release of the vacuolar content into the apoplast (Hatsugai *et al.*, 2009). The absence of the hypersensitive cell death may reduce or delay the signals that trigger DAR on adjacent tissue. In addition to suppressing local immune responses, SylA is able to migrate from the primary infection site through the vascular tissue and prevent remaining DAR on a distance by suppressing SA signaling. One mechanistic explanation might be that SylA prevents the turnover of phosphorylated NPR1, which is required for SA-induced gene expression, including *PR1* (Spoel *et al.*, 2009). Indeed, the *npr1* mutant in *Arabidopsis* showed spreading symptoms when inoculated with *PmaES4326* (Cao *et al.*, 1994). However, also NPR1-independent signaling pathways are likely targeted by proteasome inhibition.

Although this work demonstrates that there are two barriers that prevent distant colonization and that both are suppressed by SylA-producing bacteria, the molecular mechanism that underlies pathogen containment locally and systemically remains a long standing unresolved question. The hypersensitive immune response has no effect on bacterial population levels at the primary infection site (Fig. 8D), but probably does contribute to pathogen containment given that distant colonization by *syIC-GFP* bacteria is limited even in *NahG* plants (Fig. 14D). Immune responses in DAR tissues are probably similar to metabolic changes described for SAR, which includes the accumulation of PR proteins and phytoalexins (Vlot *et al.*, 2009). However, how these components act in concert to prevent distant colonization remains subject to further studies.



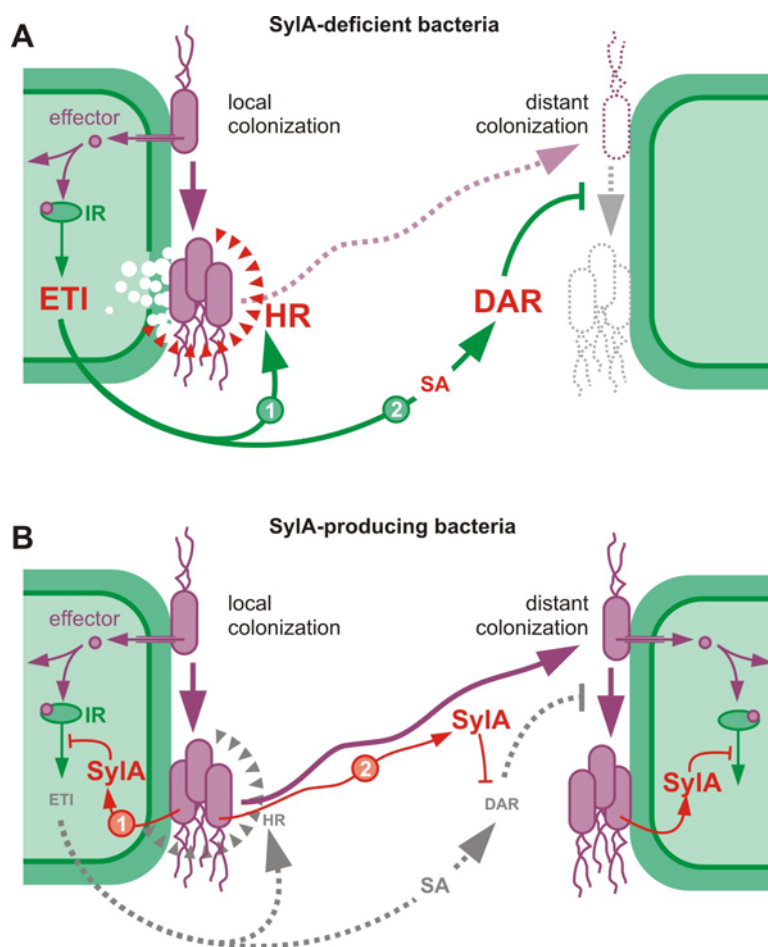


**Figure 16. Model of SyIA action**

**(A)** SyIA-deficient *sy/C* bacteria inject effectors using the type-III secretion system. These effectors initiate ETI, probably through the action of immune receptors (IRs). ETI triggers both local cell death and immune responses (HR), as well as distant acquired resistance (DAR), which is dependent on SA signalling. Distant colonization is prevented both locally by HR (1) and at a distance by DAR (2). Only some bacteria can escape (dashed purple line) to establish a few distant colonies in the absence of DAR.

**(B)** SyIA-producing bacteria secrete SyIA, which prevents HR at the primary infection site by blocking ETI (left) (1). In addition, SyIA may diffuse over a distance and prevent DAR induced by SA signalling (2). As a consequence, SyIA-producing bacteria can escape from primary infection sites and colonize distant tissue. ETI, HR and, DAR are suppressed (grey dashed lines).

In conclusion, a novel and important aspect in the life of *P. syringae* facilitated by the production of the small molecule proteasome inhibitor SyIA was uncovered. SyIA suppresses ETI SA-dependent immune response at a distance, facilitating the escape of the bacteria from primary infection sites, and thus enabling colonization of distant tissues. The ability to spread through the vascular system and thereby achieve distant colonization was a long overlooked property of

## DISCUSSION

this pathogen, and is likely to be a key aspect in the life of this pathogen in the field and in nature.

## 4 EXPERIMENTAL PROCEDURES

### 4.1 Chemicals

The AOMK P2 position inhibitor library that was used for VPE screening experiments has been previously published (Berger *et al.*, 2006) and was kindly provided by Mathew Bogyo as well as AB13, AB46, AB50, AB53, AB69, AMS-101, JCP550 and D-AOMK. The inhibitors described in this work were obtained from different sources: E-64 and MG132 were from Sigma. Epoxomicin was from BioMol. DEVD-cho and YVAD-cmk were purchased from Merk. The synthesis of MV151, SylA and RhSylA has been described previously (Verdoes *et al.*, 2006; Clerc *et al.*, 2009a; 2009b). Synthesis of MVB003, MVB070 and MVB072 has been published in a thesis (Verdoes, 2008) and N3 $\beta$ 1 has been described previously (Britton *et al.*, 2009). These probes as well as the inhibitors N3  $\beta$ 1 and N3  $\beta$ 5 were kindly provided by Hermen Overkleeft. Synthesis of SylA derivatives will be described elsewhere (Clerc & Kaiser, unpublished results).

### 4.2 Plant materials and growth conditions

*Arabidopsis thaliana* ecotype Columbia plants were grown in a growth chamber at 24°C (day)/20 °C (night) under 12-hour light regime. Rosette leaves of 4 to 6-week-old plants were used for protein extraction. *Arabidopsis*  $\gamma$ VPE-OE,  $\gamma$ VPE-KO and quadruple VPE-KO lines have been previously described (Rojo *et al.*, 2003, Gruis *et al.*, 2004). 3-4 week old *Nicotiana benthamiana* plants were grown under a 14 hour light regime at 20 °C - 24 °C, before flowering. *Phaseolus vulgaris* plants (cultivar Bush Blue Lake 274) were grown under a 10 hour light regime at 22 °C and primary leaves of 3-4 week old plants were use for inoculations.

### 4.3 Bacterial strains

*Pseudomonas syringae* wild-type strains were kindly provided by David Guttman, Jim Alfano, Jane Parker and Silke Robatzek (Table 1, appendix D). *sy/C* mutants were generated in Robert Dudler's lab as previously described (Amrein *et al.*, 2004).

#### 4.4 *In vitro* labeling of leaf extracts

Arabidopsis proteins were extracted by grinding seven rosette leaves into 700  $\mu$ l water. Leaf disks of 16 mm diameter of *N. benthamiana* (infected) leaves were ground in 100  $\mu$ l water containing 2  $\mu$ M DTT. The extract was cleared by centrifugation (2 min at 16,000g). Labelling was usually done by incubating ~100  $\mu$ g protein in 50  $\mu$ l containing 67mM Tris buffer pH 7 (for proteasome) or 67mM NaAc pH 5 (for VPE), L-cysteine (65 nM) or DTT (10  $\mu$ M) in the presence of 1  $\mu$ M and 2  $\mu$ M probe for 2 hours at room temperature (22-25 °C) in the dark. Equal volumes of DMSO were added to the no-probe controls. The extract was mixed with 4x SDS-PAGE loading buffer containing  $\beta$ -mercaptoethanol, and separated on 12% SDS gels (~ 10  $\mu$ g protein per lane). Labeled proteins were visualized by in-gel fluorescence scanning using a Typhoon 8600 scanner (Molecular Dynamics) with excitation and emission at 532 and 580 nm, respectively. Alternatively, the Fujifilm FLA6000 fluorescence scanner was used. Fluorescent signals were quantified with ImageQuant 5.2 (Molecular Dynamics). Competition or inhibition assays were done by pre-incubating protein extracts with competitor or inhibitor molecules for 30 minutes before labelling.

#### 4.5 Generation of transgenic *Pseudomonas* strains

*Pseudomonas syringae* strains were transformed with pFK78 (Kaschani *et al.*, unpublished) by electroporation and selected on gentamycin (10  $\mu$ g/ml). Several fluorescent colonies were used for infection and were found to behave similarly. Pac WT-GFP was transformed with cosmid pPL3syl carrying *syIA-E* genes of PssB301D-R (Ramel *et al.*, 2009) by triparental mating using a helper *E. coli* strain carrying pRK600 and selected with tetracyclin (10  $\mu$ g/ml), gentamycin (10  $\mu$ g/ml) and rifampicin (25  $\mu$ g/ml) (Ramel *et al.*, 2009).

#### 4.6 *Pseudomonas* infection assays

Bacteria were grown overnight in 10 ml NYG medium (5 g/l pepton, 5 g/l yeast extract, 2% glycerol), centrifuged and resuspended into 10 mM MgCl<sub>2</sub>. The OD<sub>600</sub> was measured and bacteria were diluted to OD<sub>600</sub> = 0.0002 (~2x10<sup>5</sup> bacteria/ml) in 10 mM MgCl<sub>2</sub>. Bacteria were infiltrated into *N. benthamiana* or bean leaves with a

1 ml syringe without needle. For spray inoculation, bacteria were diluted until  $OD_{600} = 0.2$  into 10 mM  $MgCl_2$ , 0.02% Silwet L-77 (Lehle seeds) and sprayed onto *N. benthamiana*, bean or Arabidopsis leaves using a 10 ml perfume spray flask. For toothpick inoculation, bacteria were taken from fresh plates with a toothpick and punched through an expanded leaf of *N. benthamiana* or bean. Pictures were taken at 5-10 dpi using fluorescence microscopy and whether or not distant colonies occurred was scored for each toothpick. The percentage of distant colonization was calculated for at least 10 toothpicks by dividing the number of times that distant colonization was scored by the number of times that colonization occurred at the toothpick inoculation site itself. The average and standard error of mean was calculated from independent biological assays.

Irrespective of the inoculation type, plants were kept under high humidity in a container with a transparent cover in the lab or climate chamber. Leaves were examined at various time points. Lactophenol trypan blue stain was performed as described previously (Koch & Slusarenko, 1990). GFP-fluorescence was detected by a Leica MZ16FA using the GFP3 filter. All experiments were done with identical acquisition settings.

#### **4.7 Quantification of bacterial densities**

Endophytic bacterial populations were determined from opposite leaf halves infiltrated with WT or *sy/C* strains as follows. Leaves were surface-sterilized in 15%  $H_2O_2$  for 5 min on a shaker at 200 rpm. Leaf disks (13 mm diameter) from two infiltrated leaves were combined and ground in 1 ml 10 mM  $MgCl_2$  using mortar and pestle or in a Retsch Mixer Mill MM 301 grinder. 10  $\mu$ l droplets of a serial 10-fold dilution series were put on selective agar medium and colonies were counted after 2 days of incubation at 28 °C. This procedure was followed for at least three sets of infiltrated leaves for each biological experiment. Samples for measuring the spread of bacterial populations from toothpick inoculation sites were taken after surface sterilization by removing a 4 mm diameter leaf disc containing the toothpick inoculation site, and taking a 25 mm diameter concentric leaf disk for determining the bacterial titer as described above. This procedure was done on at least 5 independent leaves for each biological experiment.

#### 4.8 *Hyaloperonospora* infection assays

*H. arabidopsidis* Noco1, Cala2 and Waco2 isolates used in this study have been described previously (Feys *et al.*, 2005, Rehmany *et al.*, 2000). 2-3-week-old plants grown at 14 °C or 20 °C were spray-inoculated with a suspension of  $4 \times 10^4$  conidiospores/ml and transferred to optimal conditions for pathogen growth (18 °C). To determine pathogen conidiospore numbers, samples were harvested 6 d after inoculation, vortexed in water, and spores were counted in a hemocytometer using a light microscope. The development of *Hpa* hyphae in leaf tissues were monitored 7 d after infection by staining with lactophenol trypan blue (Aarts *et al.*, 1998).

#### 4.9 Agroinfiltration of VPEs

The ORF of Arabidopsis VPEs were amplified by RT-PCR, cloned into pFK26 (Shabab *et al.*, 2008) and sequenced. Expression cassettes containing correct ORF sequences were shuttled into binary vector pTP5 (Shabab *et al.*, 2008), resulting in the vectors pFK133 ( $\alpha$ VPE), pFK134 ( $\beta$ VPE), pFK135 ( $\gamma$ VPE) and pFK136 ( $\delta$ VPE) (F. Kaschani, unpublished data). *Agrobacterium tumefaciens* strain GV3101 was transformed with binary vectors and used for agroinfiltration as described previously (Van der Hoorn *et al.*, 2000). *Agrobacterium* was grown overnight at 28°C in 10 ml Luria-Bertani medium containing 50 µg/ml kanamycin and 50 µg/ml rifampicin. The culture was centrifuged (10 min, 3000g) and the bacterial pellet was resuspended in 10 mM MgCl<sub>2</sub>, and 1 mM acetosyringone to a final OD of 2. *Agrobacterium* cultures containing binary protease expression vectors were mixed with *Agrobacterium* cultures containing binary expression vector for silencing inhibitor p19 (Voinnet *et al.*, 2003). *Agrobacterium* cultures were infiltrated into 5-week-old *N. benthamiana* plants using a syringe without a needle. Infiltrated leaves were collected at 5 dpi and ground in a mortar with water. Extract was centrifuged and the supernatant was used for further experiments.

#### 4.10 BTH treatment

The leaf surface of *Arabidopsis* and *N. benthamiana* plants was sprayed using a perfume sprayer (Roth) with 300 µM BTH (Bion, Syngenta) and 0.01% Silwet (Lenne Seeds) until the droplets ran off. As a control plants were sprayed with sterile water containing 0.01% Silwet (Lenne Seeds).

#### 4.11 PCR and RT-PCR

For the detection of the *sylA*-biosynthesis cluster, a 585 bp fragment of the *sylC* gene was amplified by colony PCR from *Pseudomonas* strains with the following primers: 5'-CCAGGGGAGTTATTCATC G-3' and 5'-TTCATTTCTACCCACGTCC-3'. For RT-PCR, RNA of infected *N. benthamiana* leaves was isolated using the Qiagen RNeasy mini kit and cDNA was synthesized using Superscript II reverse transcriptase (Invitrogen) using oligo(dT) 20 primer (Invitrogen) according to the instructions of the manufacturer. cDNA was used as a template for PCR using primer pairs for *NbHin1*: 5'-GAGCCATGCCGGAATCCAAT-3' and

5'-GCTACCAATCAAGATGGCATCTGG-3';

*NbPR1*: 5'-AATATCCCCTCTTGCCG-3' and

5'-CCTGGAGGATCATAGTTG-3'

*NbActin*: 5'-TGGACTCTGGTGATGGTGTC-3' and

5'-CCTCCAATCCAAACACTGTA-3'.

## 5 REFERENCES

- Adams, J., and Kauffman, M.** (2004) Development of the proteasome inhibitor Velcade™ (Bortezomib). *Cancer Invest.* **22**, 304-311.
- Allen, R.L., Bittner-Eddy, P.D., Grenville-Briggs, L.J., Meitz, J.C., Rehmany, A.P., Rose, L.E., and Beynon, J.L.** (2004) Host-parasite coevolutionary conflict between *Arabidopsis* and downy mildew. *Science* **306**, 1957-1960.
- Amrein, H., Makart, S., Granado, J., Shakya, R., Schneider-Pokorny, J., and Dudler, R.** (2004) Functional analysis of genes involved in the synthesis of Syringolin A by *Pseudomonas syringae* pv. *syringae* B301D-R. *Mol. Plant-Microbe Interact.* **17**, 90-97.
- Baehrecke, E.H.** (2002) How death shapes life during development. *Nat. Rev. Mol. Cell Biol.* **3**, 779-787.
- Bender, C. L., Alarcon-Chaidez, F., and Gross, D. C.** (1999) *Pseudomonas syringae* phytotoxins: mode of action, regulation, and biosynthesis by peptide and polyketide synthetases. *Microbiol. Mol. Biol. Rev.* **63**, 266-292.
- Berger, A.B., Witte, M.D., Denault, J.B., Sadaghiani, A.M., Sexton, K.M.B., Salvesen, G.S., and Bogyo, M.** (2006) Identification of early intermediates of caspase activation using selective inhibitors and activity-based probes. *Mol. Cell.* **23**, 509-521.
- Bolduc, N., and Brisson, L.F.** (2002) Antisense downregulation of NtBI-1 in tobacco BY-2 cells induces accelerated cell death upon carbon starvation. *FEBS Lett.* **532**, 111-114.
- Bozhkov, P.V., Filonova, L.H., Suarez, M.F., Helmerson, A., Smertenko, A.P., Zhivotovsky, B., and von Arnold, S.** (2004) VEIDase is a principal caspase-like activity involved in plant programmed cell death and essential for embryonic pattern formation. *Cell Death Diff.* **11**, 175-182.
- Britton, M., Lucas, M.M., Downey, S.L., Screen, M., Pletnev, A.A., Verdoes, M., Tokhunts, R.A., Amir, O., Goddard, A.I., Pelphrey, P.M., Wright, D.L., Overkleeft, H.S., and Kisselev, A.F.** (2009) Selective inhibitor of proteasome's caspase-like sites sensitizes cells to specific inhibition of chymotrypsin-like sites. *Cell* **16**, 1278-1289.
- Cao, H., Bowling, S. A., Gordon, S., and Dong, X.** (1994) Characterization of an *Arabidopsis* mutant that is nonresponsive to inducers of systemic acquired resistance. *Plant Cell* **6**, 1583-1592.
- Chang, Y.T., Germain, H., Wiermer, M., Bi, D., Xu, F., Garcia, A.V., Wirthmueller, L., Despres, C., Parker, J.E., Zhang, Y., and Li, X.** (2009) Nuclear pore complex component MOS7/Nup88 is required for innate immunity and nuclear accumulation of defense regulators in *Arabidopsis*. *Plant Cell*, **21**, 2503-2516.
- Chichkova, N.V., Kim, S.H., Titova, E.S., Kalkum, M., Morozov, V.S., Rubtsov, Y.P., Kalinina, N.O., Taliansky, M.E., and Varpetian, A.B.** (2003) A plant caspase-like protease activated during the hypersensitive response. *Plant Cell* **16**, 157-171.
- Chichkova, N.V., Shaw, J., Galiullina, R.A., Drury, G.E., Tuzhikov, A.I., Kim, S.H., Kalkum, M., Hong, T.B., Gorshkova, E.N., Torrance, L., Vartapetian, A.B., and Taliansky, M.** (2010) Phytaspase, a relocatable cell death promoting plant protease with caspase specificity. *EMBO J.* **29**, 1149-1161.
- Chini, A., Fonseca, S., Fernandez, G., Adie, B., Chico, J. M., Lorenzo, O., Garcia-Casado, G., Lopez-Vidriero, I., Lozano, F. M., Ponce, M. R., Micol, J. L., and Solano, R.** (2007) The JAZ family of repressors is the missing link in jasmonate signaling. *Nature* **448**, 666-671.



- Clerc, J., Florea, B. I., Kraus, M., Groll, M., Huber, R., Bachmann, A. S., Dudler, R., Driessen, C., Overkleef, H. S., and Kaiser, M. (2009a) Syringolin A selectively labels the 20 S proteasome in murine EL4 and wild-type and bortezomib-adapted leukaemic cell lines. *Chembiochem*. **10**, 2638-43.
- Clerc, J., Groll, M., Illich, D. J., Bachmann, A.S., Huber, R., Schellenberg, B., Dudler, R., and Kaiser, M. (2009b) Synthetic and structural studies in syringolin A and B reveal critical determinants of selectivity and potency of proteasome inhibition. *Proc. Natl. Acad. Sci. USA*. **106**, 6507-6512.
- Coates, M.E., and Beynon, J.L. (2010) Hyaloperonospora arabidopsidis as a pathogen model. *Annu. Rev. Phytopathol.* **48**, 329-345.
- Cochet, N., and Widehem, P. (2000) Ice crystallization by *Pseudomonas syringae*. *Appl. Microbiol. Biotechnol.* **54**, 153-161.
- Coleman, C.S., Rocetes, J.P., Park, D.J., Wallick, C.J., Warn-Cramer, B.J., Michel, K., Dudler, R., and Bachmann, A.S. (2006) Syringolin A, a new plant elicitor from the phytopathogenic bacterium *Pseudomonas syringae* pv. *syringae*, inhibits the proliferation of neuroblastoma and ovarian cancer cells and induces apoptosis. *Cell Prolif.* **39**, 599-609.
- Coffeen, W.C., and Wolpert, T.J. (2004) Purification and characterization of serine proteases that exhibit caspase-like activity and are associated with programmed cell death in *Avena sativa*. *Plant Cell* **16**, 857-873.
- Cravatt, B.F., Wright, A.T., and Kozarich, J.W. (2008) Activity-based protein profiling: from enzyme chemistry to proteomic chemistry. *Ann. Rev. Biochem.* **77**, 838-414.
- Cunnac, S., Lindeberg, M., and Collmer, A. (2009) *Pseudomonas syringae* type III secretion system effectors: repertoires in search of functions. *Curr. Opin. Microbiol.* **12**, 53-60.
- del Pozo, O., and Lam, E. (1998) Caspases and programmed cell death in the hypersensitive response of plants to pathogens. *Curr. Biol.* **8**, 1129-1132.
- Demon, D., van Damme, P., Vanden Berghe, T., Vandekerckhove, J., Declercq, W., Gavaert, K., and Vandenabeele, P. (2009) Caspase substrates: easily caught in deep waters? *Trends Biotech.* **27**, 680-688.
- Deslandes, L., Pileur, F., Liaubet, L., Camut, S., Can, C., Williams, K., Holub, E., Arlat, M., and Marco, Y. (1998) Genetic characterization of *RRS1*, a recessive locus in *Arabidopsis thaliana* that confers resistance to the bacterial soilborne pathogen *Ralstonia solanacearum*. *Mol. Plant-Microbe Interact.* **11**, 659-667.
- Dick, T.P., Nussbaum, A.K., Deeg, M., Heinemeyer, W., Groll, M., Schirle, M., Keilholz, W., Stevanovic, S., Wolf, D.H., Huber, R., Rammensee, H.G., and Schild, H. (1998) Contribution of proteasomal  $\beta$ -subunits to the cleavage of peptide substrates analyzed with yeast mutants. *J. Biol. Chem.* **273**, 25637-25646.
- Doukhanina, E.V., Chen, S., van der Zalm, E., Godzik, A., Reed, J., and Dickman, M.B. (2006) Identification and functional characterization of the BAG protein family in *Arabidopsis thaliana*. *J. Biol. Chem.* **281**, 18793-18801.
- Evans, M.J., and Cravatt, B.F. (2006) Mechanism-based profiling of enzyme families. *Chem. Rev.* **106**, 3279-3301.
- Feil, H., Feil, W.S., Chain, P., Larimer, F., DiBartolo, G., Copeland, A., Lykidis, A., Trong, S., Nolan, M., Goltsman, E., Thiel, J., Malfatti, S., Loper, J.E., Lapidus, A., Detter, J.C., Land, M., Richardson, P.M., Kyrpides, N.C., Ivanova, N., and Lindow, S.E. (2005) Comparison of the complete genome sequences of *Pseudomonas syringae*

## REFERENCES

- pv. *syringae* B728a and pv. *tomato* DC3000. *Proc. Natl. Acad. Sci. USA* **102**, 11064-11069.
- Feys, B.J., Wiermer, M., Bhat, R.A., Moisa, L.J., Medina-Escobar, N., Neu, C., Cabral, A., and Parker, J.E.** (2005) Arabidopsis senescence-associated gene101 stabilizes and signals within an enhanced-disease susceptibility1 complex in plant innate immunity. *Plant Cell* **17**, 2601-2613.
- Fenteany, G., Standaert, R.F., Lane, W.S., Choi, S., Corey, E.J., and Schreiber, S.L.** (1995) Inhibition of proteasome activities and subunit-specific amino-terminal threonine modification by lactacystin. *Science* **268**, 726-731.
- Goldberg, A.L., Cascio, P., Saric, T., and Rock, K.L.** (2002) The importance of the proteasome and subsequent proteolytic steps in the generation of antigenic peptides. *Mol. Immunol.* **39**, 147-164.
- Greenberg, J.T., and Vinatzer, B.A.** (2003) Identifying type III effectors of plant pathogens and analyzing their interaction with plant cells. *Curr. Opin. Microbiol.* **6**, 20-28.
- Greenberg, J.T. and Yao, N.** (2004) The role and regulation of programmed cell death in plant-pathogen interactions. *Cell. Microbiol.* **6**, 201-211.
- Groll, M., Ditzel, L., Löwe, J., Stock, D., Bochtler, M., Bartunik, H.D., and Huber, R.** (1997) Structure of 20S proteasome from yeast at 2.4Å resolution. *Nature* **386**, 463-471.
- Groll, M., Huber, R., Moroder, L.** (2008a) The persisting challenge of selective and specific proteasome inhibition. *J. Pept. Sci.* **15**, 58-66.
- Groll, M., Schellenberg, B., Bachmann, A.S., Archer, C.R., Huber, R., Powell, T.K., Lindow, S., Kaiser, M., and Dudler, R.** (2008b) A plant pathogen virulence factor inhibits the eukaryotic proteasome by a novel mechanism. *Nature* **10**, 755-758.
- Gruis, D.F., Schulze, J., and Jung, R.** (2004) Storage protein accumulation in the absence of the vacuolar processing enzyme family of cysteine proteases. *Plant Cell* **16**, 270-290.
- Gruis, D.F., Selinger, D.A., Curran, J.M., and Jung, R.** (2002) Redundant proteolytic mechanisms process seed storage proteins in the absence of seed-type members of the vacuolar processing enzyme family of cysteine proteases. *Plant Cell.* **14**, 2863-2882.
- Gu, C., Kolodziejek, I., Misas-Villamil, J., Shindo, T., Colby, T., Verdoes, M., Richau, K., Schmidt, J., Overkleeft, H., and Van der Hoorn, R. A. L.** (2010) Proteasome activity profiling: a simple, robust and versatile method revealing subunit-selective inhibitors and cytoplasmic, defence-induced proteasome activities. *Plant J.* **62**, 160-170.
- Guo, M., Tian, F., Wamboldt, Y., and Alfano, J.R.** (2009) The majority of the type III effector inventory of *Pseudomonas syringae* pv. *tomato* DC3000 can suppress plant immunity. *Mol. Plant-Microbe Interact.* **9**, 1069-1080.
- Hann, D.R., and Rathjen, J.P.** (2007) Early events in the pathogenicity of *Pseudomonas syringae* on *Nicotiana benthamiana*. *Plant J.* **48**, 607-618.
- Hara-Nishimura, I.** (2009) A novel membrane-fusion-mediated plant immunity against bacterial pathogens. *Gene Dev* **23**, 2496-2506.
- Hara-Nishimura, I., Hatsugai, N., Nakaune, S., Kuroyanagi, M., and Nishimura, M.** (2005) Vacuolar processing enzyme: an executor of plant cell death. *Curr. Opin. Plant Biol.* **8**, 404-408.
- Hara-Nishimura, I., Inoue, K., and Nishimura, M.** (1991) A unique vacuolar processing enzyme responsible for conversion of several proprotein precursors into the mature forms. *FEBS Lett.* **294**, 89-93.

- Hara-Nishimura, I., Nishimura M., Matsubara, H., and Akazaba, T.** (1982) Suborganellar localization of proteinase catalyzing the limited hydrolysis of pumpkin globulin. *Plant Physiol.* **70**, 699-703.
- Hara-Nishimura, I., Shimada, T., Hatano, K., Takeuchi, Y. and Nishimura M.** (1998) Transport of storage proteins to protein storage vacuoles is mediated by large precursor-accumulating vesicles. *Plant Cell.* **10**, 825-836.
- Hara-Nishimura, I. Takeuchi, Y., Inoue, K., and Nishimura, M.** (1993) Vesicle transport and processing of the precursor to 2S albumin in pumpkin. *Plant J.* **4**, 793-800.
- Hatsugai, N., Iwasaki, S., Tamura, K., Kondo, M., Fuji, K., Ogasawara, K., Nishimura, M., and Hara-Nishimura, I.** (2009) A novel membrane-fusion-mediated plant immunity against bacterial pathogens. *Gene Dev.* **23**, 2496-2506.
- Hatsugai, N., Iwasaki, S., Tamura, K., Kondo, M., Fuji, K., Ogasawara, K., Nishimura, M., and Hirano, S.S., and Upper, C.D.** (2000) Bacteria in the leaf ecosystem with emphasis on *Pseudomonas syringae* - a pathogen, ice nucleus, and epiphyte. *Microbiol. Mol. Biol. Rev.* **64**, 624-653.
- Hatsugai, N., Kuroyanagi, M., Nishimura, M., and Hara-Nishimura, I.** (2006) A cellular suicide strategy of plants: vacuole-mediated cell death. *Apoptosis* **11**, 905-911.
- Hatsugai, N., Kuroyanagi, M., Yamada, K., Meshi, T., Tsuda, S., Kondo, M., Nishimura, M., Hara-Nishimura, I.** (2004) A plant vacuolar protease, VPE, mediates virus-induced hypersensitive cell death. *Science* **305**, 855-858.
- Hayward, A. C.** (1991) Biology and epidemiology of *Pseudomonas solanacearum*. *Annu. Rev. Phytopathol.* **29**, 65-87.
- Hirano, S.S., and Upper, C.D.** (2000) Bacteria in the leaf ecosystem with emphasis on *Pseudomonas syringae* - a pathogen, ice nucleus, and epiphyte. *Microbiol. Mol. Biol. Rev.* **64**, 624-653.
- Hirano, S.S., Baker, L.S., and Upper, C.D.** (1996) Raindrop momentum triggers growth of leaf-associated populations of *Pseudomonas syringae* on field-grown snap bean plants. *Appl. Environ. Microbiol.* **62**, 2560-2566.
- Hofius, D., Tsitsigiannis, D.I., Jones, J.D.G., and Mundy, J.** (2007) Inducible cell death in plant immunity. *Semin. Canc. Biol.* **17**, 166-187.
- Holub, E.B., Beynon, J.L., and Crute, I.R.** (1994) Phenotypic and genotypic characterization of interactions between isolates of *Peronospora parasitica* and accessions of *Arabidopsis thaliana*. *Mol. Plant-Microbe Interact.* **7**, 223-239.
- Hou, S., Yang, Y., and Zhou, J. M.** (2009) The multilevel and dynamic interplay between plant and pathogen. *Plant Sign. Behav.* **4**, 282-293.
- Huang, L., and Chen, C. H.** (2009) Proteasome regulators: activators and inhibitors. *Curr Med Chem.* **16**, 931-939.
- Imker, J. J., Walsh, C. T., and Wuest, W. M.** (2009) SylC catalyzes ureido-bond formation during biosynthesis of the proteasome inhibitor Syringolin A. *J. Am. Chem. Soc.* **131**, 18263-18265.
- Jin, C., and Reed, J.C.** (2002) Yeast and apoptosis. *Nat Rev. Mol. Cell. Biol.* **3**, 453-459.
- Jones, J.D., and Dangl, J.L.** (2006) The plant immune system. *Nature* **444**, 323-329.
- Kaffarnik F. A., Jones, A. M., Rathjen, J P., and Peck, S. C.** (2009) Effector proteins of the bacterial pathogen *Pseudomonas syringae* alter the extracellular proteome of the host plant *Arabidopsis thaliana*. *Mol. Cell. Proteomics* **8**, 145-156.

- Kaschani, F., Verhelst, S.H.L., Van Swieten, P.F., Verdoes, M., Wong, C.S., Wang, Z., Kaiser, M., Overkleeft, H.S., Bogyo, M., and Van der Hoorn, R.A.L.** (2009) Minitags for small molecules: detecting targets of reactive small molecules in living plant tissues using 'click chemistry'. *Plant J.* **57**, 373-385.
- Katagiri, F., Thilmony, R. and He, S.Y.** (2002) The *Arabidopsis-Pseudomonas syringae* interaction. In *The Arabidopsis Book*, C.R.Somerville and E.M.Meyerowitz, eds. (Rockville, MD, USA: American Society of Plant Biologists).
- Kato, D., Boatright, K.M., Berger, A.B., Nazif, T., Blum, G., Ryan, C., Chehade, K.A.H., Salvesen, G., and Bogyo, M.** (2005) Activity based probes that target diverse cysteine protease families. *Nature Chem. Biol.* **1**, 33-38.
- Kinoshita, T., Yamada, K., Hiraiwa, N., Kondo, M., Nishimura, M., and Hara-Nishimura, I.** (1999) Vacuolar processing enzyme is up-regulated in the lytic vacuoles of vegetative tissues during senescence and under various stressed conditions. *Plant J.* **19**, 43-53.
- Kohler, A., Schwindling, S., and Conrath, U.** (2002) Benzothiadiazole-induced priming for potentiated responses to pathogen infection, wounding, and infiltration of water into leaves requires the NPR1/NIM1 gene in *Arabidopsis*. *Plant Physiol.* **128**, 1046-1056.
- Kolodziejek, I., and Van der Hoorn, R. A. L.** (2010) Mining the active plant proteome in plant science and biotechnology. *Curr. Opin. Biotechnol.* **21**, 225-233.
- Krzyszowska, M., Konopka-Postupolska, D., Sobczak, M., Macioszek, V., Ellis, B.E., and Hennig, J.** (2007). Infection of tobacco with different *Pseudomonas syringae* pathovars leads to distinct morphotypes of programmed cell death. *Plant J.* **50**, 253-264.
- Kurepa, J., and Smalle, J.A.** (2008) Structure, function and regulation of plant proteasomes. *Biochimie* **90**, 324-335.
- Kuroyanagi, M., Nishimura, M., and Hara-Nishimura, I.** (2002) Activation of *Arabidopsis* vacuolar processing enzyme by self-catalytic removal of an auto-inhibitory domain of the C-terminal propeptide. *Plant Cell Physiol.* **43**, 143-151.
- Kuroyanagi, M., Yamada, K., Hatsugai, N., Kondo, M., Nishimura, M., and Hara-Nishimura, I.** (2005) Vacuolar processing enzyme is essential for mycotoxin-induced cell death in *Arabidopsis thaliana*. *J. Biol. Chem.* **280**, 32914-32920.
- Labes M., Pühler A., and Simon R.** (1990) A new family of RSF1010-derived expression and lac-fusion broad-host-range vectors for gram-negative bacteria. *Gene* **89**, 37-46.
- Lam, E.** (2005) Vacuolar proteases livening up programmed cell death. *Trends Cell Biol.* **15**, 124-127.
- Lin, N. C., Abramovitch, R. B., Kim, Y. J., and Martin, G. B.** (2006) Diverse AvrPtoB homologs from several *Pseudomonas syringae* pathovars elicit Pto-dependent resistance and have similar virulence activities. *Appl. Environm. Microbiol.* **72**, 702-712.
- Liu, Y., Patricelli M. P., Cravatt, B.F.** (1999) Activity-based protein profiling: The serine hydrolases. *Proc. Natl. Acad. Sci. USA.* **96**, 14694-14699.
- Meiners, S., Ludwig, A., Stangl, V., and Stangl, K.** (2008) Proteasome inhibitors: poisons and remedies. *Med. Res. Rev.* **28**, 309-327.
- Melotto, M., Underwood, W., and He, S.H.** (2008) Role of stomata in plant innate immunity and foliar bacterial diseases. *Ann. Rev. Phytopathol.* **46**, 101-122.
- Melotto, M., Underwood, W., Koczan, J., Nomura, K., and He, S.H.** (2006). Plant stomata function in innate immunity against bacterial invasion. *Cell* **126**, 969-980.

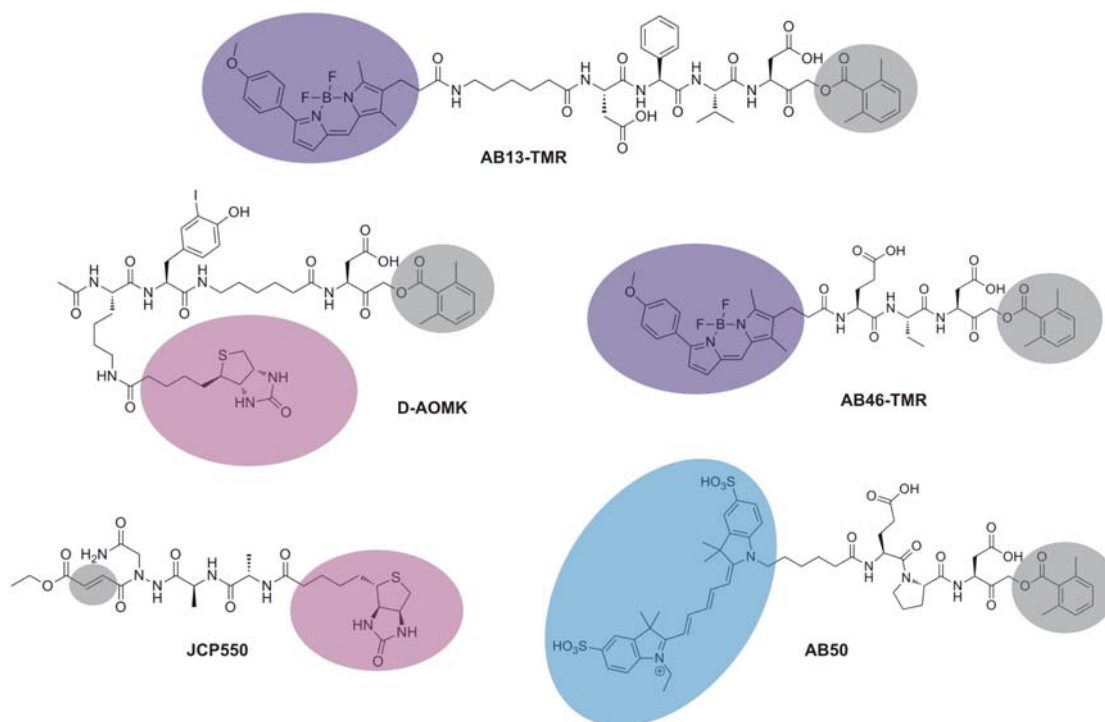
- Meng, L., Mohan, R., Kwok, B. H. B., Eloffson, M., Sin, N., and Crews, C. M.** (1999) Epoxomicin, a potent and selective proteasome inhibitor, exhibits *in vivo* antiinflammatory activity. *Proc. Natl. Acad. Sci USA* **96**, 10403-10408.
- Monier, J.M., and Lindow, S.E.** (2003) Differential survival of solitary and aggregated bacterial cells promotes aggregate formation on leaf surfaces. *Proc. Natl. Acad. Sci. USA*. **100**, 15977-15982.
- Nakaune, S., Yamada, K., Kondo, M., Kato, T., Tabata, S., Nishimura, M., and Hara-Nishimura, I.** (2005) A vacuolar processing enzyme,  $\delta$ VPE, is involved in seed coat formation at the early stage of seed development. *Plant Cell* **17**, 876-887.
- Nicholson, D.W.** (1999) Caspase structure, proteolytic substrates, and function during apoptotic cell death. *Cell Death Diff.* **6**, 1028-1042.
- Nino-Liu, D. O., Ronald, P. C., and Bogdanove, A. J.** (2006) *Xanthomonas oryzae* pathovars: model pathogens of a model crop. *Mol. Plant Pathol.* **7**, 303-324.
- Noel, L.D., Cagna, G., Stuttmann, J., Wirthmuller, L., Betsuyaku, S., Witte, C.-P., Bhat, R., Pochon, N., Colby, T., and Parker, J.E.** (2007) Interaction between SGT1 and cytosolic/nuclear HSC70 chaperones regulates Arabidopsis immune responses. *Plant Cell* **19**, 4061-4076.
- Nomura, K., DebRoy, S., Lee, Y.H., Pumplin, N., Jones, J. and He, S.Y.** (2006) A bacterial virulence protein suppresses host innate immunity to cause plant disease. *Science* **313**, 220-223.
- Okun, I., Malarchuk, S., Dubrovskaya, E., Khvat, A., Tkachenko, S., Kysil, V., Kravchenko, D., and Ivachtchenko, A.** (2006) Screening for caspase-3 inhibitors: effect of a reducing agent on identified hit chemotypes. *J. Biomol. Screen.* **11**, 694-703.
- Qiao, H., Chang, K. N., Yazaki, J., and Ecker, J. R.** (2009) Interplay between ethylene, ETP1/ETP2 F-box proteins, and degradation of EIN2 triggers ethylene responses in Arabidopsis. *Genes Dev.* **23**, 512-521.
- Ramel, C., Tobler, M., Meyer, M., Bigler, L., Ebert, M.O., Schellenberg, B., and Dudler, R.** (2009) Biosynthesis of the proteasome inhibitor syringolin A: the ureido group joining two amino acids originates from bicarbonate. *BMC Biochemistry* **10**:26
- Rethage, J., Ward, P.I., and Slusarenko, A.J.** (2000) Race-specific elicitors from the *Peronospora parasitica*/Arabidopsis thaliana pathosystem. *Physiol. Mol. Plant Pathol.* **56**, 179-184.
- Rehmany, A.P., Lynn, J.R., Tör, M., Holub, E.B., and Beynon, J.L.** (2000) A comparison of *Peronospora parasitica* (downy mildew) isolates from Arabidopsis thaliana and Brassica oleracea using amplified fragment length polymorphism and internal transcribed spacer 1 sequence analyses. *Fungal Gen. Biol.* **30**, 95-103.
- Richael, C., Lincoln, E., Bostock, R.M., and Gilchrist, D.G.** (2001) Caspase inhibitors reduce symptom development and limit bacterial proliferation in susceptible plant tissues. *Physiol. Mol. Plant Pathol.* **59**, 213-221.
- Rock, K.L., Gramm, C., Rothstein, L., Clark, K., Stein, R., Dick, L., Hwang, D., and Goldberg, A.L.** (1994) Inhibitors of the proteasome block the degradation of most cell proteins and the generation of peptides presented on MHC class I molecules. *Cell* **78**, 761-771.
- Rojo, E., Martín, R., Carter, C., Zouhar, J., Pan, S., Plotnikova, J., Jin, H., Paneque, M., Sánchez-Serrano, J.J., Baker, B., Ausubel, F.M., and Raikhel N.V.** (2004) VPEy exhibits a caspase-like activity that contributes to defense against pathogens. *Curr. Biol.* **14**, 1897-1906.

- Rojo, E., Zouhar, J., Carter, C., Kovaleva, V., and Raikhel N.V.** (2003) A unique mechanism for protein processing and degradation in *Arabidopsis thaliana*. *Proc. Natl. Acad. Sci USA* **100**, 7389-7394.
- Roos, I. M. M., and Hattingh, M. J.** (1987) Systemic invasion of plum leaves and shoots by *Pseudomonas syringae* pv. *syringae* introduced into petioles. *Phytopathol.* **77**, 1252-1257.
- Rosebrock T.R., Zeng, L., Brady, J.J., Abramovitch, R.B., Xiao, F., and Martin, G.B.** (2007) A bacterial E3 ubiquitin ligase targets a host protein kinase to disrupt plant immunity. *Nature* **448**, 370-374.
- Sadaghiani, A.M., Verhelts, S.H.L., and Bogyo, M.** (2007) Tagging and detection strategies for activity-based proteomics. *Curr. Opi. Chem. Biol.* **11**, 1-9.
- Sarkar, S. F., Gordon, J. S., Martin, G. B., and Guttman, D. S.** (2006) Comparative genomics of host-specific virulence in *Pseudomonas syringae*. *Genetics* **174**, 1041-1056.
- Sexton, K.B., Kato, D., Berger, A.B., Fonovic, M., Verhelst, S.H.L., and Bogyo, M.** (2007) Specificity of aza-peptide electrophile activity-based probes of caspases. *Cell Death Differ.* **14**, 727-732.
- Shimada, T., Yamada, K., Kataoka, M., Nakaune, S., Koumoto, Y., Kuroyanagi, M., Tabata, S., Kato, T., Shinozaki, K., Seki, M., Kobayashi, M., Kondo, M., Nishimura, M., and Hara-Nishimura, I.** (2003) Vacuolar processing enzymes are essential for proper processing of seed storage proteins in *Arabidopsis thaliana*. *J. Biol. Chem.* **278**, 32292-32299.
- Slusarenko, A.J., and Schlaich, N.L.** (2003) Downy mildew of *Arabidopsis thaliana* caused by *Hyaloperonospora parasitica* (formerly *Peronospora parasitica*). *Mol. Plant Pathol.* **4**, 159-170.
- Soylu, E.M., Soyly, S., and Mansfield, J.W.** (2004) Ultrastructural characterisation of pathogen development and host responses during compatible and incompatible interactions between *Arabidopsis thaliana* and *Peronospora parasitica*. *Physiol. Mol. Plant Pathol.* **65**, 67-78.
- Speers, A.E. and Cravatt, B.F.** (2004) Profiling enzyme activities *in vivo* using click chemistry methods. *Chem Biol*, **11**, 535-546.
- Spoel, S. H., Mou, Z., Tada, Y., Spivey, N. W., Genschik, P., and Dong, X.** (2009) Proteasome-mediated turnover of the transcription coactivator NPR1 plays dual roles in regulating plant immunity. *Cell* **137**, 860-872.
- Thines, B., Katsir, L., Melotto, M., Niu, Y., Mandaokar, A., Liu, G., Nomura, K., He, S. H., Howe, G. A., and Browse, J.** (2007) JAZ repressor proteins are targets of the SCF<sup>CO11</sup> complex during jasmonate signalling. *Nature* **448**, 661-665.
- Uren, A.G., O'Rourke, K., Aravind, L.A., Pisabarro, M.T., Seshagari, S., Koonin, E.V., and Dixit, V.M.** (2000) Identification of paracaspases and metacaspases: two ancient families of caspase-like proteins, one of which plays a key role in MALT lymphoma. *Mol. Cell* **6**, 961-967.
- van der Hoorn, R.A.L.** (2008) Plant proteases: from phenotype to molecular mechanisms. *Annu. Rev. Plant Biol.* **59**, 191-223.
- van der Hoorn, R.A., Laurent, F., and De Wit P.J.** (2000) Agroinfiltration is a versatile tool that facilitates comparative analysis of Avr9/Cf-9-induced and Avr4/Cf-4-induced necrosis. *Mol. Plant Microb. Interact.* **13**, 439-446.
- van der Hoorn, R.A.L., Leeuwenburgh, M.A., Bogyo, M., Joosten, M.H.A.J, and Peck, S.C.** (2004) Activity profiling of papain-like cysteine proteases in plants. *Plant Physiol.* **135**, 1170-1178.

- van Doorn, W.G., and Woltering, E.J.** (2005) Many ways to exit? Cell death categories in plants. *Trends Plant Sci.* **10**, 117-122
- Vercammen, D., van de Cotte, B., De Jaeger, G., Eeckhout, D., Casteels, P., Vandepoele, K., Vanderberghe, I., Beeumen, J., Inzé, D., and van Breusegem, F.** (2004) Type II metacaspases Atmc4 and Atmc9 of *Arabidopsis thaliana* cleave substrates after arginine and lysine. *J. Biol. Chem.* **279**, 54329-45336.
- Verdoes, M., Florea, B.I., Menendez-Benito, V., Maynard, C.J., Witte, M.D., Van der Linden, W.A., Van den Nieuwendijk, A.M.C.H., Hofman, T., Berkers, C.R., Van Leeuwen, F.W.B., Groothuis, T.A., Leeuwenburgh, M.A., Ovaa, H., Neefjes, J.J., Filippov, D.V., Van der Marel, G.A., Dantuma, N.P., and Overkleeft, H.S.** (2006) A fluorescent broad-spectrum proteasome inhibitor for labelling proteasomes *in vitro* and *in vivo*. *Chem. Biol.* **13**, 1217-1226.
- Vlot, A. C., Dempsey, D. A., and Klessig, D. F.** (2009) Salicylic acid, a multifaceted hormone to combat disease. *Annu. Rev. Phytopathol.* **47**, 177-206.
- Vinutzer, B.A., Teitzel, G.M., Lee, M.W., Jelenska, J., Hotton, S., Fairfax, K., Jenrette, J., and Greenberg, J.T.** (2006) The type III effector repertoire of *Pseudomonas syringae* pv. *syringae* B728a and its role in survival and disease on host and non-host plants. *Mol. Microbiol.* **62**, 26-44.
- Voinnet, O., Rivas, S., Mestre, P., and Baulcombe, D.** (2003) An enhanced transient expression system in plants based on suppression of gene silencing by the p19 protein of tomato bushy stunt virus. *Plant J.* **33**, 949-956.
- Watanabe, N., and Lam, E.** (2005) Two *Arabidopsis* metacaspases AtMCP1b and AtMCP2b are arginine/lysine specific cysteine proteases and activate apoptosis-like cell death in yeast. *J. Biol. Chem.* **280**, 14691-14699.
- Wäspi, U., Hassa, P., Staempfli, A., Molleyres, L. P., Winkler, T., and Dudler, R.** (1999) Identification and structure of a family of syringolin variants: unusual cyclic peptides from *Pseudomonas syringae* pv. *syringae* that elicit defence responses in rice. *Microbiol. Res.* **154**, 1-5.
- Wulff, B. B. H., Kruijt, M., Collins, P. L., Thomas, C. M., Ludwig, A. A., De Wit, P. J. G. M., and Jones, J. D. G.** (2004) Gene shuffling-generated and natural variants of the tomato resistance gene *Cf-9* exhibit different auto-necrosis-inducing activities in *Nicotiana* species. *Plant J.* **40**, 942-956.
- Yamada, K., Shimada, T., Kondo, M., Nishimura, M., and Hara-Nishimura, I.** (1999) Multiple functional proteins are produced by cleaving Asn-Gln bonds of a single precursor by vacuolar processing enzyme. *J. Biol. Chem.* **274**, 2563-2570.
- Yamada, K., Shimada, T., Nishimura, M., and Hara-Nishimura, I.** (2005) A VPE family supporting various vacuolar functions in plants. *Physiol. Plant, Special Issue* **123**, 369-375.

## 6 APPENDICES

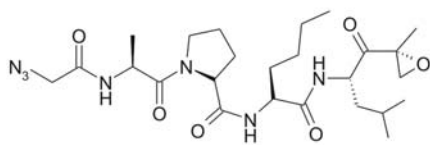
### 6.1 Appendix A. Structure of legumain probes used for VPE screening



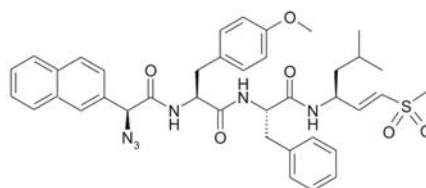
The probes contain a reactive group (grey), which in the case of JCP550 is a Michael system and for the others is an AOMK, and the reporter tags bodipy (purple), Cy5 (blue) or biotin (pink).



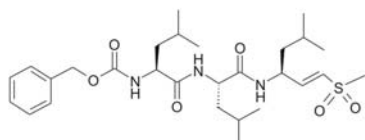
## 6.2 Appendix B. Structure of the inhibitors used in this study



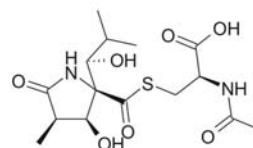
N3β1



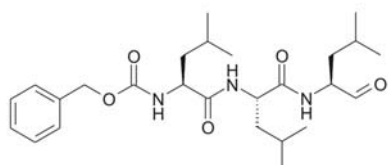
N3β5



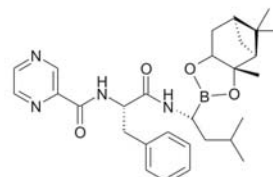
ZL3VS



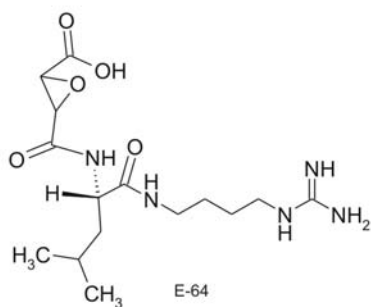
Lactacystin



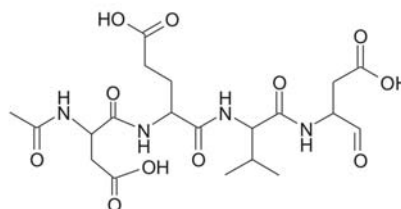
MG132



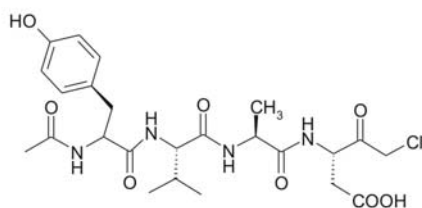
Protected Bortezomib



E-64

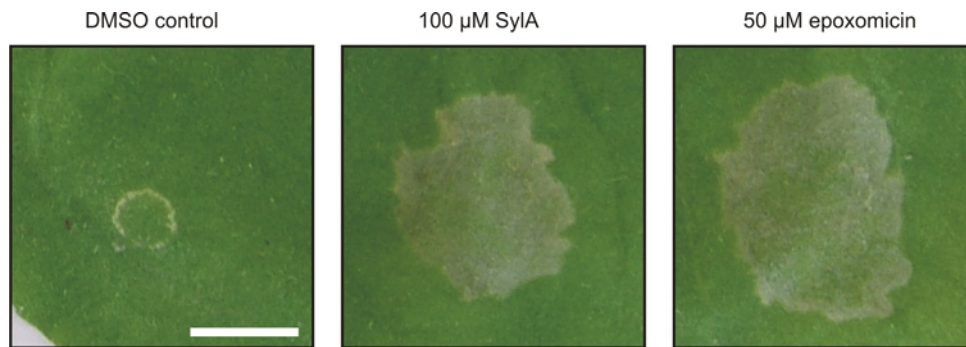


Ac-DEVD-cho



Ac-YVAD-cmk

**6.3 Appendix C. SylA and epoxomicin induce cell death in *Nicotiana benthamiana***



Leaves of *N. benthamiana* were infiltrated with 100 μM SylA or 50 μM epoxomicin and tissue collapse was observed at 5 days after infiltration (dpi). Picture was taken at 7 dpi. Scale bar, 1 cm.

6.4 Appendix D. Table 1. *Pseudomonas syringae* strains

Strain	Resistance marker <sup>a</sup>	GFP construct <sup>b</sup>	Lab
<i>Ps maculicola</i> YM7930 WT		Y	J. Alfano
<i>Ps syringae</i> B301D-R WT	Rif	Y	R. Dudler
<i>Ps syringae</i> B301D-R sylC	Rif/Tet	Y	R. Dudler
<i>Ps syringae</i> B301D-R sylD	Rif/Tet	Y	R. Dudler
<i>Ps syringae</i> B728a WT	Rif	Y	R. Dudler
<i>Ps syringae</i> B728a sylC	Rif/Tet	Y	R. Dudler
<i>Ps syringae</i> B728a hrcC	Rif//Km	Y	R. Dudler
<i>Ps syringae</i> B728a hrcC-sylC	Rif/Tet/Km	Y	R. Dudler
<i>Ps syringae</i> DC3000	Rif	Y	J. Parker
<i>Ps tabaci</i> 11528R WT	Rif	Y	J. Parker
<i>Ps thea</i> K93001 WT	Rif	Y	J. Alfano
<i>Ps aceris</i> A10853 WT	Rif	Y	J. Greenberg
<i>Ps aceris</i> A10853 SylA	Rif/Tet	Y	This lab
<i>Ps phaseolicola</i> NPS3121 WT	Rif/Km	Y	S. Robatzek
<i>Ps phaseolicola</i> RW60 WT	Rif/Spec	Y	S. Robatzek
<i>Ps glycinea</i> R4A WT		Y	S. Robatzek
<i>Ps pisi</i> H7E7 WT		Y	S. Robatzek
<i>Ps maculicola</i> 4981 WT		Y	S. Robatzek
<i>Ps syringae</i> B64 wt_GFP		Y	R. Dudler
<i>Ps syringae</i> B64 sylC-GFP	Tet	Y	R. Dudler

<sup>a</sup>. Antibiotics used for the selection of the strain. Rifampicin [25-50µg/ml] (Rif), tetracyclin [10µg/ml] (Tet), kanamycin [50µg/ml] (Km), spectromycin [10-15µg/ml].

<sup>b</sup>. GFP-expressing strains were generated by transforming WT strains with the plasmid pFK0078.01 (F. Kaschani, unpublished data). pFK0078.01 carries gentamicin resistance. Y: yes, the GFP transformant was generated and is available.

## 7 ACKNOWLEDGMENT

This is the section I like the most from my thesis. The moment, in which I have the opportunity to say thanks to everyone who has contributed to this work, without them this PhD would have not been possible.

I would like to thank Renier for giving me the opportunity to be part of the Plant Chemetics group. Your continuous support and enthusiastic encouragement have helped me to be an excellent scientist everyday. Thank you for the hours and hours of scientific discussions, for the time expended supervising me, for your help in the lab and in the writing period. Thanks a lot you for your patience, I have been learning a lot! And I hope we will find the way to finish our “never ending story”.

Thank you very much Jane for being my second supervisor, for giving me critical comments about my work and for encouraging me to search for the right answer. Special thanks for being part of my defense committee as a “Beisitzer”.

I would like to thank Paul for accepting to be my “Doktorvater”. I will never forget the PSL departmental seminars, in which you encourage us to think independently, to ask questions, and to be critical with our work. Thank you very much for encouraging us to be the best!

Special thanks to my thesis committee Prof. Dr. Marcel Bucher, Prof. Dr. Hermen Overkleeft, and Prof. Dr. Reinhard Krämer. I am very glad you were able to be part of my defense. Thank you very much for your reply even during your vacations time!

I am very thankful with all the members of the Plant Chemetics lab. Many thanks to Iza for all the days and nights collecting samples, for motivating me when I was tired, for teaching me cell biology, and specially for your friendship. Thanks a lot to Christian and Farnusch for being critical with my work; I learned a lot from you guys. Thank you my dear Selva, we had a good time in the lab. Thanks to Ilyas, Taka, Kerstin, Adriana, Leo, and all the people who pass by trough the lab. You made a very nice atmosphere in the plant chemetics lab. Special thanks to Gerrit, my first student, I hope you enjoyed the time in Cologne!

I also want to thank everyone at the institute who contributes to this work, thanks to the JP lab for advices, materials and time, specially Marco, Ana, Johannes, Katharina, and Jaqueline. You really made my work easier! Thanks to Coupland's lab, Konz's lab, and Davis's lab for sharing space, equipment, and nice departamental outings.

Thank you to "las chicas" for the nice lunch times and coffee breaks. Cami, Joha, Gabi y Linda gracias por su valiosa amistad! Pāmi vielen Dank für deine Hilfe.

Last but not least, I would like to thank my family in Germany and in Colombia. Papi y Mami, gracias por el apoyo durante todos estos años y por estar siempre conmigo en la distancia. Mi cuchis lo logramos! Gracias por las oraciones, por la compañía, por darme siempre ánimos para seguir adelante y por siempre estar tan orgullosa de mí. Gracias negris por tu confianza y tu amistad, espero ser un buen ejemplo para ti! Gracias abuelito, tito Jorge y tito Gabriel. Abuelita Ana muchas gracias por apoyarme y consentirme tanto. Vielen Dank Björnchi, ohne deine Liebe und deine Unterstützung wäre es nicht möglich gewesen! Danke Luisa, dass Du da bist und mir das Gefühl gibst was besonderes zu sein!

## 8 ERKLÄRUNG

Ich versichere, dass ich die von mir vorgelegte Dissertation selbständig angefertigt, die benutzten Quellen und Hilfsmittel vollständig angegeben und die Stellen der Arbeit – einschließlich Tabellen, Karten und Abbildungen –, die anderen Werken im Wortlaut oder dem Sinn nach entnommen sind, in jedem Einzelfall als Entlehnung kenntlich gemacht habe; dass diese Dissertation noch keiner anderen Fakultät oder Universität zur Prüfung vorgelegen hat; dass sie – abgesehen von den auf Seite 96 angegebenen Teilpublikationen – noch nicht veröffentlicht worden ist sowie, dass ich eine solche Veröffentlichung vor Abschluss des Promotionsverfahrens nicht vornehmen werde. Die Bestimmungen dieser Promotionsordnung sind mir bekannt. Die von mir vorgelegte Dissertation ist von Prof. Dr. Paul Schulze-Lefert betreut worden.

Köln, 30. August 2010

---

Johana C. Misas Villamil

## 9 LEBENS LAUF

### Angaben zur Person

Name: Johana Catherine Misas-Villamil  
 Geburtsdatum: 7. Oktober 1980  
 Geburtsort: Bogotá, Kolumbien  
 Nationalität: Kolumbianerin

### Ausbildung

- Seit 05/2007 **Promotions-Studium** an der Universität zu Köln, Köln, Deutschland.  
 Max-Planck-Institut für Pflanzenzüchtungsforschung, unter der Leitung von Prof. Dr. Paul Schulze-Lefert und Dr. Renier van der Hoorn.  
 Stipendium der Deutsche Akademische Austausch Dienst (DAAD)
- 10/2006-04/2007 **Wissenschaftlicher Mitarbeiter** am Max-Planck-Institut für Terrestrische Mikrobiologie, Marburg, Deutschland; unter der Leitung von Dr. Michael Friedrich.  
 Stipendium der Deutsche Akademische Austausch Dienst (DAAD)
- 10/2005-09/2006 **Wissenschaftlicher Mitarbeiter** am *National Coffee Research Center* (CENICAFE), Chinchiná, Kolumbien.  
 Abteilung der Phytopathologie unter der Leitung von Dr. Alvaro Gaitán.
- 02/2001-09/2005 **Diplom-Studium Biologie** and der Universidad de los Andes, Bogotá, Kolumbien.  
 Abschluss: Diplom-Biologin.

## LEBENS LAUF

- 02/1998-09/2005 **Diplom-Studium Mikrobiologie** and der Universidad de los Andes, Bogotá, Kolumbien.  
Abschluss: Diplom-Mikrobiologin.
- 02/2004-02/2005 **Diplomarbeit** am Institut für Mikrobiologie und Molekularbiologie. Justus-Liebig Universität Giessen, Giessen, Deutschland; unter der Leitung von Prof. Dr. Gabriele Klug.
- 10/2003-01/2004 **Austausch Programm** an der Justus-Liebig Universität Giessen. Giessen. Deutschland.  
Stipendium der Justus-Liebig Universität Giessen in Kooperation mit der Universidad de los Andes.
- 11/1997 **Abitur** am *Instituto Colsubsidio de Educacion Femenina* (ICEF), Bogotá, Kolumbien.

## Publikationen

- Gu, C., Kolodziejek, I., Misas-Villamil, J., Shindo, T., Colby, T., Verdoes, M., Richau, K., Schmidt, J., Overkleeft, H., and Van der Hoorn, R. A. L. (2010) Proteasome activity profiling: a simple, robust and versatile method revealing subunit-selective inhibitors and cytoplasmic, defence-induced proteasome activities. *Plant J.* 62, 160-170.
- Misas-Villamil, J. C., and Van der Hoorn, R. A. L. (2008) Enzyme-inhibitor interactions at the plant-pathogen interface. *Curr. Opin. Plant Biol.* 11, 380-388.

Köln, 30. August 2010

---

Johana C. Misas-Villamil